

**On the Function and Regulation of Human
STIL – a Centrosomal Protein Implicated in
Autosomal Recessive Primary
Microcephaly**

Inauguraldissertation

zur

Erlangung der Würde eines Doktors der Philosophie

vorgelegt der

Philosophisch-Naturwissenschaftlichen Fakultät

der Universität Basel

von

Christian Arquint

aus Tarasp, Schweiz

Basel 2014

Originaldokument gespeichert auf dem Dokumentenserver der Universität Basel edoc.unibas.ch

Dieses Werk ist unter dem Vertrag „Creative Commons Namensnennung-Keine kommerzielle Nutzung-Keine Bearbeitung 3.0 Schweiz“ (CC BY-NC-ND 3.0 CH) lizenziert. Die vollständige Lizenz kann unter creativecommons.org/licenses/by-nc-nd/3.0/ch/ eingesehen werden.

Genehmigt von der Philosophisch-Naturwissenschaftlichen Fakultät

Auf Antrag von

Erich A. Nigg

Markus Affolter

Basel, den 24.06.2014

Prof. Dr. Jörg Schibler

- Dekan-



Namensnennung-Keine kommerzielle Nutzung-Keine Bearbeitung 3.0 Schweiz
(CC BY-NC-ND 3.0 CH)

Sie dürfen: **Teilen** — den Inhalt kopieren, verbreiten und zugänglich machen

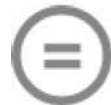
Unter den folgenden Bedingungen:



Namensnennung — Sie müssen den Namen des Autors/Rechteinhabers in der von ihm festgelegten Weise nennen.



Keine kommerzielle Nutzung — Sie dürfen diesen Inhalt nicht für kommerzielle Zwecke nutzen.



Keine Bearbeitung erlaubt — Sie dürfen diesen Inhalt nicht bearbeiten, abwandeln oder in anderer Weise verändern.

Wobei gilt:

- **Verzichtserklärung** — Jede der vorgenannten Bedingungen kann **aufgehoben** werden, sofern Sie die ausdrückliche Einwilligung des Rechteinhabers dazu erhalten.
- **Public Domain (gemeinfreie oder nicht-schützbare Inhalte)** — Soweit das Werk, der Inhalt oder irgendein Teil davon zur Public Domain der jeweiligen Rechtsordnung gehört, wird dieser Status von der Lizenz in keiner Weise berührt.
- **Sonstige Rechte** — Die Lizenz hat keinerlei Einfluss auf die folgenden Rechte:
 - Die Rechte, die jedermann wegen der Schranken des Urheberrechts oder aufgrund gesetzlicher Erlaubnisse zustehen (in einigen Ländern als grundsätzliche Doktrin des **fair use** bekannt);
 - Die **Persönlichkeitsrechte** des Urhebers;
 - Rechte anderer Personen, entweder am Lizenzgegenstand selber oder bezüglich seiner Verwendung, zum Beispiel für **Werbung** oder Privatsphärenschutz.
- **Hinweis** — Bei jeder Nutzung oder Verbreitung müssen Sie anderen alle Lizenzbedingungen mitteilen, die für diesen Inhalt gelten. Am einfachsten ist es, an entsprechender Stelle einen Link auf diese Seite einzubinden.

TABLE OF CONTENTS

1. SUMMARY	1
2. INTRODUCTION	3
2.1 Centrosome Research – A Short Historical Overview.....	4
2.2 Centrioles, Centrosomes, Cilia and Flagella	5
2.3 Centriole and Centrosome Structure.....	8
2.4 Centriole and Centrosome Function	12
2.5 Centriole and Centrosome Regulation	17
2.5.1 Centrosome Duplication	17
2.5.2 Centrosome Cohesion and Separation	18
2.5.3 Centrosome Maturation	18
2.5.4 Centriole Disengagement	19
2.6 Centriole Biogenesis	21
2.6.1 RNAi Screens in <i>C. elegans</i> Reveal a Small Set of Centriole Duplication Factors.....	21
2.6.2 The Centriole Duplication Machinery is Conserved from Worm to Man.....	22
2.6.3 Additional Duplication Factors in <i>Drosophila</i> , Human Cells and Other Organisms.....	25
2.6.4 Regulation of Centriole Duplication.....	29
2.6.4.1 Two Modes of Centriole Duplication.....	29
2.6.4.2 Cell Cycle Cues that Regulate Centriole Duplication..	30

2.6.4.3 Regulation of Centriole Numbers by Proteasomal Degradation.....	30
2.7 Centrosomes in Brain Disease and Primordial Dwarfism.....	32
2.8 STIL – A Centriole Duplication Factor in Human Cells?.....	35
3. AIM OF THIS PROJECT	37
4. RESULTS	39
4.1 Publication in Journal of Cell Science, 2012	40
Cell-cycle Regulated Expression of STIL Controls Centriole Numbers in Human Cells	
4.2 Publication in Current Biology, 2014.....	58
STIL Microcephaly Mutations Interfere with APC/C-Mediated Degradation and Cause Centriole Amplification	
5. DISCUSSION	78
5.1 On the Relation of SAS-5, Ana-2 and STIL.....	79
5.2 Do STIL and E2F Cooperate in Centriole Duplication?.....	83
5.3 Is STIL a Genuine Cartwheel Protein?.....	83
5.4 Is STIL Required for Cartwheel Stability?.....	84
5.5 APC/C-Mediated Degradation of STIL.....	85
5.6 STIL Microcephaly Mutations are Gain-of-Function.....	87
5.7 Is Centriole Amplification a Root Cause of Microcephaly?.....	90

6. ABBREVIATIONS.....	92
7. REFERENCES	95
8. ACKNOWLEDGMENTS	119

1. SUMMARY

Here, we have characterized human STIL (SCL/TAL1 interrupting locus), a distant member of the *Drosophila* Ana2 and *C. elegans* SAS-5 family of centriole duplication factors and a protein, which causes autosomal recessive primary microcephaly (MCPH) when mutated in patients. We show that depletion of STIL from human cells blocks centriole duplication, whereas overexpression of STIL triggers the near-simultaneous formation of multiple daughter centrioles. A similar phenotype had previously been observed for HsSAS-6 and the kinase Plk4, two key regulators of centriole duplication that contribute to cartwheel assembly, a template for centriole formation. In line with these results, we observed a prominent co-localization of STIL and HsSAS-6 at the cartwheel region. Together with two independent studies (Tang et al., 2011; Vulprecht et al., 2012), our work suggests that STIL cooperates with Plk4 and HsSAS-6 in cartwheel formation and thus represents a key centriole duplication factor in human cells.

The observation that excess STIL triggers centriole amplification, a condition that is associated with genome instability, prompted us to analyse the controls governing STIL cell-cycle regulation in more detail. By fluorescence time-lapse imaging, we revealed a two-step process that results in complete elimination of STIL towards the end of mitosis. First, during nuclear envelope breakdown, Cdk1 triggers the translocation of STIL from daughter centrioles into the cytoplasm. This event might initiate cartwheel disassembly, as HsSAS-6, a major cartwheel component, follows a similar trend. The bulk of cytoplasmic STIL is then degraded at the metaphase to anaphase transition by the anaphase promoting complex/cyclosome (APC/C), which involves a KEN box located at the C-terminus of STIL. Interestingly, we found that truncations of STIL that cause MCPH in human patients delete this KEN box, but preserve the overall function of STIL as a centriole duplication factor. We readily confirmed that STIL MCPH truncations resist APC/C-mediated degradation, and demonstrated that stabilization of mutant STIL is strong enough to trigger centriole amplification in our cell culture model. Therefore, by analysing STIL cell cycle regulation, we uncovered a provocative link to primary microcephaly. This leads us to propose that centriole amplification, triggered by STIL stabilization, is the underlying cause of MCPH in patients with STIL mutations.

2. INTRODUCTION

2.1 Centrosome Research – A Short Historical Overview

The centrosome has been discovered and described by cell biologists Edouard van Beneden (van Beneden, 1876) and Theodor Boveri (Boveri, 1887) more than 100 years ago. Despite its important roles in cell physiology, our understanding of the centrosome's structure and function is only beginning to emerge. For a long time, research on the centrosome has remained static due to technical limitations, mainly posed by the small size and low copy number of this organelle. The introduction of new methods in the late 20th century, such as usage of fluorescently labeled antibodies in light microscopy, possibilities to deplete proteins by RNA interference or the application of mass spectrometry to protein analysis have stimulated a new rise in centrosome research.

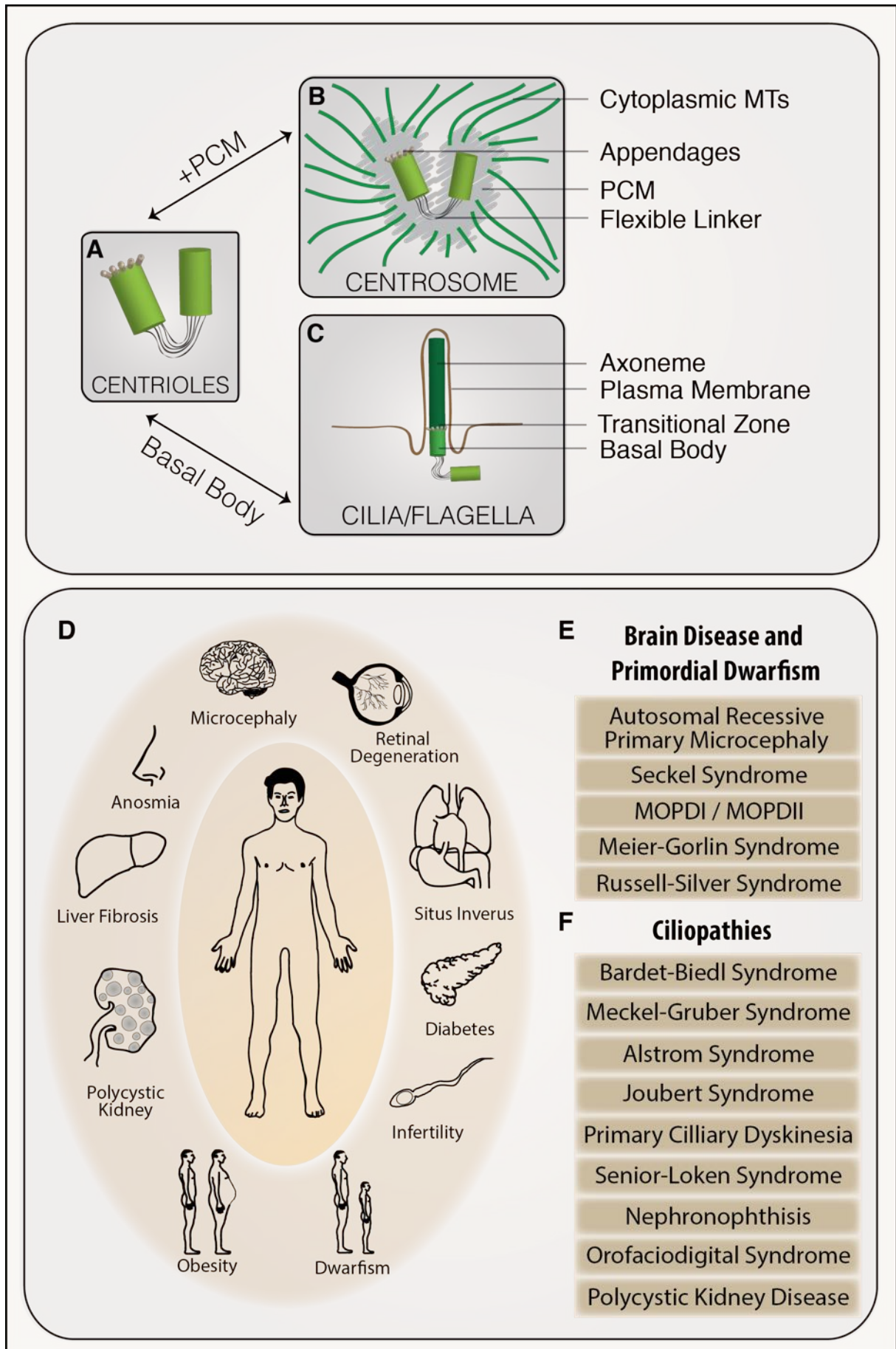
Likewise, the discovery of frequent centrosomal anomalies in cancer (Lingle et al., 2002; Nigg, 2002; Zyss and Gergely, 2009) and the realization that many centrosomal proteins are involved in genetic disorders, such as ciliopathies (Schwartz et al., 2011; Sharma et al., 2008), dwarfism (Klingseisen and Jackson, 2011) or brain disease (Thornton and Woods, 2009) (Figure 1), has steadily increased the awareness on this organelle's impact in human health and disease (Bettencourt-Dias et al., 2011; Nigg, 2006; Nigg and Raff, 2009). The precise roles that centrosomes play in the development of those disorders remains largely to be understood. The elucidation of mechanisms and controls underlying centrosome biogenesis and function will therefore undoubtedly lead to a better understanding and treatment of centrosome-related diseases.

2.2 Centrioles, Centrosomes, Cilia and Flagella

Centrioles are small cylinders made up of stabilized microtubules (MTs) (Figure 1A). They are required for the formation of two different, yet related cellular organelles: centrosomes and cilia/flagella. A pair of centrioles surrounded by a matrix of coiled-coil proteins is defined as the centrosome (Figure 1B). The matrix, called pericentriolar material (PCM), contains factors that allow the nucleation and anchorage of cytoplasmic MTs (Bornens, 2002; Gould and Borisy, 1977; Lüders and Stearns, 2007). Therefore, the centrosome is the primary MT-organizing center (MTOC) in animal cells (Bornens, 2012; Nigg and Stearns, 2011). Centrioles are core centrosomal building blocks for several reasons. First, the PCM has been shown to scatter within the cytoplasm upon centriole disassembly (Bobinnec et al., 1998a), demonstrating that centrioles are important for centrosome stability. Second, centrioles self-replicate and thereby duplicate the centrosome (Nigg and Stearns, 2011).

In quiescent cells, the oldest centriole can furthermore transform into a basal body that associates with the plasma membrane and acts as a template to grow cilia and flagella (Ishikawa and Marshall, 2011; Kim and Dynlacht, 2013), hair-like membrane protrusions, generated by the outgrowth of MT bundles (also called axonemes) (Figure 1C). These organelles can be motile or immotile (Kobayashi and Takeda, 2012) and are important for movement of extracellular fluids or locomotion of whole cells, such as sperm or protists. They can also act as cellular antennae in chemo- and mechanosensation (Goetz and Anderson, 2010; Marshall and Nonaka, 2006).

Mutations in genuine centrosomal and ciliary components have been associated with a large number of diseases (Bettencourt-Dias et al., 2011; Nigg and Raff, 2009) (Figure 1D). Mutations in centrosomal proteins often cause defects in brain development (microcephalies) (Thornton and Woods, 2009) or growth retardation (dwarfism) (Klingseisen and Jackson, 2011) (Figure 1E), whereas malfunction of cilia and flagella results in a large spectrum of disorders, collectively termed ciliopathies (Figure 1F) (Marshall, 2008; Schwartz et al., 2011). Typical phenotypes include polycystic kidneys, liver fibrosis, retinal degeneration, infertility or obesity.



(for figure legend, see next page)

Figure 1: Centrioles, Centrosomes and Cilia in Health and Disease (A) Centrioles are small MT cylinders. They can either associate with pericentriolar material (PCM) to form an MTOC called centrosome (B) or transform into basal bodies to seed the growth of cilia and flagella (C). Mutations in centrosomal and ciliary genes have been linked to numerous pathogenic phenotypes in humans, affecting a wide range of tissues and organs (D). Mutations in centrosomal genes often result in brain disease and primordial dwarfism (E), whereas mutations in ciliary genes lead to a large spectrum of syndromes termed ciliopathies (F).

2.3 Centriole and Centrosome Structure

The canonical vertebrate centriole is a highly-ordered, MT-based cylindrical structure that measures about 500 nm in length and is 250-300 nm wide (Azimzadeh and Marshall, 2010) (Figure 2). Centrioles replicate by the outgrowth of new centrioles (called pro- or daughter centrioles) perpendicular to the wall of preexisting centrioles (called mother centrioles) (Azimzadeh and Bornens, 2007; Nigg and Stearns, 2011). The part of the newly formed centriole, which lies closest to the preexisting centriole, is defined as the proximal part, whereas the opposite end is defined as distal (Figure 2A). The duplication of centrioles involves a template called cartwheel structure. The cartwheel consists of a central hub and nine emanating spokes with associated pinheads that display a 9-fold radial symmetry (Gönczy, 2012; Guichard et al., 2012; van Breugel et al., 2014). Attached to the cartwheel pinheads are nine MT triplets that build the centriole wall. Therefore, the cartwheel is pivotal for establishing the conserved 9-fold symmetric arrangement of mature centrioles (Figure 2A and B).

The first MTs to attach to the cartwheel pinheads, presumably nucleated by γ -tubulin ring complexes (γ -TuRCs) (Fuller et al., 1995), are the A-tubules, which are conventional 13-protofilament MTs. Subsequently, B- and C-tubules assemble, which are both incomplete MTs with less than 13 protofilaments (Dippell, 1968; Guichard et al., 2010) (Figure 2B). In comparison to cytoplasmic MTs, centriolar MTs are cold and detergent resistant. This high degree of stability is due to tubulin modifications, such as polyglutamylation, which protect centriolar MTs from depolymerization (Bobinnec et al., 1998a; 1998b). In vertebrates, the C- tubules are shorter in length, therefore, the distal end of centrioles is composed of A and B tubules only (Figure 2A). Strong deviations from the vertebrate canonical centriole structure can be found in some organisms, e.g. in *C. elegans* (Figure 2C). These centrioles are formed by MT singlets instead of triplets and the assembly platform is a central tube, rather than a cartwheel structure (Pelletier et al., 2006).

To become fully mature, each newborn centriole has to acquire distal and subdistal appendage proteins in a process called centriole maturation (Nigg and Stearns, 2011). Distal appendages, such as Cep164, Cep89, Cep83, SCLT1 or

FBF1, enable basal bodies to dock to the plasma membrane (Tanos et al., 2013), whereas subdistal appendages are needed for the MT organizing capacity of centrioles (Bornens, 2002; Piel et al., 2000). Thus, the older of the two centrioles normally present in one centrosome has the competence to anchor cytoplasmic MTs (Piel et al., 2000), which correlates with the presence of subdistal appendage proteins, such as ninein, Cep170, ODF2 (also known as cenexin) or centriolin.

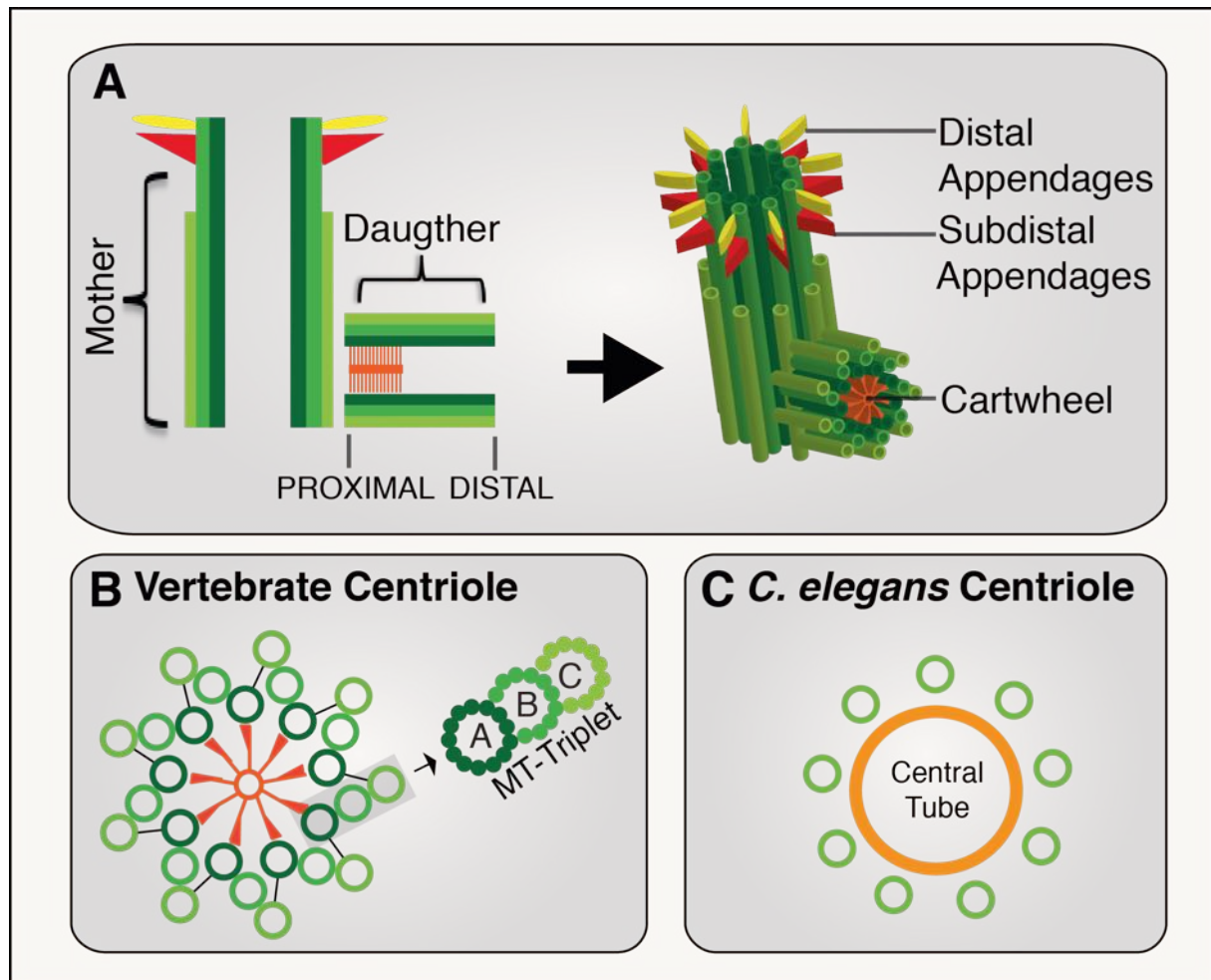


Figure 2: Centriole Structure (A and B) Centrioles are small cylinders formed by a 9-fold symmetrical arrangement of MT triplets (called A, B and C tubules). Centrioles are polarized along the proximo-distal axis. Mature centrioles carry distal and subdistal appendages important for cilia formation and MT nucleation. Nascent centrioles contain a proximal cartwheel structure that serves as a centriole assembly platform. (C) Centriole structure in *C. elegans* is divergent and displays singlet instead of triplet MTs and a central tube, rather than a cartwheel, as assembly platform.

In proliferating cells, centrioles associate with PCM to form the centrosome (Figure 3A). As MT organizers (Figure 3B), centrosomes are implicated in a variety of MT-dependent processes (Bornens, 2012). MTs are nucleated and anchored either directly at centrioles (via subdistal appendages) or via protein complexes that reside within the PCM (Bornens, 2002). The main factor for MT nucleation at centrosomes is γ -tubulin (Félix et al., 1994; Oakley et al., 1990; Oakley and Oakley, 1989; Stearns and Kirschner, 1994). This tubulin variant forms, along with members of a conserved protein family called gamma complex proteins (GCPs), γ -tubulin ring complexes (γ -TuRCs) (Moritz et al., 2000; 1995). These protein complexes allow the nucleation and stabilization of MT minus ends (Stearns and Kirschner, 1994; Wiese and Zheng, 2000; Zheng et al., 1995) (Figure 3C). Therefore, MT minus ends are concentrated around centrosomes, whereas MT plus ends are projecting outwards into the cytoplasm (Figure 3B). The PCM is built from a large number of proteins, such as pericentrin, CDK5RAP2/Cep215 or NEDD1/GCP-WD, many of which contain extensive coiled-coil domains. Following its observation in electron and conventional light microscopy, the PCM has been mainly described as an amorphous mass of proteins. Recent studies, using superresolution light microscopy, however, have revealed a higher order, concentric organization of individual PCM components (Fu and Glover, 2012; Lawo et al., 2012; Mennella et al., 2012; Sonnen et al., 2012). A mysterious and yet to be explored component of centrosomes are the centriolar satellites, electron dense spherical granules of unknown function that appear around centrosomes and move along MTs (Kubo et al., 1999).

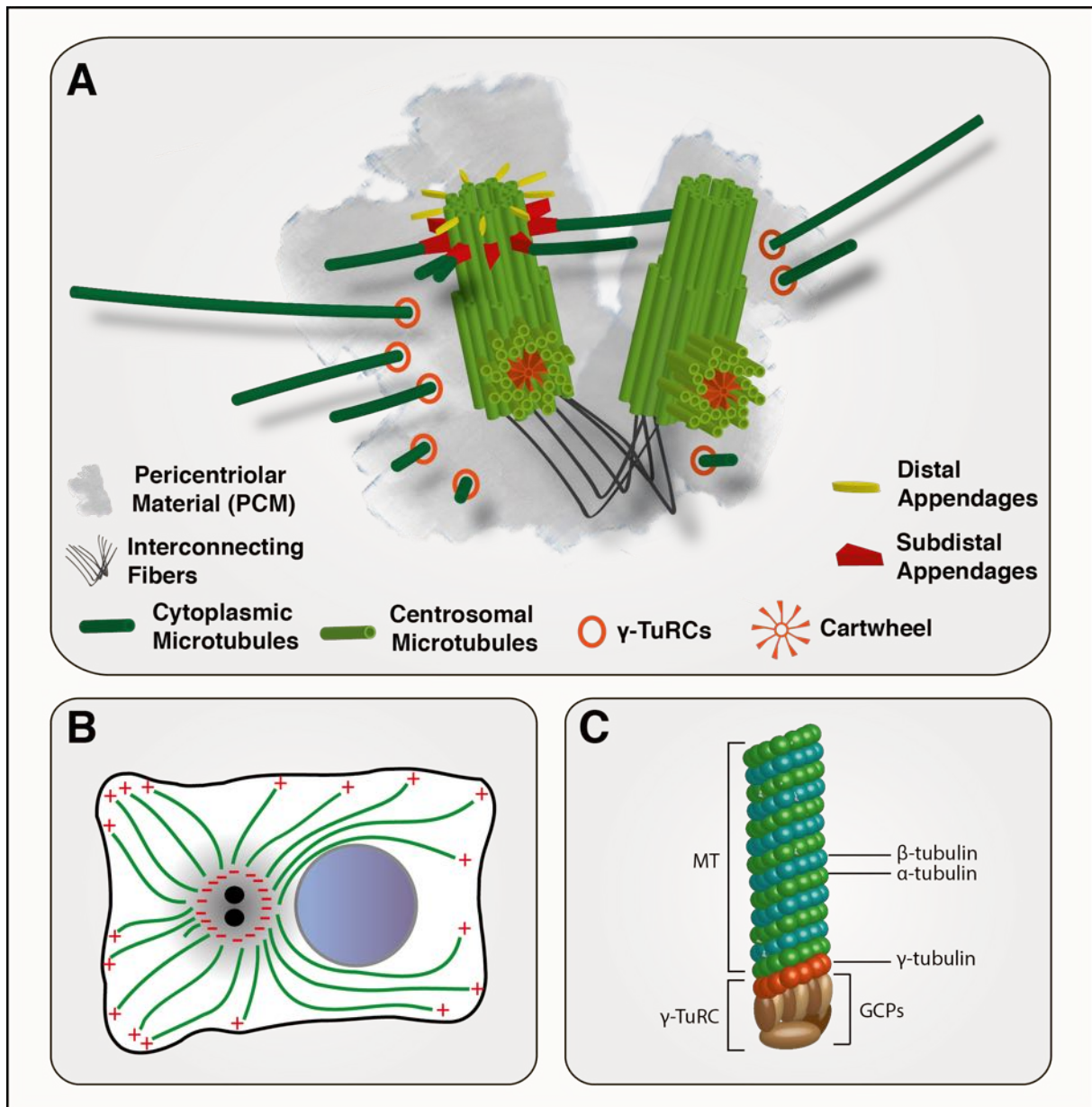


Figure 3: Structure of the Mammalian Centrosome (A) Centrosomes are a combination of centrioles and PCM. One of the centrioles (the oldest one) carries appendages that allow it to attach MTs or to initiate ciliogenesis. The PCM contains protein complexes (such as γ -TuRCs) that are important for MT nucleation. (B) Centrosomes, as the primary MTOCs of animal cells, tether MT minus ends and thereby organize the MT network. This leads to a polarization of the MT network (light green) with MT minus ends concentrating around the centrosome and MT plus ends projecting outwards into the cytoplasm. Centrioles are shown as black dots, PCM is depicted in grey (C) Model of a MT minus end that is capped by a γ -TuRC.

2.4 Centriole and Centrosome Function

Centrioles, in their function as basal bodies nucleating cilia and flagella, are ancestral structures that exist in all major eukaryotic taxa, ranging from uni- to multicellular organisms (Carvalho-Santos et al., 2011; Marshall, 2009). The presence of centrioles in any organism usually correlates with the need to form cilia and flagella (Azimzadeh et al., 2012; Bornens and Azimzadeh, 2007), pointing to the important role of the centriole in the formation and function of these organelles. The situation is different when considering the function of centrioles as organizers of centrosomes. Organisms, especially those that do not rely on cilia and flagella function, often have evolved alternative, acentriolar MTOCs. Yeasts and other fungi, for example, rely on so called spindle pole bodies (SPBs) to organize their MTs (Jaspersen and Winey, 2004). SPBs are multilayered, nuclear membrane-associated organelles. These MTOCs do not contain centrioles, but both centrosomes and SPBs share components that are important for MT nucleation, such as γ -tubulin (Horio et al., 1991; Oakley et al., 1990; Stearns et al., 1991; Zheng et al., 1991) or XMAP215 (Stu2 in yeast) (Wang and Huffaker, 1997). Therefore, in contrast to the widely distributed basal body, the centrosome is mainly restricted to animal cells and centriole structure is probably evolutionarily linked to cilia and flagella, rather than centrosome function.

Despite their limited phylogenetic distribution, centrosomes serve essential functions in animal cells. As primary MTOCs, they orchestrate number, distribution and length of MTs in a temporal and spatial manner (Lüders and Stearns, 2007) (Figure 4). Thus, they are implicated in a variety of MT-dependent processes, with mitotic spindle formation being the most prominent (Figure 5A, see also below). Centrosomes also function in cell migration, intracellular transport or cell fate determination (Figure 5B-D), and these processes are also dependent on the centrosome's MTOC function. For example, in migrating nerve cells, the centrosome positions between the cell nucleus and the leading edge (Cooper, 2013). This polarizes the MT network and allows for stabilization of the leading edge and transport of membrane vesicles towards the site of movement (Figure 5B). Similarly,

in cytotoxic T lymphocytes (CTLs) (Figure 4C), centrosome positioning concentrates the transport of lytic granules to the site of target recognition, called immunological synapse (Angus and Griffiths, 2013; Ritter et al., 2013) (Figure 5C). Centrosomes furthermore play important roles in establishment of polarity axes, such as in the *C. elegans* embryo. Upon fertilization, the sperm centrosome and its MT aster initiate a symmetry breaking event that results in the redistribution of cortical polarity proteins and thus allows asymmetric division of the one-cell embryo (Gönczy and Rose, 2005). Furthermore, many regulatory proteins, including kinases and phosphatases, attach to centrosomes. On one hand, it is well established that the action of these proteins lead to cell-cycle dependent changes in centrosome structure and function, thereby affecting its MTOC function (Lüders and Stearns, 2007). On the other hand, several studies suggest that this organelle also serves MT-independent functions, probably providing a platform for the integration of diverse signaling pathways (Figure 5E). Indeed, there is increasing evidence which implicates the centrosome in signaling related responses (for reviews, see Arquint et al., 2014; Doxsey et al., 2005a; Rieder et al., 2001; Sluder, 2005). The centrosome might therefore act as a hub that integrates and generates intracellular signals, which directly modulate cell cycle progression, such as mitotic entry (Hachet et al., 2007; Portier et al., 2007) or cytokinesis (Piel et al., 2001) (Figure 5F).

The most obvious function of centrosomes is the formation of a bipolar mitotic spindle (Figure 4 and 5A) (Gadde and Heald, 2004). At the onset of mitosis, the two centrosomes separate and accumulate PCM in a process called centrosome maturation, which drastically enhances their MT nucleation activity in prophase (see also chapter 2.5.3). From the two spindle poles, the centrosomes then organize a bipolar MT array that connects to the kinetochore regions of chromosomes. Astral MTs radiate from each spindle pole and associate with the cell cortex to aid in spindle orientation (Kotak and Gönczy, 2013), a process which is important for asymmetric cell division and maintenance of tissue architecture (Siller and Doe, 2009) (Figure 5A). Abnormal mitotic spindles, caused by numerical or structural centrosome aberrations, are a characteristic of many cancer cells and likely contribute to genomic instability, which is a hallmark of cancer progression (Lingle et al., 2002; 2005; Nigg, 2002; Zyss and Gergely, 2009).

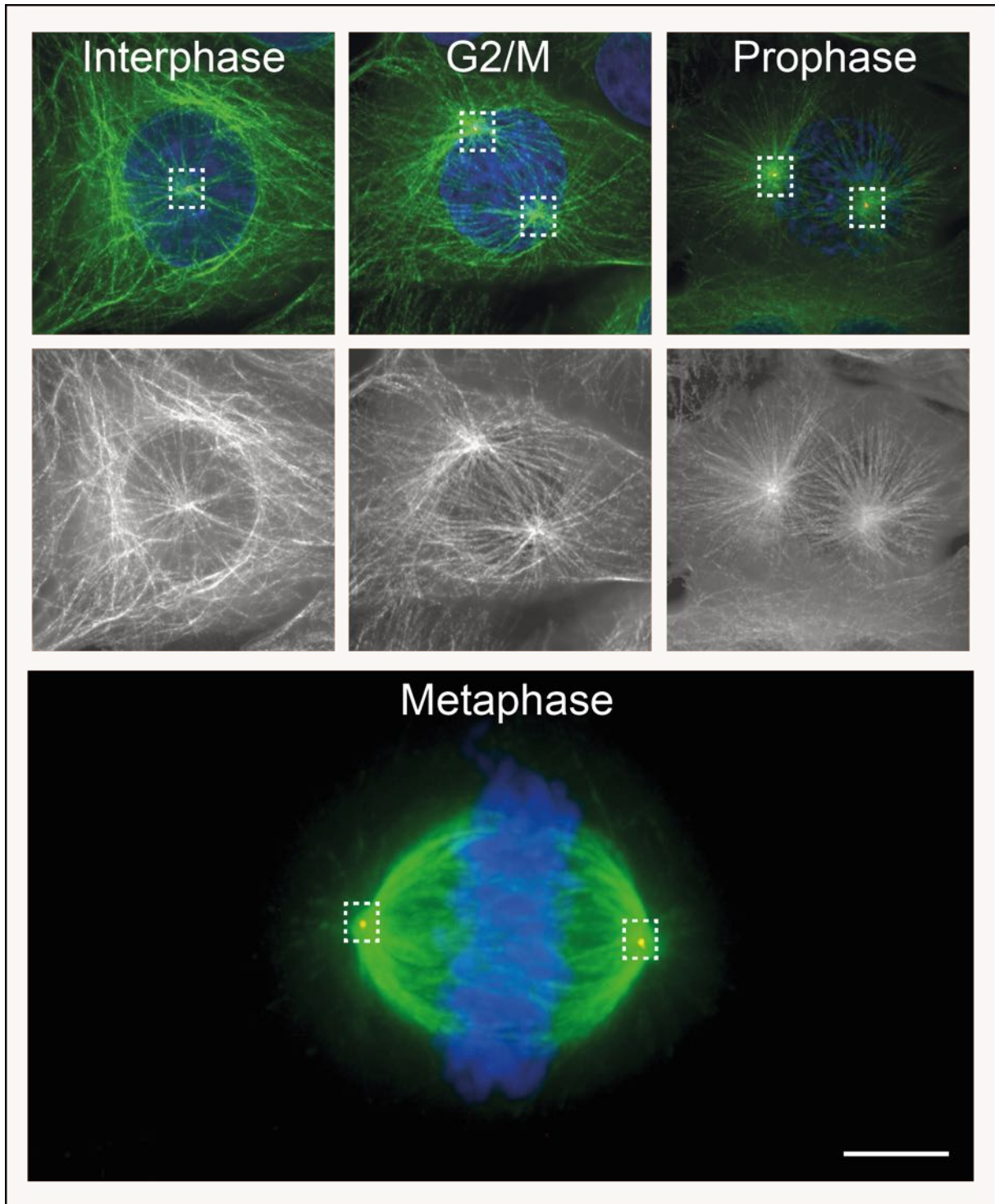


Figure 4: The Centrosome Functions as MTOC in Animal Cells Immunofluorescence micrographs depicting the MT network (green) and centrosomes (red) in U2OS cells of different cell cycle stages. Centrosomes are stained in red and surrounded by white boxes, DNA is shown in blue. Scale bar denotes: 5 μm .

Even though cellular rescue mechanisms, such as the clustering of extra centrosomes to spindle poles (Kwon et al., 2008; Quintyne, 2005; Ring et al., 1982) or inactivation of supernumerary centrosomes (Basto et al., 2008), allow for bipolar cell division in such a context, the error rate for segregation of chromosomes are likely to be higher (Ganem et al., 2009; Silkworth et al., 2009). It remains therefore attractive to postulate that centrosome aberrations are cause and not simply consequence of tumorigenesis (Nigg, 2006; Nigg and Raff, 2009; Zyss and Gergely, 2009), even though a direct link, already proposed by Theodor Boveri 100 years ago (Boveri, 1914), has not yet been provided.

Despite the central role that centrosomes play in spindle formation, it is obvious that bipolar spindles can form in the complete absence of centrosomes, such as in the mouse oocyte (Szollosi et al., 1972) or in planarians (Azimzadeh et al., 2012). Furthermore, bipolar spindles were shown to assemble *in vitro* without the help of centrosomes (Heald et al., 1996) and removal of centrosomes by microsurgery or laser ablation did not interfere with mitotic progression of vertebrate cells (Hinchcliffe et al., 2001; Khodjakov and Rieder, 2001; Uetake et al., 2007). In support of all these observations, *Drosophila* mutant embryos which lack centrioles due to genetic removal of the centriole duplication factor DSAS-4 developed into morphologically normal adult flies (Basto et al., 2006). Only asymmetric divisions of neuroblasts were abnormal, suggesting important functions of centrosomes in this, but not other types of divisions (reviewed in Yamashita and Fuller, 2008). However, these flies do possess centrosomes in very early embryonic stages, and it is those first zygotic divisions that the centrosome seems to be essential for in both *Drosophila* (Stevens et al., 2007) and *C. elegans* development (Pelletier et al., 2005). Furthermore, centrosomes seem to be more essential for vertebrate development, as exemplified by mice lacking the centriole duplication factor Plk4 (Hudson et al., 2001), as well as by chicken cells from which essential centrosomal proteins have been genetically deleted (Sir et al., 2013).

But how do acentriolar cells manage to form a bipolar mitotic spindle? These cells manage to divide due to the existence of an alternative pathway for spindle formation, in which a RanGTP gradient around chromosomes plays a central role (Gruss and Vernos, 2004; O'Connell and Khodjakov, 2007; Wadsworth and Khodjakov, 2003). This pathway allows for MT nucleation at chromosomes, and MTs

are subsequently focused into a bipolar array by help of minus-end directed motor proteins, resulting in the formation of an acentriolar spindle.

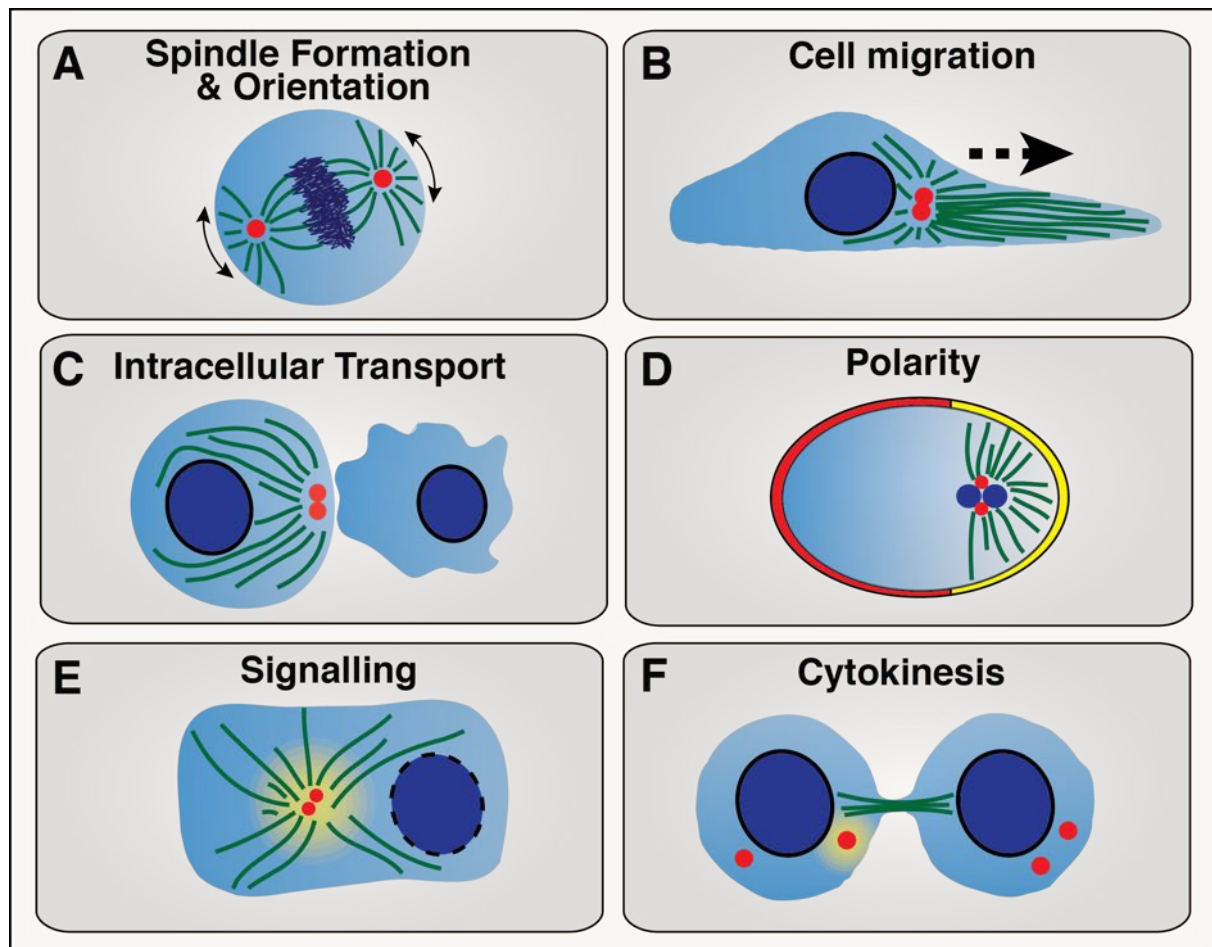


Figure 5: Function of Centrosomes in Animal Cells Centrosomes serve a multitude of cellular functions. (A) In mitosis, the two centrosomes organize the mitotic spindle array by forming the spindle poles. Astral MTs that radiate from centrosomes interact with the cell cortex to allow for precise spindle orientation. (B) In migrating cells, the centrosome positions between the nucleus and the leading edge and acts as a stabilizer for cell movement, thereby also providing vesicles to the site of migration. (C) In CTLs, the centrosome positions near the immunological synapse, which allows for intracellular transportation of lytic granules to the site of target recognition. (D) In the *C. elegans* one-cell embryo, the sperm centrosome and its astral MTs are initiating a symmetry-breaking event that enables redistribution of cortical polarity proteins and asymmetric cell division. (E) Centrosomes also function as signaling hubs that allow for integration of different signaling responses and release of diffusible signals (yellow gradient). (F) As signaling centers, centrosomes might directly have an influence on cellular processes. For example, centrosomes have been shown to play a role in cytokinesis.

2.5 Centriole and Centrosome Regulation

Numerous events act on centrosomes to modulate centrosome/centriole structure or function during cell cycle progression (Nigg and Stearns, 2011). Those events can be divided into several discrete steps, known as the centrosome cycle (Figure 6A).

2.5.1 Centrosome Duplication

A G1-phase centrosome contains two centrioles that are linked to each other via flexible protein fibers. One of the two centrioles (the older) contains appendages that allow it to dock to the plasma membrane for formation of a primary cilia in quiescent cells (Tanos et al., 2013). When cells proliferate, cilia retract and the centrosome duplicates at the G1/S-phase transition. The centrosome is duplicated by duplication of its centrioles (Figure 6B). Centriole duplication is the outgrowth of new centrioles (so called pro- or daughter centrioles) at the proximal base of pre-existing (or mother) centrioles (Azimzadeh and Bornens, 2007; Strnad and Gönczy, 2008) (Figure 5B). Centriole growth involves the formation of a template structure, which in vertebrate and most other species resembles a cartwheel (except for *C. elegans*, where the template is a central tube) (Gönczy, 2012; Pelletier et al., 2006). Centriole duplication requires a set of evolutionarily conserved proteins that have first been identified by RNAi screens in *C. elegans* (Leidel and Gönczy, 2005). Related and additional duplication factors have subsequently been identified in both *Drosophila* and humans (Balestra et al., 2013; Dobbelaere et al., 2008; Kleylein-Sohn et al., 2007), suggesting strong conservation of the centriole duplication pathway. A more detailed description of the molecular players involved in centriole duplication can be found in chapter 2.6. After template formation, centrioles start to grow by deposition of MTs onto the template structure. The newly assembled procentrioles elongate throughout G2 phase and remain tightly associated with their parental centrioles until the end of the next mitosis (see also chapter 2.5.4).

2.5.2 Centrosome Cohesion and Separation

The two parental centrioles are connected via a flexible protein linker (Bornens et al., 1987) to form a single MTOC throughout interphase. The linker consists of C-Nap1 and rootletin fibers (Bahe et al., 2005; Fry et al., 1998; Mayor et al., 2000), but also Cep68, Cdk5rap2/Cep215 (Graser et al., 2007) and β -catenin (Bahmanyar et al., 2008) have been implicated in cohesion. At the G2/M transition, the linker is resolved via protein phosphorylation, mainly triggered by the protein kinase Nek2 that phosphorylates C-Nap1 (Faragher and Fry, 2003; Fry et al., 1998), rootletin (Bahe et al., 2005) and possibly other substrates (Bahmanyar et al., 2008) (Figure 6C). This process is counteracted by protein phosphatase 1 (PP1) (Helps et al., 2000), which is inactivated at the onset of mitosis to allow centrosome separation. In addition, localized Nek2 activity has recently been shown to be regulated by components of the Hippo pathway (Mardin and Schiebel, 2012; Mardin et al., 2010). The separated centrosomes are moved apart by the action of MT-dependent motor proteins, such as the mitotic kinesin Eg5 (Bertran et al., 2011; Blangy et al., 1995; Smith et al., 2011), which allows the centrosomes to participate in mitotic spindle formation.

2.5.3 Centrosome Maturation

The MTOC activity of centrosomes oscillates throughout the cell cycle, reaching its highest levels in mitosis, when centrosomes expand their PCM. This process, called centrosome maturation, is triggered via activities of the mitotic kinases Plk1 (Conduit et al., 2014; Lane and Nigg, 1996; Lee and Rhee, 2011; Sunkel and Glover, 1988) and Aurora A (Berdnik and Knoblich, 2002; Hannak et al., 2001) at the G2/M phase transition (Figure 6D). Maturation not only acts on PCM structure, but also leads to modification of parental and nascent centrioles. Parental centrioles acquire distal and subdistal appendage proteins (Lange and Gull, 1995; Nakagawa et al., 2001), which allows them to anchor cytoplasmic MTs (Bornens, 2002; Piel et al., 2000) or to initiate ciliogenesis (Tanos et al., 2013). Centrioles that have been generated in the same cell cycle (nascent centrioles) have no inherent replication and PCM organisation potentials. Therefore, Plk1-dependent modification at the G2/M phase

transition enables them to replicate and to recruit PCM in the following cell cycle (Wang et al., 2011).

2.5.4 Centriole Disengagement

Centriole disengagement is defined as the loss of the tight orthogonal orientation between the daughter-mother centriole pair (Kuriyama and Borisy, 1981). This process is a prerequisite for another round of centriole duplication (licensing), as the attachment of a newborn centriole to a parental one serves as a block for reduplication, ensuring that one and only one centriole gets formed each cell cycle (Tsou and Stearns, 2006a; Wong and Stearns, 2003), for reviews see Nigg, 2007; Tsou and Stearns, 2006b). However, there are notable exceptions leading to failure in the coordination between cell and centriole duplication cycle, which potentially results in the generation of supernumerary centrosomes (Brownlee and Rogers, 2013; Lingle et al., 2005). First, the block can be overridden by overexpression of certain centriole duplication factors, such as Plk4 (Habedanck et al., 2005; Kleylein-Sohn et al., 2007) and HsSAS-6 (Strnad et al., 2007), which trigger the near-simultaneous formation of several daughter centrioles per mother centriole. Second, some transformed cells can undergo repeated rounds of centriole duplication (including maturation and disengagement of newborn centrioles) when arrested for an extended timespan in interphase (Balczon et al., 1995; Inanc et al., 2010; Loncarek et al., 2010; Wong and Stearns, 2003).

Centriole disengagement requires separase and Plk1 activities (Thein et al., 2007; Tsou and Stearns, 2006a; Tsou et al., 2009) (Figure 5E). Separase is a well-known protease which cleaves cohesin rings that hold sister-chromatids together, and therefore activation of separase (by the APC/C-mediated degradation of its partner securin) marks the timepoint for chromosome segregation (Uhlmann, 2003). The substrate for separase at centrosomes has been elusive for a long time, but increasing evidence suggests that separase might indeed cleave cohesin rings at centrosomes (Nakamura et al., 2009; Schöckel et al., 2011). By using the same molecular „glue“ for centriole and chromosome cohesion, this model therefore provides intriguing provocative explanation for how the centrosome and chromosome cycles might be coupled. In addition, the PCM component kendrin has been identified as an attractive separase substrate (Matsuo et al., 2012).

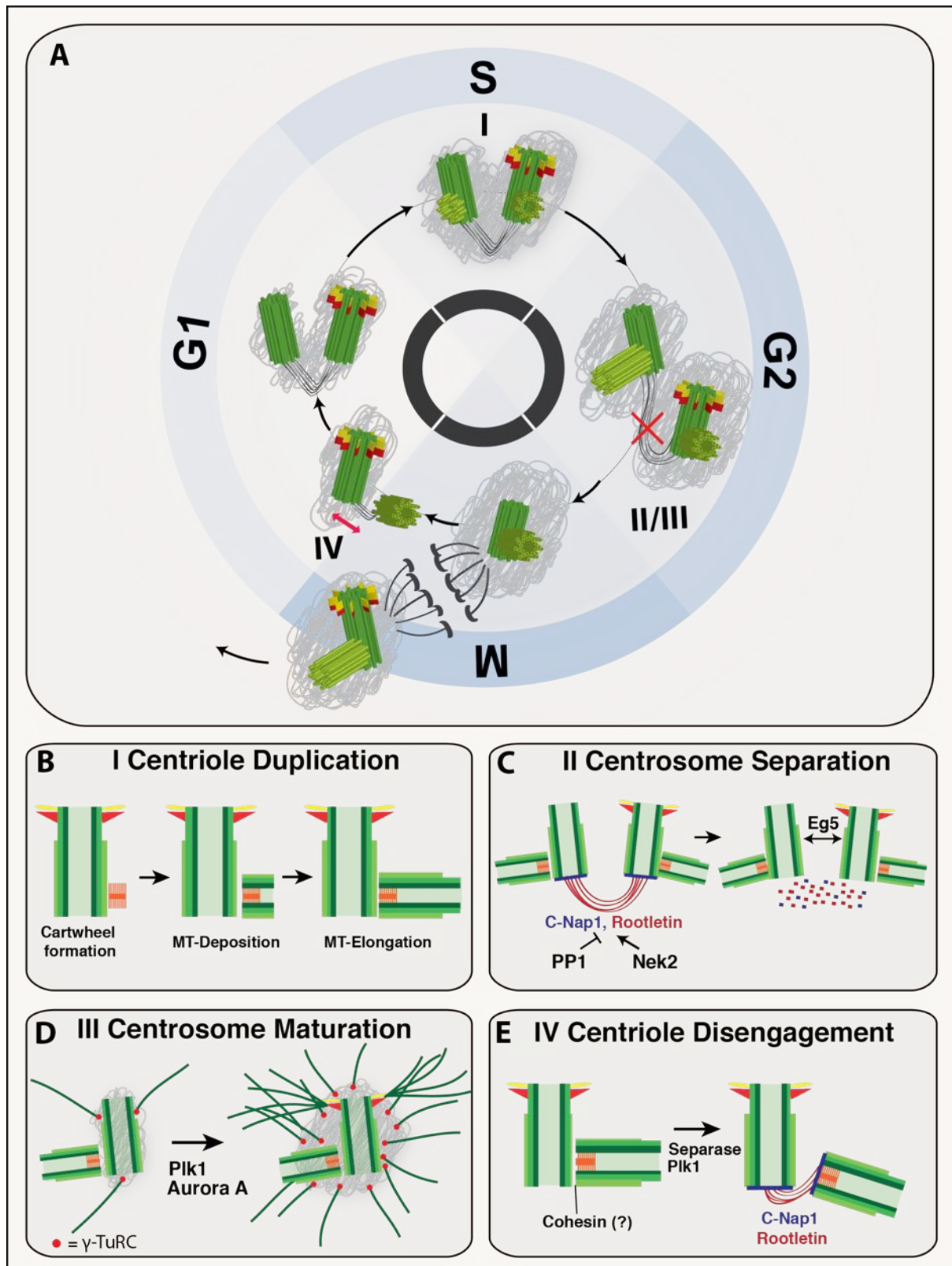


Figure 6: The Centrosome Cycle (A) Illustration of the mammalian centrosome cycle, depicting the processes of centriole duplication (B), centrosome separation (C), centrosome maturation (D) and centriole disengagement (E). For a more detailed explanations, see text.

2.6 Centriole Biogenesis

2.6.1 RNAi Screens in *C. elegans* Reveal a Small Set of Centriole Duplication Factors

Many of the genes that play important roles in cell division processes were identified by genetic screens in *C. elegans* embryos (Fraser et al., 2000; Gonczy et al., 2000; O'Connell et al., 1998; Sönnichsen et al., 2005; Zipperlen et al., 2001). Of those, only five gene products (Figure 7) have been described to be essential for centriole duplication (reviewed in Leidel and Gönczy, 2005). Subsequent functional analysis has led to an understanding of how these proteins, called centriole duplication factors, cooperate to form a new centriole (Dammermann et al., 2004; Delattre et al., 2006; Pelletier et al., 2006).

Centriole duplication factors are consecutively recruited to the site of centriole formation and gradually incorporate into the growing procentriole (Delattre et al., 2006; Pelletier et al., 2006). Most upstream in the pathway acts SPD-2, a protein which plays dual roles in centriole as well as PCM formation (Kemp et al., 2004; Pelletier et al., 2004). SPD-2 is required for localization of the four other proteins (Delattre et al., 2006; Pelletier et al., 2006). Next in the hierarchy is ZYG-1, a kinase that can not be placed into one of the known kinase subfamilies (O'Connell et al., 2001). ZYG-1 triggers the recruitment of a complex of two coiled-coil proteins, named SAS-6 and SAS-5 (Dammermann et al., 2004; Delattre et al., 2006; 2004; Leidel et al., 2005; Pelletier et al., 2006; Qiao et al., 2012). Localization of this complex to the site of centriole assembly coincides with the formation of the central tube (orange tube in Figure 7), a scaffold for the formation of a new centriole (Pelletier et al., 2006). SAS-4 assists in the deposition of singlet MTs onto the central tube, which completes the process (Dammermann et al., 2008; Delattre et al., 2006; Kirkham et al., 2003; Leidel and Gönczy, 2003; Pelletier et al., 2006).

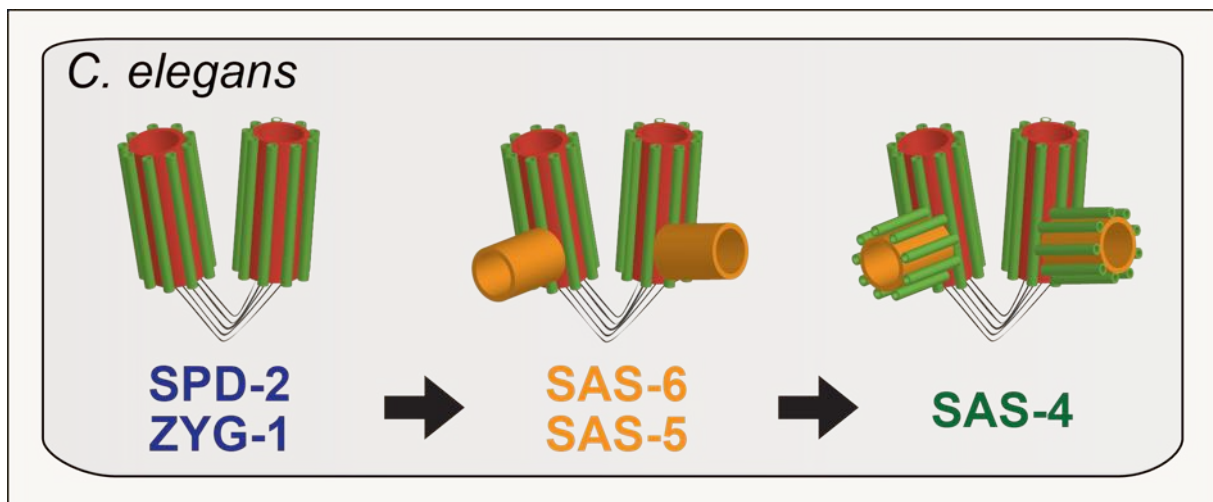


Figure 7 : Centriole Duplication Pathway in *C. elegans* Upstream in the pathway operates SPD-2, which recruits the kinase ZYG-1 to the site of pro-centriole formation. ZYG-1 triggers the recruitment of SAS-6 and SAS-5, a complex of two structural proteins that form the central tube. The central tube is a template onto which singlet MTs are deposited in a SAS-4 dependent manner.

2.6.2 The Centriole Duplication Machinery is Conserved from Worm to Man

All of the five *C. elegans* centriole duplication factors have been conserved in *Drosophila*, humans and many other organisms, suggesting that centriole duplication is a highly conserved process (Figure 8). However, the degree of conservation varies amongst the different components.

A key conserved centriole duplication factor is SAS-6, indicating that this protein is essential for the construction of any new centriole (Dammermann et al., 2004; Leidel et al., 2005; Rodrigues-Martins et al., 2007b). Indeed, SAS-6 is a major component of the cartwheel which establishes the 9-fold symmetry of centrioles (Gopalakrishnan et al., 2010; Nakazawa et al., 2007; Rodrigues-Martins et al., 2007b). In unprecedented detail, recent structural studies have shown that SAS-6 can self-assemble into ring-shaped oligomers *in vitro* that resemble cartwheel structures *in vivo* (Guichard et al., 2013; Kitagawa et al., 2011b; van Breugel et al., 2014; 2011). In contrast, *C. elegans* SAS-6 assembles into a spiral arrangement, which might explain the formation of a central tube (instead of a cartwheel) in this species (Hilbert et al., 2013). In summary, SAS-6 seems to be a universal component of the scaffold that precedes centriole formation (Figure 9).

Another well conserved component of the centriole duplication machinery is SAS-4 (Dammermann et al., 2008; Kirkham et al., 2003), which in vertebrates is known as CPAP (or CENP-J) (Hung et al., 2000). Several studies have implicated

CPAP in positive regulation of centriole length, as CPAP overexpression results in overly long centrioles (Kohlmaier et al., 2009; Schmidt et al., 2009; Tang et al., 2009). In addition, two recent studies have uncovered a cooperation between Cep120, SPICE1 and CPAP in centriole elongation (Comartin et al., 2013; Lin et al., 2013a). Therefore, the function of *C. elegans* SAS-4, which is the organization of centriolar MTs around the central tube, seems to be conserved in mammals. In *Drosophila*, SAS-4 has furthermore been implicated in tethering of PCM complexes to the centrosome (Gopalakrishnan et al., 2012; 2011; Zheng et al., 2014).

Although they are related on an amino acid sequence level, some duplication factors changed functions in some organisms. This is the case for SPD-2, which in *C. elegans* is required for centriole duplication and PCM maturation (Kemp et al., 2004; Pelletier et al., 2004), but in *Drosophila* only the function in PCM recruitment has been conserved (Dix and Raff, 2007; Giansanti et al., 2008). However, the SPD-2 homolog in vertebrates, called Cep192, has been implicated in both centrosome maturation (Gomez-Ferreria et al., 2007; Joukov et al., 2010; Zhu et al., 2008) and centriole duplication (Kim et al., 2013; Sonnen et al., 2013; Zhu et al., 2008).

On the other extreme, the kinase ZYG-1 is not well conserved at the amino acid sequence level (O'Connell et al., 2001), but this kinase has been functionally replaced in *Drosophila* (Bettencourt-Dias et al., 2005) and human cells (Habedanck et al., 2005) by Plk4 (SAK), a member of the family of polo-like kinases (Plks). Intriguingly, ZYG-1 and Plk4 also seem to share similar mechanisms of regulation, as both kinases are targeted for proteasomal degradation by the SCF β TrCP (Slimb in *Drosophila*; LIN-23 in *C. elegans*) (Cunha-Ferreira et al., 2009; Guderian et al., 2010; Holland et al., 2012; 2010; Peel et al., 2012; Rogers et al., 2009).

Poorly conserved is also the duplication factor SAS-5. This protein has not been assigned any homologs outside of nematodes, because obvious candidates were lacking. A recent study then suggested that Ana2, which is required for centriole duplication in *Drosophila*, might be the SAS-5 homolog in flies (Stevens et al., 2010a). Based on sequence alignments, the same study suggested that a protein called STIL might be the long-sought-after SAS-5 homolog in vertebrates (Stevens et al., 2010a) (see also chapter 2.8). Similar to SAS-5, which cooperates with SAS-6 in central tube formation (Pelletier et al., 2006), both Ana2 and STIL were therefore predicted to participate in cartwheel assembly. In line with these predictions, Ana2

localizes specifically to daughter centrioles (Stevens et al., 2010a) and co-expression of Ana2 and DSAS-6 resulted in assembly of extended tubules that bear striking resemblance to the inner cartwheel structure (Stevens et al., 2010b). However, sequence conservation between Ana2/SAS-5 and vertebrate STIL is very low and restricted to a small sequence stretch named STAN (STIL/Ana2) motif, leaving doubts as to whether these functions were truly conserved. Therefore, it was important to characterize STIL in regard to centriole biogenesis in human cells (see results and discussion sections).

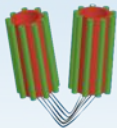
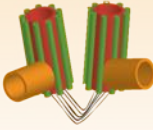
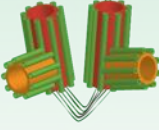
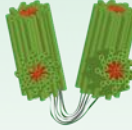
	<i>C. elegans</i>	<i>D. melanogaster</i>	<i>H. sapiens</i>
Initiation	 <p>SPD-2 ZYG-1</p>	 <p>DSpd-2* Asterless Pik4 (SAK)</p>	 <p>Cep192+ Cep152 Cep63 Pik4 (SAK)</p>
Assembly	 <p>SAS-5 SAS-6</p>	 <p>Ana2 DSAS-6 DBld10*</p>	 <p>STIL (?) HsSAS-6 Cep135 γ-Tubulin (?)</p>
Elongation	 <p>SAS-4</p>	 <p>DSAS-4 POC5 Centrobin* DCP110* Ana1</p>	 <p>CPAP Cep120 SPICE Centrins+ hPOC1 hPOC5 Centrobin CP110 CEP97 CEP67</p>

Figure 8 : A Comprehensive List of Centriole Duplication Factors. Proteins that play essential roles in centriole duplication in *C. elegans*, *D. melanogaster* and *H. sapiens* are listed. Duplication factors that are conserved in all three organisms are marked in red. Additional duplication factors in *D. melanogaster* or *H. sapiens* are marked in blue. Proteins marked with * are not required for centriole duplication in all species, whereas for proteins marked with +, controversial data were reported. For more information on the role of individual duplication factors, see text.

2.6.3 Additional Centriole Duplication Factors in *Drosophila*, Human Cells and Other Organisms

Besides the five duplication factors described in *C. elegans*, additional proteins required for centriole formation have been identified by genomic screens in human cells (Balestra et al., 2013; Kleylein-Sohn et al., 2007) or *Drosophila* (Dobbelaere et al., 2008; Goshima et al., 2007) (Figure 8). Also, large proteomic studies have been performed to identify novel centrosome (Andersen et al., 2003; Jakobsen et al., 2011) or basal body components (Keller et al., 2009; 2005; Kilburn et al., 2007), some of which were also shown to be essential for centriole formation.

Not conserved in *C. elegans*, but crucial for centriole biogenesis in other organisms, is for example the protein Cep135. Its homolog Bld10p in the green algae *Chlamydomonas reinhardtii* has long been implicated in cartwheel formation (Hiraki et al., 2007; Matsuura et al., 2004). Bld10p localizes to the cartwheel tip region (also called pinheads), where it connects the cartwheel spokes to centriolar MTs. Similar conclusions have been reached for Bld10p in *Paramecium tetraurelia*, a ciliate (Jerka-Dziadosz et al., 2010). In agreement with this work from lower eukaryotes, Cep135 is required for centriole duplication in mammalian cells (Kleylein-Sohn et al., 2007; Ohta et al., 2002), where it binds to HsSAS-6 and CPAP (Lin et al., 2013b). However, despite the central role Cep135/Bld10 plays in centriole formation, Bld10 in *Drosophila* seems to be dispensable for cartwheel assembly and hence centriole duplication (Carvalho-Santos et al., 2012; Mottier-Pavie and Megraw, 2009; Roque et al., 2012).

Similarly, it has been suggested that γ -tubulin might function in early steps of centriole formation by providing a template for the outgrowth of centriolar MT triplets (Fuller et al., 1995). Indeed, γ -tubulin like structures capping the proximal part of A-MTs were detected when analyzing purified human centrioles by cryo-electron tomography (Guichard et al., 2010).

Another module for centriole duplication that has been subject to large evolutionary changes concerns the upstream factors that recruit the kinase, ZYG-1 in *C. elegans* or Plk4 in other systems, to the site where a new centriole starts to grow. In *C. elegans*, ZYG-1 is recruited via SPD-2 (Delattre et al., 2006; Pelletier et al.,

2006). In *Drosophila* and *H. sapiens*, however, an additional duplication factor, called Cep152 (asterless in *Drosophila*), plays an important role in recruitment of Plk4 (Cizmecioglu et al., 2010; Dzhindzhev et al., 2010; Hatch et al., 2010). In human cells, it has been shown that Cep152 functions in cooperation with the vertebrate SPD-2 homolog, called Cep192 (Kim et al., 2013; Sonnen et al., 2013) and a protein called Cep63 (Brown et al., 2013; Sir et al., 2011), in recruitment of Plk4. However, whether Cep192 is required for centriole duplication or not remains controversial (Gomez-Ferreria et al., 2007; Zhu et al., 2008).

Centrins are a family of core centriolar proteins that have also been implicated in centriole duplication. The homolog of Centrin-2 in yeast (*cdc31p*) is clearly required for SPB duplication (Schiebel and Bornens, 1995), and centrin homologs in ciliates play essential roles in basal body formation (Ruiz et al., 2005; Stemm-Wolf et al., 2005). However, whether centrin-2 is required for centriole formation in vertebrates (Salisbury et al., 2002), probably in cooperation with Sfi1 (Kilmartin, 2003) and hPOC5 (Azimzadeh et al., 2009), is controversial (Kleylein-Sohn et al., 2007). In fact, genetic deletion of centrins from chicken DT40 cells demonstrates that normal centrosomes can form in the absence of all centrins, at least in this vertebrate species and cell type (Dantas et al., 2011).

Centrobin is a daughter centriole specific protein that has been attributed a function in centriole duplication and centriole elongation in human cells (Gudi et al., 2011; Zou et al., 2005). In *Drosophila*, its function in centriole duplication seems not to be conserved (Januschke et al., 2013). However, it has adopted an important role in control of asymmetric centrosome distribution during neuroprogenitor cell divisions. In short, neuroprogenitor cells divide in asymmetric fashion, giving rise to one daughter cell with stem cell character and one cell that will differentiate into a neuron. Interestingly, the stem cell always retains the daughter centrosome (Januschke et al., 2011), a process which requires centrobin at the daughter centrosome, relies on Plk1-mediated centrosome maturation (Januschke et al., 2013) and is counteracted by pericentrin-like protein (PLP) at the mother centrosome (Lerit and Rusan, 2013).

Finally, the tip of centrioles in vertebrates and flies is decorated by a protein called CP110. In vertebrates, this protein has been implicated in the control of centriole duplication (probably in cooperation with Cep67) (Chen et al., 2002; Kleylein-Sohn et al., 2007; Tsang et al., 2009), centriole elongation (Schmidt et al.,

2009) and the inhibition of cilia formation (Schmidt et al., 2009; Spektor et al., 2006; Tsang et al., 2008). In contrast to CPAP, which regulates centriole length in a positive manner (Comartin et al., 2013; Kohlmaier et al., 2009; Lin et al., 2013a; Schmidt et al., 2009; Tang et al., 2009), CP110 seems to restrict the length of newly formed centrioles. Therefore, removal of CP110 from cells leads to overly long centrioles (Schmidt et al., 2009). In line with a repressive function in centriole elongation, CP110, probably in cooperation with Cep97, Cep290, Kif24 and Talpid3, has an inhibitory effect on primary cilium formation (Spektor et al., 2006; Tsang et al., 2008), which requires basal bodies to grow out MTs in order to form an axoneme. Conversely, in *Drosophila*, removal of CP110 does not abrogate centriole duplication, but also influences centriole length control (Delgehyr et al., 2012; Franz et al., 2013). Similar to CP110, a role in centriole duplication, centriole elongation and ciliogenesis has been identified for Poc1 in diverse organisms (Blachon et al., 2009; Fourrage et al., 2010; Keller et al., 2009; Pearson et al., 2009; Venoux et al., 2013).

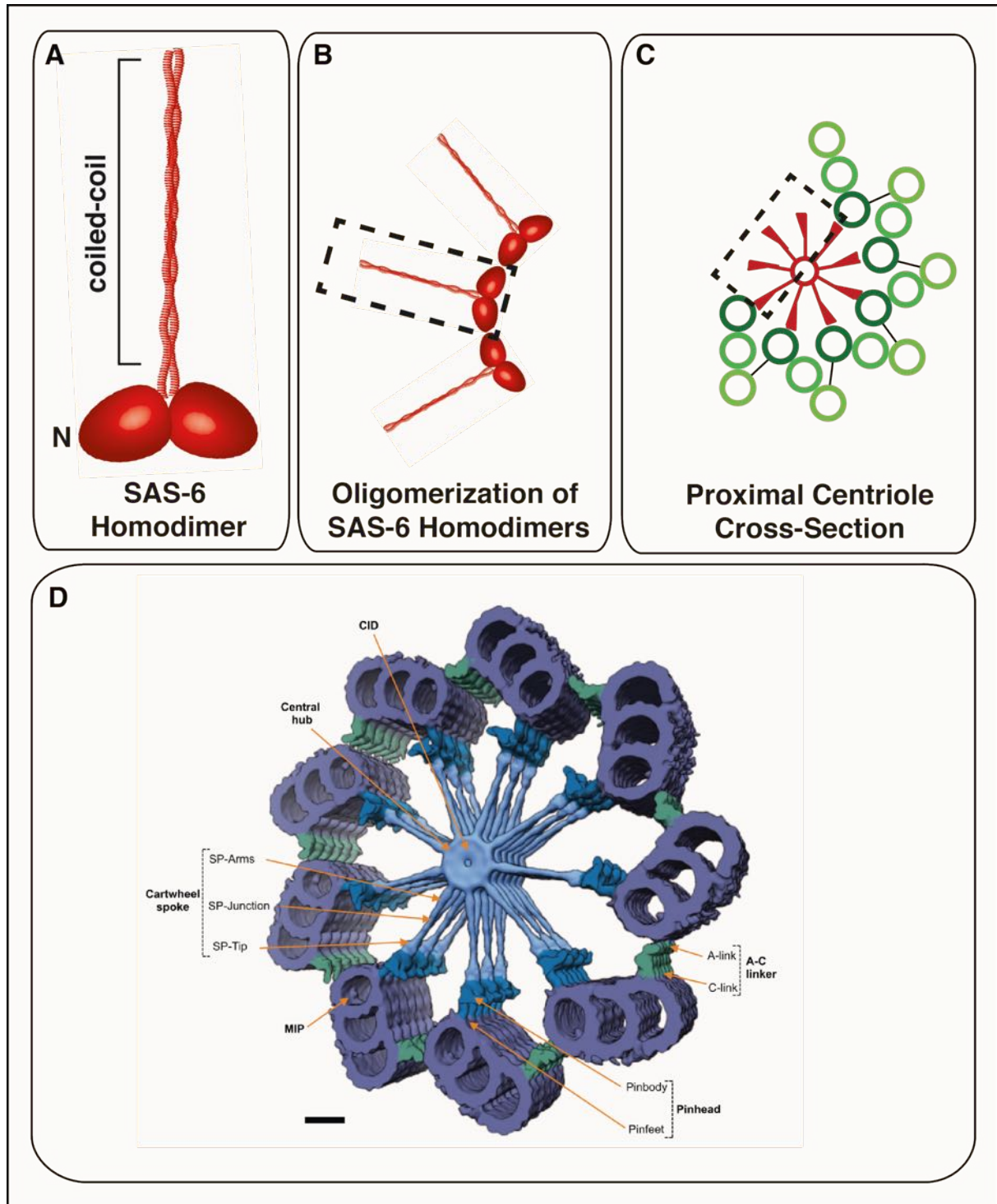


Figure 9 : SAS-6 Oligomerization Dictates the 9-fold Symmetry of Centrioles (A) SAS-6 forms homodimers through dimerization of its C-terminal coiled-coil domain. The N-terminus of SAS-6 adopts a globular fold (N). (B) SAS-6 homodimers interact through their N-terminal globular domains and form the cartwheel central hub, while their coiled-coil domains project outwards to form the spokes. (C) Cross-section through the mammalian procentriole proximal region. The cartwheel, which is formed by nine SAS-6 homodimers, is depicted in red, centriolar MTs are shown in green. (D) Cryo-electron tomography 3D map of the proximal centriole region from *Trichonympha*. The cartwheel is colored in light blue, the pinheads that connect to the centriolar MT triplets (purple) are shown in dark blue. The A-C linkers that connect the A and C MTs are colored in green. Scale bar represents 20 nm. Part D of this figure has been adapted from (Guichard et al., 2013).

2.6.4 Regulation of Centriole Duplication

2.6.4.1 Two Modes of Centriole Duplication

Two main pathways exist to build a new centriole, canonical centriole duplication and *de novo* centriole formation. Whereas canonical centriole duplication relies on a preexisting centriole (probably providing a structural platform) to form a new centriole, *de novo* centriole duplication can take place in the absence of any centrioles.

Overexpression of certain centriole duplication factors can trigger centriole *de novo* formation in unfertilized *Drosophila* eggs (Peel et al., 2007; Rodrigues-Martins et al., 2007a). *De novo* centriole formation can also be observed in vertebrate cycling cells, but only if pre-existing centrioles were experimentally removed (Khodjakov et al., 2002; Rodrigues-Martins et al., 2007a). This suggests that the presence of centrioles in cells somehow inhibits *de novo* centriole formation under normal conditions, but how this is achieved remains unknown.

In specialized cell types and under certain developmental contexts, *de novo* centriole formation can occur on a natural basis. For example, *de novo* centriole formation can be observed in early mouse development. The mouse sperm does not, as is common in many other organisms, contribute a centriole to form a centrosome in the emerging zygote. Centrioles and centrosomes therefore arise at later developmental stages *de novo* (Szollosi et al., 1972). A similar phenomenon can also be observed in terminally differentiated, multiciliated epithelial cells. These cells assemble hundreds of motile cilia at their plasma membrane and therefore have to undergo massive centriole amplification *de novo*, as canonical centriole duplication might not be efficient enough to meet such high demands. This involves a structure called deuterosome, an amorphous proteinaceous structure at which centrioles assemble (Song et al., 2008).

Although disparate, the two modes of centriole duplication basically use the same proteins to form centrioles, and therefore represent variations of the same mechanism, rather than distinct pathways. So far, a difference that has been clearly revealed concerns the upstream duplication factors called Cep63 and Deup1. Whereas Cep63 is used in canonical centriole biogenesis to recruit Cep152 and Plk4

to mother centrioles, deuterosomes are decorated with Deup1, a Cep63 paralog, which recruits the same duplication factors for *de novo* centriole formation (Zhao et al., 2013). In addition, a protein named CCDC78 has been identified to be essential for centriole amplification in multiciliated cells (Klos Dehring et al., 2013).

2.6.4.2 Cell Cycle Cues that Regulate Centriole Duplication

Much has been learned about the structural components that are directly involved into the assembly of centrioles (see chapter 2.6.1-2.6.3). Surprisingly little is known, however, about the extrinsic cell cycle cues that control when and where a centriole starts to grow, and how cells coordinate centriole duplication with other prominent cell cycle events, such as DNA replication. A key factor in the temporal regulation of centriole duplication is the kinase Cdk2 in conjunction with either cyclins E or A, as has been demonstrated in *Xenopus* (Hinchcliffe et al., 1999; Lacey et al., 1999) and somatic mammalian cells (Matsumoto et al., 1999; Meraldi et al., 1999). In addition, E2F transcription factors have also been associated with timely initiation of centriole duplication (Meraldi et al., 1999). Both Cdk2 and E2F are also involved in initiation of DNA replication and thus might elegantly coordinate centrosome duplication with DNA replication.

Centrosomal substrates of Cdk2 might be CP110 (Chen et al., 2002) or nucleophosmin (Okuda et al., 2000), both playing distinct roles in centriole duplication. Other kinases, that are potentially involved in centriole duplication include MPS1 (Fisk and Winey, 2001), Plk1 (Liu and Erikson, 2002) and Plk2 (Chang et al., 2010; Cizmecioglu et al., 2012; Warnke et al., 2004).

2.6.4.3. Regulation of Centriole Numbers by Proteasomal Degradation

Precise regulation of centriole duplication ensures genome stability, as extra centrioles are likely to trigger multipolar spindle formation which brings along chromosome missegregation and aneuploidy. Centriole duplication therefore is a tightly regulated process and several mechanisms exist to restrict centriole numbers in proliferating cells. One important aspect in the control of centriole numbers is the utilization of proteasomal degradation to keep levels of individual centriole duplication factors, many of which cause massive centriole amplification, at low levels.

For example, Plk4 harbors a DSG motif that is required for its degradation by the multi-protein E3 ubiquitin ligase complex SCF β TrCP. Interestingly, Plk4 kinase activity is required for its own degradation, as the protein, which exists as a dimer, autophosphorylates itself *in trans* and thereby primes its own degradation (Cunha-Ferreira et al., 2009; 2013; Guderian et al., 2010; Holland et al., 2010; Klebba et al., 2013; Rogers et al., 2009). This mechanism prevents Plk4 activity to rise above a certain threshold level which could trigger the formation of more than one procentriole per pre-existing centriole. Nevertheless, Plk4 activity rises towards mitosis and this might be accomplished by phosphatase activities, as shown in *Drosophila*, where the protein phosphatase PP2A counteracts Plk4 autophosphorylation at this cell cycle stage (Brownlee et al., 2011). Furthermore, one study has linked Plk4 to control of HsSAS-6 proteasomal degradation. HsSAS-6 is a target of the SCF FBXW5, an E3 ubiquitin ligase which is inhibited by Plk4 phosphorylation. Plk4 might therefore, via inhibition of SCF FBXW5, stabilize HsSAS-6 levels at the G1/S phase transition (Puklowski et al., 2011).

In addition, both SAS-6 and CPAP have been implicated in APC/C-mediated degradation (Strnad et al., 2007; Tang et al., 2009). Complete degradation of SAS-6 and CPAP might serve to reset components of the centriole duplication machinery at the onset of each new cell cycle transition. Furthermore, the levels of the duplication factor CP110 are also subject to proteasomal degradation. CP110 is controlled by the SCF CyclinF (D'Angiolella et al., 2010), which is antagonized by USP33, an enzyme that specifically deubiquitinates and protects CP110 from degradation (Li et al., 2013).

2.7 Centrosomes in Brain Disease and Primordial Dwarfism

Improvements in DNA sequencing methods have led to the rapid identification of genes that are associated with rare genetic disorders. Of special interest in regard to centrosomes is a disease called autosomal recessive primary microcephaly (MCPH). Out of 12 gene products that have been associated with MCPH, 9 are localizing to centrosomes (see table 1) (Kaindl et al., 2010; Pagon et al., 1993; Thornton and Woods, 2009). MCPH is a neurodevelopmental disorder that interferes with human fetal brain growth. This results in smaller than usual brains at birth and mental retardation, but the brain architecture is normal. The disease is caused by a deficit in neuron production. In developing brains, neurons are generated by asymmetric divisions of the neuroprogenitor pool. The progenitors first expand by symmetric divisions, which require the mitotic spindle to be oriented in parallel to the ventricular surfaces. Upon rotation of the mitotic spindle axis, which goes along with a switch to asymmetric divisions, each cell produces a progenitor and a neuron (Lehtinen and Walsh, 2011). A reduction of the neuroprogenitor pool is underlying the development of MCPH, which can arise due to either defects in spindle rotation (Noatynska et al., 2012) or via apoptosis (Komada et al., 2010).

Another condition that is associated with mutations in centrosomal proteins is primordial dwarfism (PD). These patients suffer from varying degrees of proportionately short stature and symptoms can clinically overlap with MCPH, which is especially the case for Seckel syndrome patients (see table 1, MCPH-Seckel combination) (Verloes et al., 2013). Other subtypes of PD encompass Meier Gorlin syndrome, microcephalic osteodysplastic primordial dwarfism type I and II (MOPDI /II) or Russell Silver syndrome (reviewed in Klingseisen and Jackson, 2011).

However, how exactly centrosomal defects cause spindle misorientation, apoptosis or other cellular damage that results in MCPH or PD is not yet fully established. Some proteins, such as Cdk5rap2 (Barr et al., 2010; Choi et al., 2010; Fong et al., 2008; Haren et al., 2009; Lucas and Raff, 2007), pericentrin (Dictenberg et al., 1998; Doxsey et al., 1994) and ninein (Delgehyr et al., 2005; Mogensen et al., 2000) have been implicated in PCM organization and MT nucleation. Such defects might well interfere with either spindle orientation or chromosome segregation. Chromosome segregation defects might also be caused by mutations in CASC5, a kinetochore protein (Genin et al., 2012). Cdk5rap2 has furthermore been implicated

in centriole cohesion (Barr et al., 2010; Barrera et al., 2010; Graser et al., 2007) and engagement (Barrera et al., 2010), and failure in these processes are likely to result in aberrant spindle formation. Other proteins, such as ASPM and WDR62, might also be directly involved in spindle orientation (Bogoyevitch et al., 2012; Farag et al., 2013; Fish et al., 2006; Higgins et al., 2010; van der Voet et al., 2009). Interestingly, a considerable fraction of these disease-associated proteins are key centriole duplication factors, such as STIL, Cep135, CPAP, Cep152 or Cep63 (Arquint et al., 2012; Blachon et al., 2008; Brown et al., 2013; Ching et al., 2002; Cizmecioglu et al., 2010; Hatch et al., 2010; Kleylein-Sohn et al., 2007; Kohlmaier et al., 2009; Schmidt et al., 2009; Sir et al., 2011; Tang et al., 2009; 2011; Vulprecht et al., 2012). Mutations might therefore either result in less efficient centriole duplication or trigger centriole overduplication. Both scenarios could interfere with proper spindle formation/orientation (Ganem et al., 2009; Kitagawa et al., 2011a) and cell cycle progression (Arquint et al., 2014; Doxsey et al., 2005b). A recent study has analyzed the effect of centrosome amplification on brain development in the mouse and concluded that centrosome amplification is sufficient to trigger a phenotype resembling microcephaly (Marthiens et al., 2013). Even though defects in spindle orientation have not been observed, it has been suggested that increased apoptosis of neuroprogenitors might be the underlying cause (Marthiens et al., 2013).

Also, some proteins, such as Cdk6 or microcephalin, might directly control cell cycle progression (Alderton et al., 2006; Gruber et al., 2011; Morgan, 1997; Tibelius et al., 2009). Furthermore, many of the involved gene products have functions in DNA-related processes, such as DNA damage responses (microcephalin, Cdk5rap2, ATR, ATRIP) (Alderton et al., 2006; Barr et al., 2010; Nam and Cortez, 2011), DNA repair (RBBP8) (Limbo et al., 2007), epigenetic modifications (ZNF335, PHC1) (Isono et al., 2005; Mahajan et al., 2002), initiation of DNA replication (ORC1, ORC4, ORC6, CDT1, CDC6) (Stillman, 2005) or RNA splicing (RNU4ATAC) (Schneider et al., 2002).

In summary, mutations in centrosomal proteins or proteins that have DNA damage and repair functions are interfering with human brain development and/or body growth. The underlying defects most likely lead to errors in cell cycle progression, mitotic spindle orientation or they might trigger apoptosis of neuroprogenitors.

MCPH			
Genetic Locus	Protein name	Localization	Function
MCPH1	Microcephalin	Centrosome	DNA damage response, Control of mitotic entry
MCPH2	WDR62	Centrosome	JNK signaling, Spindle formation
MCPH3	CDK5RAP2 or Cep215	Centrosome	PCM organization, Centriole cohesion/engagement, DNA repair
MCPH4	CASC5 or KNL-1	Kinetochores	MT attachment to kinetochores, SAC function
MCPH5	ASPM	Centrosome	Spindle orientation
MCPH7	STIL	Centrosome	Centriole duplication factor
MCPH8	CEP135	Centrosome	Centriole duplication factor
MCPH10	ZNF335	Nucleus	Component of a chromatin remodeling complex
MCPH12	Cdk6	Centrosome?	Control of G1/S phase transition
MCPH-Seckel combination			
MCPH11	PHC1	Nucleus	Polycomb group protein (epigenetic modification of DNA)
MCPH6/SCKL4	SAS-4 (CENPJ)	Centrosome	Centriole duplication factor
MCPH9/SCKL5	Cep152	Centrosome	Centriole duplication factor
SCKL2	RBBP8	Nucleus	DNA repair (Endonuclease)
SCKL6	Cep63	Centrosome	Centriole duplication factor
Seckel Syndrome			
SCKL1	ATR	Nucleus	DNA damage response
SCKL7	Ninein	Centrosome	Subdistal appendage protein, MT nucleation at centrioles
SCKL8	ATRIP	Nucleus	DNA damage response
Meier Gorlin Syndrome			
MGS1	ORC1	Nucleus	Initiation of DNA replication
MGS2	ORC4	Nucleus	Initiation of DNA replication
MGS3	ORC6	Nucleus	Initiation of DNA replication
MGS4	CDT1	Nucleus	Initiation of DNA replication
MGS5	CDC6	Nucleus	Initiation of DNA replication
Microcephalic Osteodysplastic Primordial Dwarfism, Type I			
MOPD I	RNU4ATAC	Nucleus	snRNA, part of spliceosome
Microcephalic Osteodysplastic Primordial Dwarfism, Type II			
MOPDII	Pericentrin	Centrosome	PCM protein, MT nucleation at centrosomes

Table 1: Gene Products Implicated in MCPH or PD. List of proteins associated with autosomal recessive primary microcephaly (MCPH), primordial dwarfism (Seckel Syndrome, Meier Gorlin Syndrome, MOPDI/II) or both diseases (MCPH-Seckel combination). Protein names, their subcellular localization and protein functions are listed. Green background color indicates localization of respective proteins to centrosomes/spindle poles, blue background color was used for nuclear localization and orange background color indicates localization to kinetochores. RNU4ATAC is not a protein but an snRNA. For more information, see text. Table was partially adapted from (Verloes et al., 2013).

2.8 STIL – a Centriole Duplication Factor in Human Cells?

The *STIL* (SCL/TAL1 interrupting locus, also called *SIL*) gene has first been identified due to its involvement in a common chromosomal rearrangement that leads to T-cell acute lymphoblastic leukemia, by alteration of *SCL* (*Tal1*) transcriptional regulation (Aplan et al., 1991; 1990; Carlotti et al., 2002). *STIL* codes for a large cytosolic protein of 1287 amino acids (Aplan et al., 1991; Izraeli et al., 1997). Its expression in proliferating cells has been shown to depend on E2F transcription factors (Erez et al., 2008), which trigger the expression of cell cycle regulators that bring about the G1/S phase transition. This protein has initially been characterized as a mitotic regulator required for mitotic entry (Erez et al., 2007) and *STIL* has furthermore been proposed to cooperate with Pin1, a peptidyl-prolyl cis-trans isomerase, in regulation of the duration of mitotic checkpoint signaling (Campaner et al., 2005). *STIL* has also been implicated in carcinogenesis as its overexpression in multiple cancers, such as melanoma or lung cancer (Erez et al., 2004), correlates with increased metastatic potential (Ramaswamy et al., 2003).

Interestingly, *STIL* seems to be strictly required for vertebrate development, as *STIL* disruption in both mouse and zebrafish results in early embryonic death (Izraeli et al., 1999; Pfaff et al., 2007). *STIL* (-/-) mouse embryos die after embryonic day 10.5 with defects in axial development and left-right specification, which might arise due to inadequate sonic hedgehog (*shh*) signaling (Izraeli et al., 1999). In line with these findings, a genetic interaction between *STIL* and the *shh* pathway has later on been confirmed (Izraeli et al., 2001), suggesting that *STIL* is strictly required for *shh* signaling.

Similarly, *STIL* loss of function in zebrafish resulted in embryonic death and increased numbers of mitotic cells. The increase in mitotic cells correlated with an increase in monopolar spindles, suggesting that *STIL* might be required for mitotic spindle assembly, which has been confirmed by the observed localization of *STIL* to mitotic spindle poles. Even though a lower number of centrosomes in *STIL* deficient zebrafish cells was described, a function of *STIL* in centriole duplication had not been taken into account at that time.

Finally, mutations in STIL have been associated with MCPH (Kumar et al., 2009), a brain disease which is linked to centrosomal defects. These latter findings are interesting in regard to a proposed function of STIL in centriole biogenesis. Based on sequence alignments, it has recently been suggested that STIL might be related to the *C. elegans* SAS-5 and *Drosophila* Ana2 duplication factors (Stevens et al., 2010a). The observation that *STIL* (-/-) mouse cells lack clear centrosomes strengthens this proposal (Castiel et al., 2011). However, STIL and Ana2/SAS-5 exhibit large size differences (with STIL being roughly three times as large as Ana2 or SAS-5), and sequence similarity is low and restricted to a short, 87 amino acid stretch called STAN motif. This left doubts as to whether these proteins might be true relatives. Therefore, we considered it important to test the role of STIL in centriole biogenesis in human cells (subject of this thesis, see results section). Intriguingly, if confirmed, a function of STIL in centriole duplication could explain previous findings that implicated STIL in the regulation of mitotic progression and shh signaling, as loss of centrioles would be predicted to interfere with both of these processes.

3. AIM OF THIS PROJECT

Here, we have analyzed the role of human STIL in centriole biogenesis. Two reasons prompted us to study whether this protein is implicated in centriole duplication: First, mutations in STIL have been linked to autosomal recessive primary microcephaly (MCPH), a neurodevelopmental disease which is connected to centrosomes, although the precise nature of this link is unknown. Second, and most intriguingly, sequence alignments led to the proposal that STIL might be a distant relative of the *C. elegans* SAS-5 and *Drosophila* Ana2 duplication factors.

After having revealed that human STIL cooperates with Plk4 and HsSAS-6 in centriole formation, we were intrigued by the finding that excess STIL triggers robust centriole amplification, which is a hallmark of many cancer cells. We therefore decided to study the mechanisms that regulate the abundance of STIL throughout the cell cycle. By doing so, we not only uncovered a mechanism that results in complete destruction of STIL, but also found a provocative link to MCPH that might explain why mutations in STIL interfere with human brain development.

4. RESULTS

4.1 Cell-Cycle-Regulated Expression of STIL Controls Centriole Number in Human Cells

Christian Arquint, Katharina F. Sonnen, York-Dieter Stierhof and Erich A. Nigg

Published in Journal of Cell Science

Volume 125

Accepted 24 October 2011

Published 01 March 2012

Cell-cycle-regulated expression of STIL controls centriole number in human cells

Christian Arquint¹, Katharina F. Sonnen¹, York-Dieter Stierhof² and Erich A. Nigg^{1,*}

¹Biozentrum, University of Basel, Klingelbergstr. 50/70, CH-4056 Basel, Switzerland

²Electron Microscopy Unit, Center for Plant Molecular Biology, University of Tübingen, Auf der Morgenstelle 5, 72076 Tübingen, Germany

*Author for correspondence (erich.nigg@unibas.ch)

Accepted 24 October 2011

Journal of Cell Science 125, 1342–1352

© 2012. Published by The Company of Biologists Ltd

doi: 10.1242/jcs.099887

Summary

Control of centriole number is crucial for genome stability and ciliogenesis. Here, we characterize the role of human STIL, a protein that displays distant sequence similarity to the centriole duplication factors Ana2 in *Drosophila* and SAS-5 in *Caenorhabditis elegans*. Using RNA interference, we show that STIL is required for centriole duplication in human cells. Conversely, overexpression of STIL triggers the near-simultaneous formation of multiple daughter centrioles surrounding each mother, which is highly reminiscent of the phenotype produced by overexpression of the polo-like kinase PLK4 or the spindle assembly abnormal protein 6 homolog (SAS-6). We further show, by fluorescence and immunoelectron microscopy, that STIL is recruited to nascent daughter centrioles at the onset of centriole duplication and degraded, in an APC/C^{C^{dc20}-C^{dh1}}-dependent manner, upon passage through mitosis. We did not detect a stable complex between STIL and SAS-6, but the two proteins resemble each other with regard to both localization and cell cycle control of expression. Thus, STIL cooperates with SAS-6 and PLK4 in the control of centriole number and represents a key centriole duplication factor in human cells.

Key words: APC/C, Centrosome, Centriole duplication, Centriole number, Daughter centriole, STIL

Introduction

Vertebrate centrioles are cylindrical structures that are made up of nine triplet microtubules and display an evolutionarily conserved ninefold rotational symmetry (Azimzadeh and Marshall, 2010). Two centrioles, embedded in a meshwork of proteins termed pericentriolar material (PCM), constitute the centrosome, the main microtubule-organizing center (MTOC) of animal cells (Bornens, 2002; Luders and Stearns, 2007). By nucleating and anchoring microtubules, centrosomes influence important cellular properties such as intracellular transport of organelles and vesicles, cell shape, polarity and motility (Doxsey et al., 2005). Centrosomes also promote the formation of a bipolar spindle at the onset of mitosis, thus contributing to the faithful segregation of chromosomes during cell division (Bettencourt-Dias and Glover, 2007; Nigg and Raff, 2009). The second major role of centrioles relates to their ability to function as basal bodies for the formation of cilia and flagella, which in turn play key roles in motility as well as in chemo- and mechanosensation (Goetz and Anderson, 2010). Mutations in genes coding for centrosomal proteins or centriole and basal body components have been linked to brain diseases and ciliopathies (Nigg and Raff, 2009; Bettencourt-Dias et al., 2011). Moreover, numerical and/or structural centrosome aberrations have long been implicated in carcinogenesis (Nigg, 2002; Zyss and Gergely, 2009). Biogenesis and propagation of appropriate numbers of centrioles is crucial for cell function and genome integrity. During the cell cycle, the two centrioles that make up the G1 centrosome need to be duplicated exactly once (Strnad and Gonczy, 2008). Centriole duplication begins at the onset of S phase, when one new centriole (termed procentriole or daughter

centriole) forms at a perpendicular angle next to the proximal end of each pre-existing centriole (termed the parental or mother centriole). Procentriole elongation then continues through G2 phase so that before mitosis each centrosome contains one pair of centrioles. At the onset of mitosis, the duplicated centrosomes separate and contribute to the formation of the bipolar mitotic spindle. Association with the spindle ensures the equal distribution of centrioles to nascent daughter cells. Late in mitosis, the tight connection between mother and daughter centriole is severed in a process termed centriole disengagement, which requires the protease separase as well as the mitotic polo-like kinase PLK1 (Tsou and Stearns, 2006a; Tsou et al., 2009). Furthermore, daughter centrioles acquire the competence to organize PCM during passage through mitosis and this also requires the activity of PLK1 (Wang et al., 2011). Thus, traverse of mitosis sets the stage for a new round of centriole duplication in the ensuing cell cycle (Tsou and Stearns, 2006b).

Pioneering work in the nematode *Caenorhabditis elegans* led to the identification of five proteins, a kinase termed ZYG-1 and four coiled-coil proteins, named SPD-2, SAS-4, SAS-5 and SAS-6, whose recruitment to the preexisting centriole is essential for centriole duplication (Strnad and Gonczy, 2008). The first protein to be recruited to the centriole in *C. elegans* is SPD-2, which in turn is essential for the localization of ZYG-1. Subsequently, the assembly of a complex of SAS-5 and SAS-6 promotes the formation and elongation of a central tube and SAS-4 is thought to assist in the deposition of singlet microtubules onto this tube, resulting in the formation of a new daughter centriole (Pelletier et al., 2006). In other organisms, notably in *Chlamydomonas* and vertebrates, procentriole formation is characterized by the

assembly of a so-called cartwheel structure, which presumably serves as an assembly platform for the outgrowth of the procentriole. Importantly, SAS-6 has recently been identified as a key component of the cartwheel (Nakazawa et al., 2007) and shown to confer ninefold symmetry to this structure (Kitagawa et al., 2011; van Breugel et al., 2011).

Of the centriole duplication factors described above, SPD-2, SAS-4 and SAS-6 show clear evolutionary conservation in other species. Curiously, no obvious homolog of ZYG-1 has been identified outside of nematodes, but polo-like kinase 4 (PLK4; also known as SAK) clearly plays a functionally analogous role in *Drosophila* and vertebrates. *C. elegans* SAS-5 also lacks obvious structural homologs outside of nematodes. Thus, it is of considerable interest that the *Drosophila* protein Ana2 has recently been identified as a potential functional ortholog of SAS-5 (Stevens et al., 2010). Furthermore, database searches led to the suggestion that STIL (SCL/TAL1 interrupting locus), a large cytosolic protein in human cells, could represent a SAS-5 and Ana2 ortholog in vertebrates. In support of this view, all three proteins share sequence similarity within a short, ~90 aa C-terminal domain called the STAN (STIL/Ana2) motif (Stevens et al., 2010). The human *STIL* gene was first identified in the context of a genomic rearrangement that leads to T-cell acute lymphoblastic leukemia (Aplan et al., 1991). In mouse and zebrafish, STIL was shown to be essential for early vertebrate development (Izraeli et al., 1999; Golling et al., 2002; Pfaff et al., 2007). Moreover, STIL expression was reported to be high in lung cancer (Erez et al., 2004) and most interestingly, mutations in STIL were recently shown to cause primary microcephaly (Kumar et al., 2009). Additional studies point to a possible role for STIL in cell proliferation, mitotic regulation and centrosome integrity (Izraeli et al., 1997; Campaner et al., 2005; Erez et al., 2007; Castiel et al., 2011), but the precise function of this protein remains unknown.

Here, we have explored a possible role for STIL in centriole biogenesis in human cells. In view of the close relationship between SAS-6 and SAS-5 in *C. elegans*, we have focused particular attention on a possible functional interaction between STIL and human SAS-6. Our results unequivocally identify human STIL as a key centriole duplication factor that is essential for cell-cycle-regulated centriole formation. Although no stable complex between STIL and SAS-6 could be observed in human cells, we show that the two proteins strongly resemble each other with regard to their localization and cell-cycle-regulated expression. We further show that overexpression of STIL leads to the near-simultaneous formation of multiple daughter centrioles surrounding each mother, a phenotype previously observed for overexpression of both SAS-6 and the kinase PLK4 (Habadanck et al., 2005; Leidel et al., 2005; Strnad et al., 2007). This argues for a tight cooperation between STIL, SAS-6 and PLK4 in centriole biogenesis in human cells.

Results

STIL is required for centriole duplication

To test whether STIL is necessary for centriole duplication in human cells, we depleted the protein from asynchronously growing U2OS cells by RNA interference. Three different siRNA oligonucleotides efficiently depleted STIL after 72 hours of treatment, as confirmed by western blot analysis using a commercial antibody against STIL (Fig. 1A). Centrioles were counted after staining of cells with antibodies against Cep135 and CP110, which mark, respectively, the proximal and distal ends of

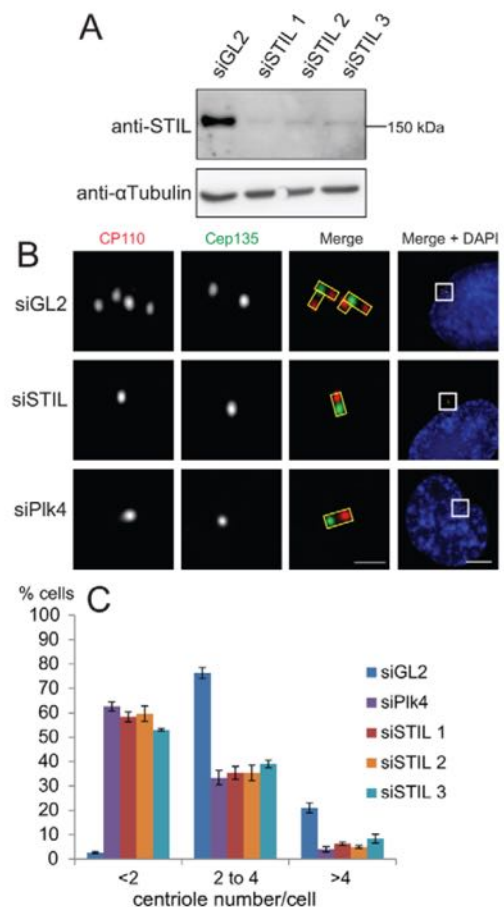


Fig. 1. STIL is required for centriole duplication in U2OS cells.

Asynchronously growing U2OS cells were transfected for 72 hours with control siRNA (GL2), three different *STIL* siRNAs (STIL1–STIL3) or *PLK4* siRNA oligonucleotides. (A) Western blot analysis of STIL protein levels in control (GL2) and STIL-depleted U2OS cell lysates (STIL1–STIL3), using the STIL antibody ab89314 and an antibody against α -tubulin as a loading control. (B) After siRNA treatment, U2OS cells were fixed and stained with antibodies against CP110 (red) and Cep135 (green) for immunofluorescence microscopy. DNA was stained with DAPI (blue). Yellow rectangles illustrate probable orientation of centrioles. (C) Centriole numbers per cell in response to treatment with *GL2*, *STIL* or *PLK4* siRNA, as in B. ($n=3$, 100 cells were analyzed in each experiment, error bars denote s.d.). Scale bars: 1 μ m (magnifications) and 5 μ m (overview; Merge + DAPI).

centrioles (representative images are shown in Fig. 1B). Owing to the proximity of their proximal ends, mother and daughter centrioles are difficult to resolve by anti-Cep135 staining, so that anti-Cep135 antibodies generally produce a two-dot staining pattern throughout interphase, regardless of centriole duplication state. By contrast, the distal ends of mother and daughter centrioles are well separated so that anti-CP110 antibodies usually stain four dots shortly after daughter centrioles begin to form (Kleylein-Sohn et al., 2007). Cells with either two or four CP110-positive dots were regarded as normal, whereas cells harboring only a single centriole or lacking centrioles altogether were considered defective in centriole duplication. The majority of cells treated with control siRNA oligonucleotides (GL2)

contained either two or four centrioles (CP110 dots). By stark contrast, about 60% of STIL-depleted cells possessed fewer than two centrioles (Fig. 1C). A similar reduction in centriole number was observed when PLK4, a key regulator of centriole duplication (Bettencourt-Dias et al., 2005; Habedanck et al., 2005), was depleted. Virtually identical results were also obtained after siRNA treatment of HeLa S3 cells (supplementary material Fig. S1A,B). Concomitant with a reduction of centriole numbers in approximately 90% of STIL-depleted HeLa cells, we also observed a significant increase in abnormal mitotic spindles, as reported previously (Pfaff et al., 2007). About 60% of STIL-depleted mitotic HeLa cells contained monopolar spindles, whereas nearly 30% showed bipolar spindles with one acentriolar pole (supplementary material Fig. S1C).

Taken together, these data strongly support the notion that STIL is required for centriole duplication.

STIL localizes to the proximal end of daughter centrioles

Because the antibody used above did not detect endogenous STIL by immunofluorescence microscopy, we generated a polyclonal antibody targeting the C-terminus of STIL (amino acids 938–1287, supplementary material Fig. S2A). In western blots, this antibody (termed ca66) readily recognized FLAG-tagged STIL ectopically expressed in HEK293T cells, but endogenous protein was undetectable (supplementary material Fig. S2B). By immunofluorescence microscopy, ca66 clearly stained the centrosome and this staining was lost upon siRNA-mediated depletion of STIL, confirming antibody specificity

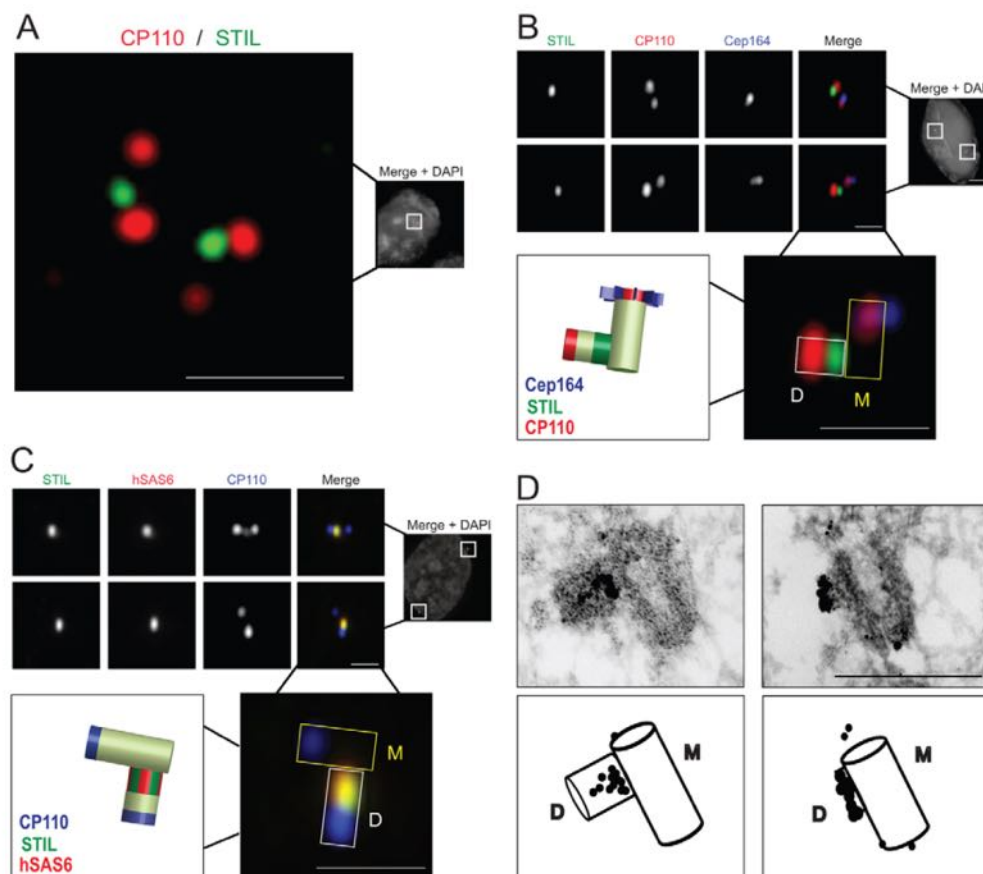


Fig. 2. STIL specifically localizes to the proximal end of daughter centrioles. (A) U2OS cells fixed and stained with antibodies against STIL (ca66, green) and CP110 (red); DNA (DAPI) is shown in gray. (B) STIL localizes closer to Cep164-negative centrioles. U2OS cells fixed and stained with antibodies against STIL (ca66, green), CP110 (red) and Cep164 (blue); DNA (DAPI) is shown in gray. The presumed orientation of the Cep164-positive mother centriole (M) is depicted with a white rectangle, the orientation of the respective Cep164-negative daughter centriole (D) with a white rectangle. The scheme to the left illustrates the relative localization of STIL (green), CP110 (red) and Cep164 (blue) within this centriole pair. (C) STIL colocalizes with SAS-6. U2OS cells were fixed and stained with antibodies against STIL (ca66, green), SAS-6 (red) and CP110 (blue); DNA (DAPI) is shown in gray. The presumed orientation of the SAS-6-negative mother centriole (M) is depicted with a yellow rectangle, the orientation of the respective SAS-6-positive daughter centriole (D) with a white rectangle. The scheme to the left illustrates the relative localization of STIL (green), SAS-6 (red) and CP110 (blue) within this centriole pair. (D) As shown by immunoelectron microscopy STIL localizes close to the interphase between mother and daughter centrioles (top row). U2OS cells were fixed and incubated with antibodies against STIL (ca66), followed by gold-labeled secondary antibodies. Schematic representations (bottom row) illustrate the orientation of mother (M) and daughter (D) centrioles; the localization of gold particles is denoted by black dots. Scale bars: 5 μ m (A–C, Merge + DAPI) and 1 μ m (A–C, all higher magnifications), 0.5 μ m (D).

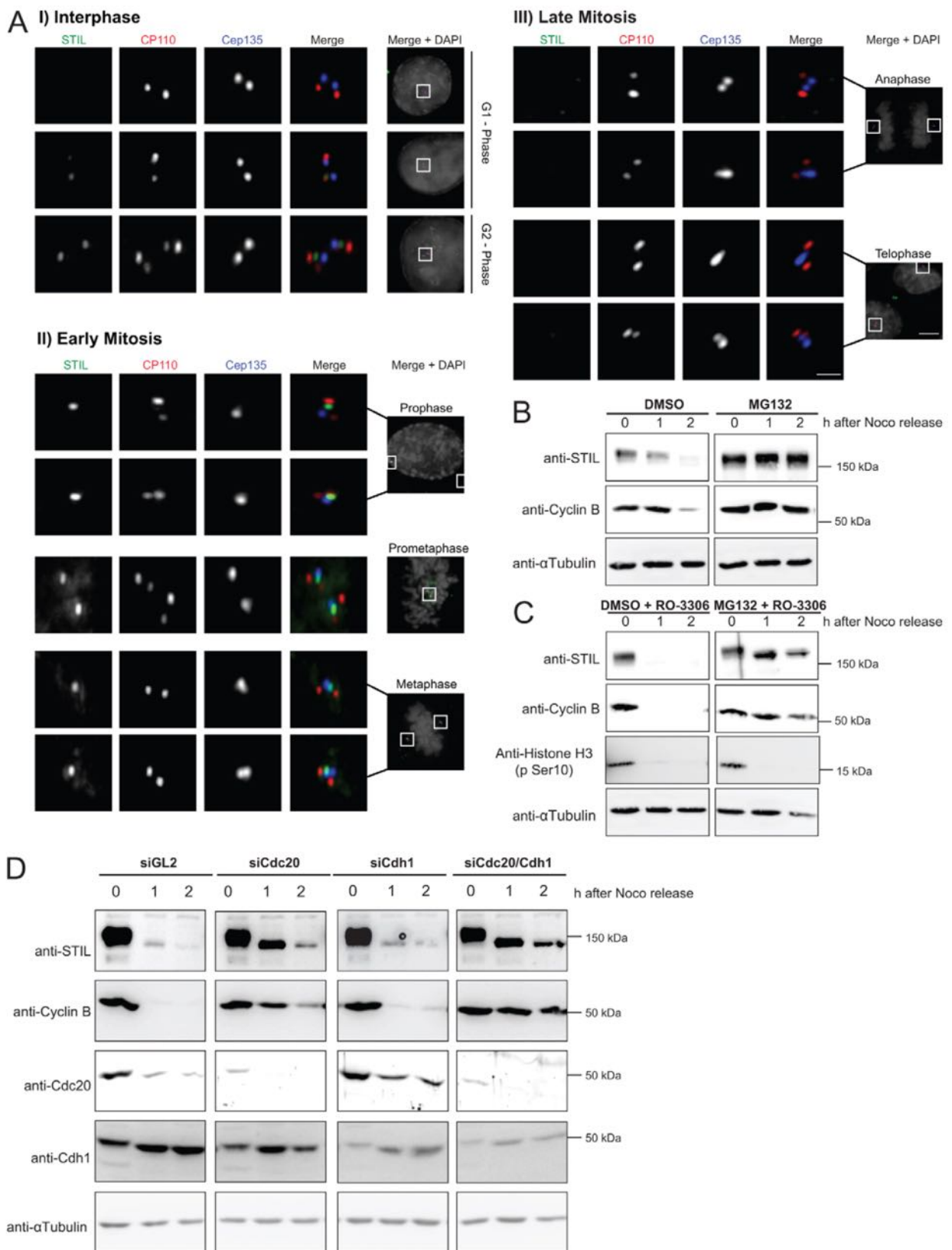


Fig. 3. See next page for legend.

(supplementary material Fig. S2C). Ca66 was then used to determine the precise subcellular localization of STIL by immunofluorescence microscopy. When co-staining S, G2 or early mitotic cells with antibodies against STIL and CP110, STIL was consistently detected as a single dot at each centriole pair (marked by two CP110 dots) (Fig. 2A). To distinguish between mother and daughter centrioles within each pair, co-staining was performed using antibodies against Cep164, a distal appendage protein that marks mature mother centrioles (Graser et al., 2007). Invariably, STIL was found closer to the Cep164-negative CP110 dot, implying that it associates with the daughter centriole (Fig. 2B). This conclusion was further strengthened by the observation that STIL colocalized with SAS-6 (Fig. 2C), an evolutionarily conserved component of the cartwheel structure that assembles transiently at the proximal end of newly forming daughter centrioles (Leidel et al., 2005; Kleylein-Sohn et al., 2007; Strnad et al., 2007; Kitagawa et al., 2011; van Breugel et al., 2011). Finally, the association of STIL with newly forming daughter centrioles could also be demonstrated by immunoelectron microscopy (Fig. 2D). Taken together, these data indicate that STIL localizes specifically to the proximal part of daughter centrioles, where it colocalizes with the centriole duplication factor SAS-6.

Association of STIL with centrioles is regulated during the cell cycle

To study the association of STIL with centrioles throughout the cell cycle, we stained asynchronously growing U2OS cells with antibodies against STIL, CP110 and Cep135. Cep135 served as a marker for centrioles and CP110 was used to time the emergence of newly forming centrioles during S phase (Chen et al., 2002; Kleylein-Sohn et al., 2007). In parallel, DNA was stained with DAPI to distinguish between interphase and mitotic cells and to identify different mitotic stages. Of the G1 cells, characterized by the presence of only two centrioles, some lacked detectable STIL, whereas others were clearly positive for STIL, even though no CP110-positive daughter centrioles could yet be seen (Fig. 3A). This strongly suggests that STIL associates with nascent daughter centrioles at a very early stage of centriole duplication, in excellent agreement with our immunoelectron microscopy data (Fig. 2D, right panel). To analyze the timing of STIL recruitment

more precisely, nocodazole-arrested U2OS cells were released into G1 phase and both the abundance and localization of STIL were monitored at different time points (supplementary material Fig. S3). Western blot analysis revealed that STIL protein levels were low in early G1 phase (4 hours after release) and progressively augmented towards the G1–S transition (8–12 hours after release; marked by the appearance of the CDK2 activator cyclin E1) (supplementary material Fig. S3A). As shown by immunofluorescence microscopy, the vast majority of cells lacked STIL at their two (unduplicated) centrioles 4 hours after the nocodazole release; however, by 8 hours after release, STIL was present at centrioles in all cells showing duplicated centrioles (four CP110 dots) and also in half of those that showed only two CP110 dots (unduplicated centrioles) (supplementary material Fig. S3B). This indicates that STIL is recruited to daughter centrioles before these can be resolved by CP110 staining. Finally, by 12 hours after release, most cells had undergone centriole duplication and about 90% of all cells showed STIL-positive centrioles (supplementary material Fig. S3B,C). Thus, whenever a cell contained duplicated centrioles, STIL was invariably present, confirming that STIL is recruited very early during the formation of new centrioles.

After the G1–S transition, centriolar STIL staining gradually increased as cells approached mitosis, so that maximal staining was seen at the poles of pro- and prometaphase cells (Fig. 3A). However, at around the time of the metaphase-to-anaphase transition, STIL staining began to decline and was completely abolished in late anaphase and telophase cells, suggesting that STIL either gets displaced from centrosomes or degraded during exit from mitosis. To distinguish between these possibilities, we analyzed STIL protein levels in U2OS cells released from a nocodazole-induced prometaphase arrest. As revealed by western blotting, STIL levels diminished 1–2 hours after release from nocodazole, coincident with a drop in levels of cyclin B1, a prominent substrate of the anaphase promoting complex/cyclosome (APC/C) (Peters, 2006) (Fig. 3B). Identical results were also seen in HeLa S3 cells (supplementary material Fig. S4), confirming and extending an earlier study showing that levels of murine STIL protein, but not mRNA, are reduced in late mitosis (Izraeli et al., 1997). Addition of the proteasome inhibitor MG132 completely blocked STIL degradation, indicating a requirement of the proteasome (Fig. 3B). To rule out cell-cycle effects, nocodazole-arrested cells were also treated with the Cdk1 inhibitor RO-3306 to enforce exit from mitosis even in the presence of MG132 (Fig. 3C). Under these conditions, mitotic exit occurred, as demonstrated by use of an anti-phospho-histone H3 (Ser10) antibody, and STIL was rapidly degraded in the control sample, but stable in the absence of proteasomal activity. Interestingly, inactivation of Cdk1 by RO-3306 resulted in a noticeable increase in the electrophoretic mobility of STIL (Fig. 3C, right panel), suggesting that STIL is a Cdk1-dependent phosphorylation substrate (Campaner et al., 2005). The above results suggested that STIL is a likely substrate of APC/C^{Cdc20} and/or APC/C^{Cdh1}. To explore this possibility, Cdc20 and/or Cdh1 were depleted by siRNA before synchronizing HeLa S3 cells in prometaphase and monitoring STIL levels upon release of cells in the presence of the Cdk1 inhibitor RO-3306. As shown in Fig. 3D, STIL was clearly stabilized in response to depletion of Cdc20, which is similar to results with cyclin B1. Depletion of Cdh1 alone did not produce major effects, but co-depletion of Cdh1 with Cdc20 clearly enhanced stabilization of STIL. The

Fig. 3. Localization of STIL to centrioles is cell-cycle dependent.

(A) Asynchronously growing U2OS cells fixed and stained for immunofluorescence microscopy with antibodies against STIL (ca66, green), CP110 (red) and Cep135 (blue); DNA (DAPI) is shown in gray. Representative images are shown for the different cell cycle stages (determined by the number of centrioles in interphase and DNA stain in mitosis). (B) Nocodazole (Noco)-arrested U2OS cells were released into mitosis in the presence or absence of MG132 and subjected to western blot analysis at different time points after release, using antibodies against STIL (ab89314) and cyclin B1. α -tubulin was monitored as loading control. (C) Same experiment as described in B except that Cdk1 inhibitor (RO-3306) was added to both MG132-treated and untreated cells. Anti-phospho-histone H3 (Ser10) antibodies were used to monitor mitotic progression. (D) Nocodazole (Noco)-arrested HeLa S3 cells previously treated with GL2 (control) or siRNA oligonucleotides targeting Cdc20 and/or Cdh1 were released into mitosis in the presence of Cdk1 inhibitor (RO-3306) and subjected to western blot analysis at different time points after release, using antibodies against STIL (ab89314), cyclin B1, Cdc20 and Cdh1. α -tubulin was monitored as a loading control. Scale bars: 5 μ m (Merge + DAPI) and 1 μ m (higher magnifications).

most likely interpretation of these results is that Cdc20 is the major APC/C adaptor responsible for STIL degradation and that Cdh1 contributes at later stages of mitosis.

Relationship between STIL, Ana2 and SAS-5

To analyze the structural and functional relationship between STIL, Ana2 and SAS-5 in more detail, we first performed a BLAST (Basic Local Alignment Search Tool) analysis to search for homologs of human STIL in other organisms. To our surprise, we readily identified apparent STIL homologs not only in other vertebrate species, but also in Hemichordata (*Saccoglossus kowalevskii*; 24% identity, 38% similarity), Cnidaria (*Nematostella vectensis*; 20% identity, 39% similarity) and even Placozoa (*Trichoplax adhaerens*; 17% identity, 26% similarity) (Fig. 4A). However, although the STIL-related proteins of Chordata, Hemichordata and Cnidaria comprise up to 1300 amino acids, those of *Drosophila* species (Ana2) comprise only about 400 residues (Fig. 4A). As emphasized previously (Stevens et al., 2010), extensive sequence similarity

between the various STIL-related proteins is seen in the STAN motif (Fig. 4B). In addition, we noticed a second region with high sequence similarity between the STIL and Ana2 families (Fig. 4B). We refer to this second motif as TIM (truncated in microcephaly), because it localizes to the extreme C-terminus of STIL that is truncated in microcephaly patients (Kumar et al., 2009). Notably, the nematode protein SAS-5 shows lower sequence conservation over the STAN and the TIM motif (Fig. 4B).

In *C. elegans*, SAS-5 has been shown to form a complex with SAS-6 (Leidel et al., 2005) and likewise, *Drosophila* Ana2 was found to bind DSAS-6 (Stevens et al., 2010). Thus, we asked whether human STIL might similarly interact with SAS-6. We co-expressed FLAG- or Myc-tagged versions of STIL and SAS-6 and performed co-immunoprecipitation experiments, followed by western blotting. Regardless of whether tags were placed at the N- or C-termini of the two proteins, we have so far been unable to detect any stable complex between STIL and SAS-6 (supplementary material Fig. S5A,B). Likewise, neither

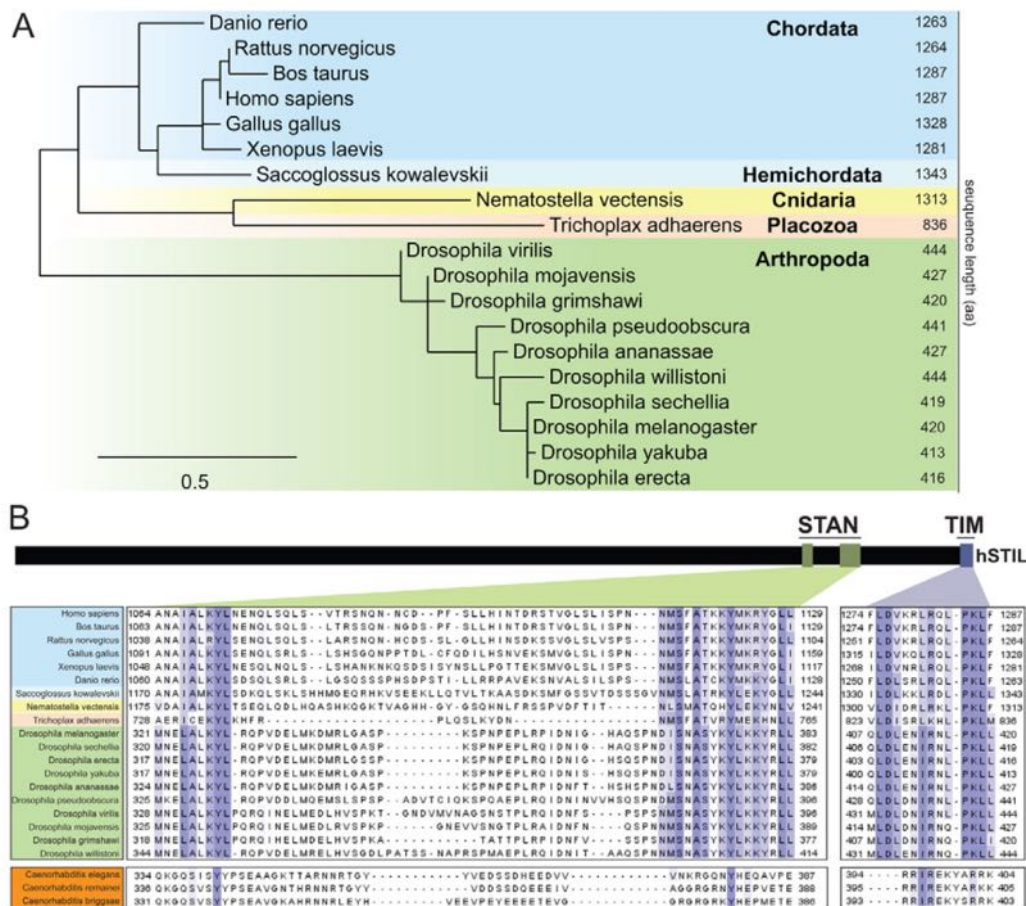


Fig. 4. Relationship between STIL, Ana2 and SAS-5. (A) Phylogenetic tree illustrating relationship between metazoan STIL and *Drosophila* Ana2 protein families. The tree was generated on phylogeny.fr (www.phylogeny.fr) using MUSCLE for alignment of amino acid sequences and PhyML (maximum likelihood method) for phylogeny. Number of amino acids (aa) for each sequence are indicated to the right. The scale bar indicates 0.5 substitutions per site. (B) Multiple protein sequence alignment (MUSCLE; colored according to the BLOSUM62 score, conservation visibility value was set to 30) of STIL/Ana2-related protein sequences. Regions encompassing highest sequence conservation (colored boxes on a scheme of human STIL) are shown. Alignment of three SAS-5 protein sequences of nematodes is shown below. STAN, STIL/ANA2; TIM, truncated in microcephaly.

endogenous nor overexpressed STIL could be seen after immunoprecipitation of endogenous SAS-6 (supplementary material Fig. S5C). Although these results do not exclude that subpopulations of STIL and SAS-6 might interact *in vivo*, we have so far been unable to demonstrate such an interaction.

To determine whether STIL and SAS-6 exhibit mutual dependencies for centriole localization, we depleted the two proteins separately from asynchronously growing U2OS cells and stained prophase cells (selected by DAPI staining) with antibodies against STIL, SAS-6 and CP110. Upon depletion of STIL, SAS-6 was readily detected at centrioles, even though levels were reduced to about 35% of those seen in control siRNA-treated cells (Fig. 5A,B). Similar to STIL, SAS-6 is completely degraded during each passage through mitosis (Strnad et al., 2007). This argues against the possibility that the SAS-6 protein detected in the STIL-depleted prophase cells could represent residual SAS-6 that localized to centrioles before the 72 hour siRNA treatment. Rather, it seems likely that SAS-6 can localize to centrioles in the absence of STIL, although STIL apparently contributes to its efficient integration into newly forming daughter centrioles. Conversely, STIL could not be detected at centrioles when SAS-6 was depleted (Fig. 5A,B), suggesting that SAS-6 is essential for efficient recruitment and/or maintenance of STIL at centrioles. To rule out the possibility that these observations reflect changes in the respective protein levels, siRNA-treated U2OS cells were analyzed in parallel by western blotting. As shown in Fig. 5C, the efficient depletion of STIL did not reduce the total abundance of SAS-6 or vice versa, suggesting

that the two proteins do not depend on each other for expression or stability.

Overexpression of STIL results in centriole amplification

Overexpression of PLK4 or SAS-6 results in centriole amplification (Leidel et al., 2005; Peel et al., 2007; Strnad et al., 2007; Cunha-Ferreira et al., 2009; Rogers et al., 2009). To ask whether overexpression of STIL might produce a similar phenotype, we overexpressed FLAG-tagged STIL in asynchronously growing U2OS cells and scored centriole numbers (Fig. 6). About 60% of all STIL-transfected cells showed extra copies of centrioles, which was similar to the extent of centriole amplification seen upon overexpression of PLK4 or SAS-6 (Fig. 6A). Strikingly, about 25% of the STIL-transfected cells showed centrioles arranged in a flower-like pattern (Fig. 6B), which was highly reminiscent of the arrangements seen upon overexpression of PLK4 and SAS-6 (Habedanck et al., 2005; Leidel et al., 2005; Duensing et al., 2007; Kleylein-Sohn et al., 2007; Strnad et al., 2007). Co-staining of STIL-transfected cells with antibodies against Cep164, a distal appendage marker present only on mature mother centrioles (Graser et al., 2007), confirmed the formation of multiple daughter centrioles around a single mother centriole (Fig. 6C). In agreement with STIL localization to the proximal ends of daughter centrioles (Fig. 2), STIL localized as a ring around the mother centriole and co-staining with antibodies against SAS-6 revealed extensive colocalization to these ring-like structures, indicating that the two proteins act in close proximity (Fig. 6D).

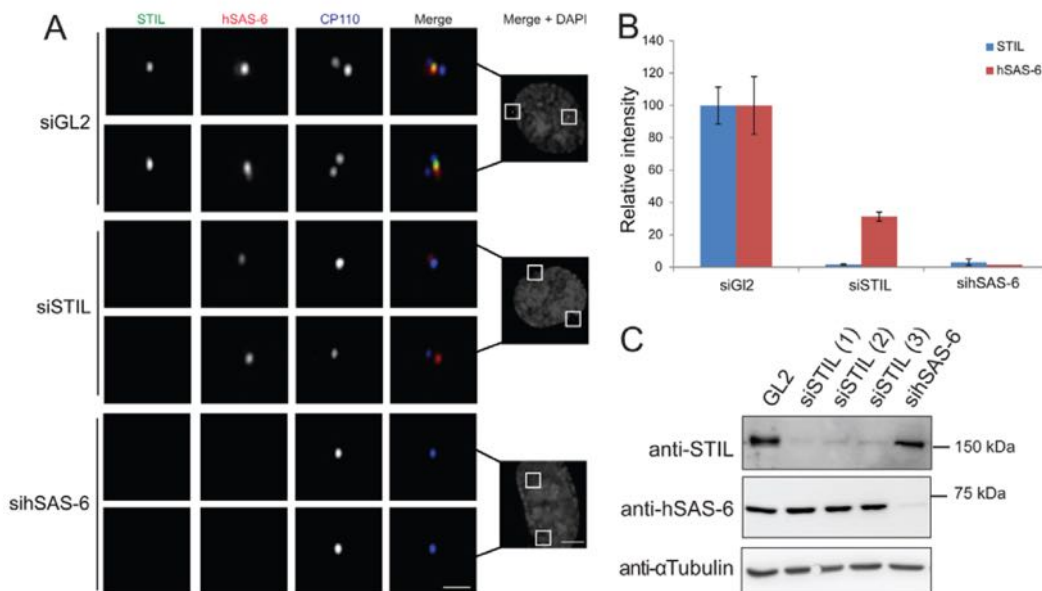


Fig. 5. SAS-6 localizes to centrioles in the absence of STIL. (A) Asynchronously growing U2OS cells transfected for 72 hours with GL2, STIL or SAS-6 siRNA oligonucleotides. Cells were fixed and stained with antibodies against STIL (ca66, green), SAS-6 (red) and CP110 (blue) for immunofluorescence microscopy; DNA (DAPI) is depicted in gray. Representative images of prophase cells are shown (determined by DAPI staining). (B) Quantification of centriolar levels of STIL and SAS-6 fluorescence in cells treated as described in A. Only prophase cells (determined by DAPI staining) were considered. ($n=3$, 10 centriolar pairs were analyzed in each experiment, error bars denote s.d.). Note that in SAS-6-depleted cells, STIL is completely absent from centrioles, whereas in STIL-depleted cells, SAS-6 localizes to centrioles (albeit in reduced amounts). (C) Western blot analysis of STIL and SAS-6 protein levels in control- (GL2), STIL- (STIL 1-3) and SAS-6-depleted U2OS cell lysates, probed with antibodies against STIL (ab89314), SAS-6 and α -tubulin for loading control. Scale bars: 5 μ m (Merge + DAPI) and 1 μ m (higher magnifications).

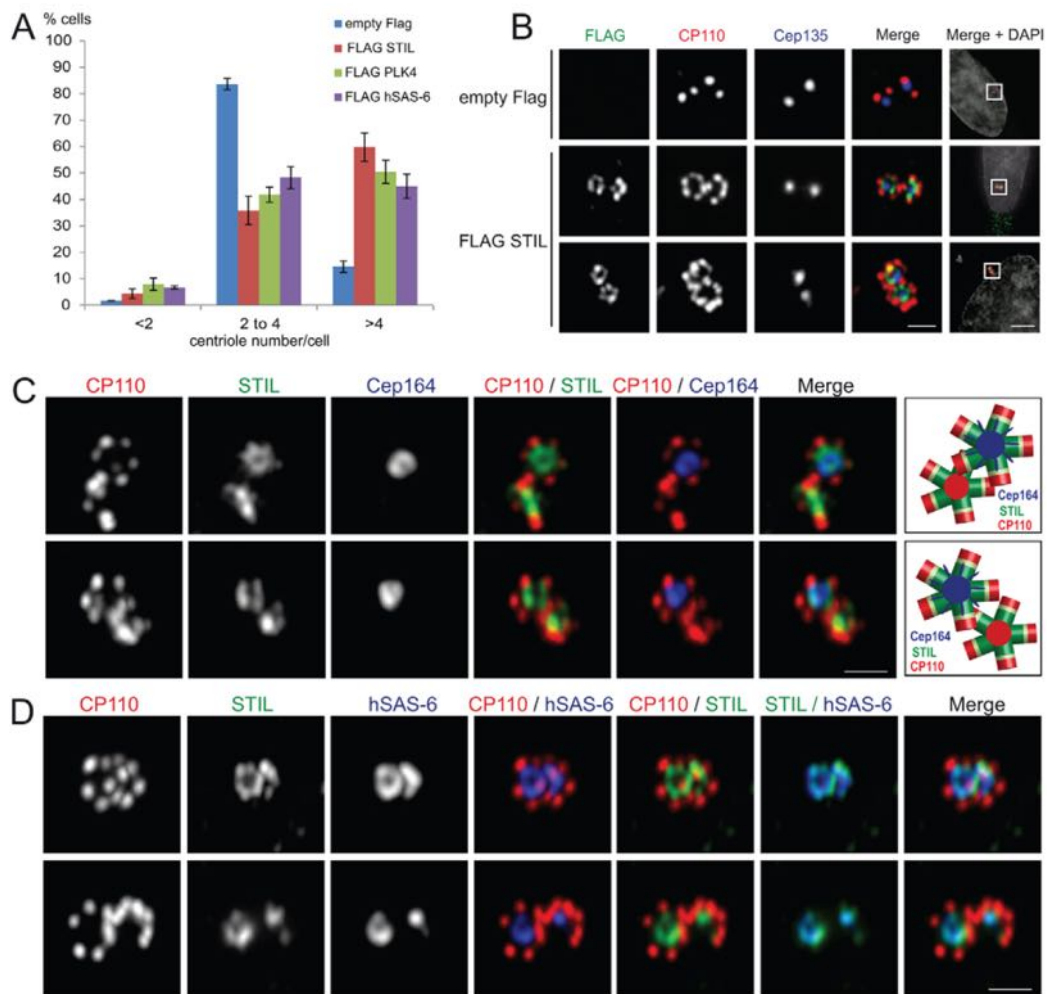


Fig. 6. STIL overexpression results in centriole amplification. Asynchronously growing U2OS cells were transfected with plasmids encoding FLAG-tagged STIL, PLK4 or SAS-6 or empty vector. After 48 hours, cells were fixed and stained with antibodies against the FLAG tag (green), CP110 (red) and Cep135 (blue); DNA (DAPI) is shown in gray. Cells were then analyzed by fluorescence microscopy. **(A)** The number of centrioles per transfected cell was determined based on CP110 staining. The graph illustrates the percentage of cells in each indicated category for control-, STIL-, PLK4- and SAS-6-transfected cells ($n=3$, 50 cells were analyzed in each experiment, error bars denote s.d.). **(B)** Representative images are shown for STIL-transfected and control cells. Note that in cells overexpressing STIL, multiple procentrioles form around a single centriole. **(C)** U2OS cells transiently expressing FLAG-tagged STIL were further stained with antibodies against CP110 (red), STIL (ca66, green) and Cep164 (blue). Representative images are shown and a scheme illustrates the localization of CP110 (red), STIL (green) and Cep164 (blue) to the flower-like structures. Note that Cep164, a marker for mature mother centrioles, localizes to the central centriole. **(D)** U2OS cells transiently expressing FLAG-tagged STIL were stained with antibodies against CP110 (red), STIL (ca66, green) and SAS-6 (blue). Note that both STIL and SAS-6 colocalize as a ring around the central centriole. Scale bars: 5 μm (Merge + DAPI) and 1 μm (all higher magnifications).

In conclusion, our data demonstrate that depletion of STIL interferes with daughter centriole formation, whereas overexpression of STIL causes the near-simultaneous formation of multiple daughter centrioles. This indicates that STIL plays a crucial and direct role in centriole duplication and further suggests that levels of this protein must be tightly controlled in human cells to prevent centriole overduplication.

Discussion

Here we demonstrate that STIL participates directly in the formation of new centrioles in human cells. We further show that STIL expression is regulated during the cell cycle and that physiological levels of STIL are crucial for the control of

centriole numbers. siRNA-mediated depletion of STIL from human cells severely suppresses centriole duplication. Conversely, overexpression of STIL triggers centriole amplification, characterized by the formation of multiple daughter centrioles around a single preexisting mother centriole, which is similar to the phenotypes seen upon overexpression of PLK4 and SAS-6. So far, we have not been able to detect stable complexes between STIL and SAS-6. However, the two proteins partly depend on each other for centriole association and they are subject to strikingly similar cell cycle regulation. Similar to SAS-6, STIL associates with newly forming procentrioles at an early stage of centriole formation during G1 phase. STIL then remains associated with daughter

centrioles until the metaphase-to-anaphase transition of mitosis, when the protein undergoes APC/C^{Cdc20-Cdh1}-dependent proteasomal degradation. Collectively, these data identify STIL as a protein that is crucial for the formation of centrioles in correct numbers and they point to close cooperation between STIL, SAS-6 and PLK4 in centriole biogenesis.

Of the five gene products required for centriole duplication in *C. elegans* (Strnad and Gonczy, 2008), three (SPD-2, SAS-4 and SAS-6) have obvious structural homologs (CEP192, CPAP and SAS-6, respectively) in humans. Furthermore, PLK4/Sak almost certainly represents a functional homolog of nematode ZYG-1. By striking contrast, bioinformatics approaches failed to identify a clear ortholog (outside nematodes) for the coiled-coil protein SAS-5. Our current study suggests that proteins of the STIL/Ana2 family are present throughout Metazoa, but show only limited sequence similarity to nematode SAS-5. This notwithstanding, we provide direct evidence for a crucial role of STIL in centriole biogenesis and number control. By both immunofluorescence and immunoelectron microscopy we show that STIL localizes at the proximal end of newly forming daughter centrioles. At this site, it colocalizes with SAS-6, a highly conserved centriole duplication factor and component of the cartwheel structure (Leidel et al., 2005; Nakazawa et al., 2007; Strnad et al., 2007; van Breugel et al., 2011). Importantly, although the localization of STIL to the centriole depends on SAS-6, SAS-6 can associate with centrioles in the absence of STIL, albeit in reduced amounts. This observation illustrates a striking difference to *C. elegans*, where SAS-5 and SAS-6 are mutually dependent for their centriolar localization (Leidel et al., 2005). A further difference between STIL and nematode SAS-5 concerns the fact that we have not been able to recover a stable complex between STIL and human SAS-6. Clearly, these negative results do not exclude a transient interaction between the two proteins. However, we emphasize that STIL and SAS-5 also differ with regard to localization. Whereas STIL localization is clearly restricted to daughter centrioles (this study) and Ana2 also shows an asymmetrical localization (Stevens et al., 2010), SAS-5 shuttles between the cytoplasm and both mother and daughter centrioles throughout the cell cycle (Delattre et al., 2004). Thus, the question of whether or not STIL should be considered a genuine ortholog of *C. elegans* SAS-5 remains difficult to answer.

The properties of STIL in vertebrate organisms have been explored in previous studies. Although these have not directly addressed a role of STIL in centriole biogenesis, we propose that a centriole-related function of STIL can explain most, if not all, of the phenotypes that were previously observed upon inactivation of the gene encoding STIL in zebrafish and mouse. In particular, loss-of-function mutations of STIL (SIL) in zebrafish resulted in embryonic lethality, with embryos showing an increase in mitotic index and disorganized mitotic spindles (Pfaff et al., 2007). The same authors also reported mitotic spindle defects in HeLa cells, as confirmed in our present study. Similarly, STIL-deficient mouse embryonic fibroblasts were shown to display defects in cell cycle progression (Castiel et al., 2011). STIL-knockout (*Stil*^{-/-}) mice die at embryonic day 10.5, with prominent axial midline defects and randomized cardiac looping, consistent with a block in Sonic hedgehog (Shh) signaling (Izraeli et al., 1999). These phenotypes are in line with the notion that Shh signaling operates through the ciliary apparatus (Wong and Reiter, 2008; Goetz and Anderson, 2010). In humans, mutations in the *STIL* gene have been linked to

primary autosomal microcephaly (Kumar et al., 2009), a neurodevelopmental disease characterized by abnormally small brain size. Interestingly, most of the genes identified to date that cause this disease code for centrosomal proteins (Thornton and Woods, 2009). Finally, it is intriguing that *STIL* expression is regulated by the transcription factor E2F (Erez et al., 2008), which has previously been shown to be important for the induction of centriole duplication in somatic cells (Meraldi et al., 1999). Thus, as a target of E2F, *STIL* might represent an important element in the coupling of centriole duplication to cell cycle cues.

STIL expression is tightly regulated during the cell cycle, with maximal protein levels seen during early mitosis. This might explain why a previous immunolocalization study (Pfaff et al., 2007) emphasized an association of STIL with mitotic spindle poles, but did not detect the association of STIL with interphase centrioles that we report in this study. Although STIL levels at daughter centrioles increase as cells approach mitosis, STIL disappears from centrioles at around the metaphase-to-anaphase transition, as a result of proteasome-mediated degradation. Regulation of STIL protein levels is crucial because overexpression of STIL induces centriole amplification. In particular, excess STIL causes the near-simultaneous formation of multiple daughter centrioles, which is highly reminiscent of the phenotype seen upon overexpression of PLK4 and SAS-6 (Habedanck et al., 2005; Leidel et al., 2005; Duensing et al., 2007; Kleylein-Sohn et al., 2007; Strnad et al., 2007). Thus, STIL cooperates with PLK4 and SAS-6 in the maintenance of constant centriole numbers during cell proliferation. The same conclusion has independently been drawn in a parallel study (Tang et al., 2011).

Materials and Methods

Cloning procedures

A full-length cDNA for *STIL* (clone IRCmp5012H1125D) was obtained from ImaGenes and amplified by PCR using the following oligonucleotides: 5'-CAAGCGGCCGCTTAAATAATTTGGTAACTGTC-3' and 5'-CAAGCGGCCGCAATGGAGCCTATATATCCTTTTG-3'. A *NotI* digest of the PCR product was cloned into pcDNA3.1-NFLAG and pcDNA3.1/3xmyc-A (Invitrogen). The full-length cDNA of *STIL* was further amplified using oligonucleotides 5'-TTTTGGCCGGCCATCATGGAGCCTATATCCTTTTG-3' and 5'-TTTTCTCGAGATCATGGAGCCTATATATCCTTTTG-3' and cloned into pcDNA3.1-CFLAG using restriction enzymes *FseI* and *XhoI*. A full-length *SAS6* cDNA was amplified using oligonucleotides 5'-TTTTGGTACCATCATGAGCCAAGTGTGTC-3' and 5'-TTTTGGCCGGCCGACTGTTGGTAACTG-3'. The PCR product was digested with *NotI* and *KpnI* and cloned into pcDNA3.1-Cmyc, using restriction enzymes *NotI* and *KpnI*. Full-length *SAS6* cDNA was further cloned into pcDNA3.1-NFLAG using restriction enzymes *AflIII* and *XhoI*. Cloning of PLK4 plasmids was described previously (Habedanck et al., 2005).

Antibody production and immunofluorescence microscopy

Rabbit polyclonal antibodies against His-STIL (aa 938–1287) were raised at Eurogentec (LIEGE Science Park, Seraing, Belgium) and immunoglobulins purified on a Protein A column according to standard protocols. Anti-CP110 (Schmidt et al., 2009), anti-Cep135 (Kleylein-Sohn et al., 2007), anti-PLK4 (Guderian et al., 2010), anti-SAS-6 (Kleylein-Sohn et al., 2007) and anti-Cep164 (Graser et al., 2007) antibodies were described previously. Anti- α -tubulin-FITC and anti-FLAG antibodies were purchased from Sigma. CP110 and SAS-6 antibodies were directly coupled to Alexa Fluor 555, Cep135 antibodies to Alexa Fluor 488 and Cep164, CP110 and Cep135 antibodies to Alexa Fluor 647, using labeling kits (Invitrogen). Alexa-Fluor-488-labeled secondary anti-mouse and anti-rabbit antibodies were purchased from Invitrogen. Cells were fixed in methanol for 5 minutes at -20°C. Antibody incubations and washings were performed as described previously (Meraldi et al., 1999). Stainings were analyzed using a DeltaVision microscope on a Nikon TE200 base (Applied Precision), equipped with a PlanApo 100 \times /1.4 NA oil-immersion objective. Serial optical sections were collected 0.2 μ m apart along the z-axis and processed using a deconvolution algorithm and projected into one picture using Softworx (Applied Precision). For quantification of centrosomal STIL and SAS-6 protein levels in ImageJ, images from control and treated samples were acquired with the same exposure time and

sum projected. Background signal intensity was subtracted from STIL and SAS-6 signal intensity.

Immunoelectron microscopy

For electron microscopy, cells were grown on coverslips and fixed with methanol for 5 minutes at -20°C . Blocking in PBS with 2% BSA was performed for 30 minutes. Primary antibody incubations were performed for 60 minutes, followed by incubation with goat-anti-rabbit IgG–Nanogold (1:50, Nanoprobes) for 45 minutes. Cells were then fixed with 2.5% glutaraldehyde for 1 hour. Nanogold was silver enhanced with HQ Silver (Nanoprobes). Cells were further processed as described previously (Fry et al., 1998).

Cell culture and transfections

U2OS, HeLa S3 or HEK293T cells were grown under standard conditions. Transient transfections were performed using TransIT-LT1 transfection reagent (Mirus Bio) according to the manufacturer's protocol.

siRNA-mediated protein depletion

STIL, Cdc20 and Cdh1 were depleted using siRNA duplex oligonucleotides targeting the following sequences: STIL1, 5'-CTGTCACCTGATCGAACCAAA-3'; STIL2, 5'-AAGTAAAGAACCTTAAACCA-3'; STIL3, 5'-AACTGAGGATTGGAAATTA-3'; Cdc20, 5'-AACATCAGAAAGCCTGGGCTT-3'; Cdh1, 5'-AATGAGAAGTCTCCAGTCA-3'. PLK4 and SAS-6 were depleted using the siRNA duplex oligonucleotides described previously (Habedanck et al., 2005; Leidel et al., 2005). Luciferase duplex GL2 was used as a control (Elbashir et al., 2001). siRNA duplex oligonucleotides were purchased from Qiagen. Transfections were performed using Oligofectamin (Invitrogen) according to the manufacturer's protocol.

Cell extracts, immunoprecipitation and western blots

Cell lysates and western blot analysis were performed as described previously (Chan et al., 2009) using Tris lysis buffer (20 mM Tris-HCl, pH 7.4, 150 mM NaCl, 0.5% IGEPAL CA-630) containing protease and phosphatase inhibitors. For immunoprecipitation experiments, 20 μg of antibody crosslinked to Protein A beads (Affi-Prep protein A matrix, Bio-Rad Laboratories) were used. Beads were incubated with 2–5 mg of lysate for 2 hours at 4°C . Beads were washed twice with Tris lysis buffer followed by three washes in PBS. Bound proteins were resolved by SDS-PAGE. The following antibodies were used for western blotting: polyclonal anti-STIL antibodies (ab89314, Abcam), monoclonal anti-myc (9E10) (Evan et al., 1985), monoclonal anti-cyclin-B1 (GNS3, Millipore), monoclonal anti-cyclin-E (HE12, Abcam), monoclonal anti-SAS-6 (Kleylein-Sohn et al., 2007), monoclonal anti- α -tubulin (Sigma), polyclonal anti-phospho-Histone H3 (Millipore), polyclonal anti-Cdc20 (sc8358, Santa Cruz) and monoclonal anti-Cdh1 (DH01, Millipore).

Cell cycle synchronization and proteasome inhibition

To analyze endogenous STIL protein levels during mitosis, HeLa S3 cells were presynchronized in thymidine (2 mM, Sigma) before they were released and arrested at prometaphase by incubation for 14 hours with nocodazole (50 ng ml^{-1} , Sigma). U2OS cells were directly arrested at prometaphase by incubation with nocodazole (as for HeLa S3 cells). After mitotic shake off and release into fresh medium, the synchronized cells were collected at different time points for western blot analysis. To inhibit the 26S proteasome, nocodazole-arrested cells were released and treated with MG132 (10 μM , Calbiochem). To force mitotic exit of MG132-treated or Cdc20- and Cdh1-depleted cells, Cdk1 inhibitor RO-3306 (9 μM , Enzo Life Science) was provided in addition.

Phylogenetic analysis

STIL homologs were identified by BLAST (Basic Local Alignment Search Tool) analysis. Protein sequences were aligned using the MUSCLE (multiple sequence alignment by log-expectation) sequence aligning algorithm (Edgar, 2004) in Jalview (Waterhouse et al., 2009) and were colored according to the BLOSUM62 coloring scheme (conservation color increment value was set to 30). Regions with high sequence conservation were subsequently determined by using the Blocks Multiple Alignment Processor (minimum block width was set to 5, maximum block width was set to 200) (Fred Hutchinson Cancer Research Center, Washington, DC). Phylogenetic trees were calculated on the phylogeny.fr platform (<http://www.phylogeny.fr>) (Dereeper et al., 2008). Protein sequences were first aligned with MUSCLE (Edgar, 2004), alignments were checked for accuracy with G-blocks (Castresana, 2000) and PhyML was used for tree building (maximum-likelihood method) (Guindon and Gascuel, 2003; Anisimova and Gascuel, 2006). Trees were rendered using Treedyn (Chevenet et al., 2006).

Acknowledgements

We thank Elena Nigg for excellent technical assistance and all members of our laboratory for helpful discussions. We also thank Conrad von Schubert for critical reading of our manuscript.

Funding

This work was supported by the Swiss National Science Foundation [grant number 31003A_132428/1]. C.A. was funded by a PhD fellowship from the Werner Siemens Foundation (Zug, Switzerland). K.F.S. was supported by a PhD fellowship from the Boehringer-Ingelheim Fonds and the International Max Planck Research School for Molecular and Cellular Life Sciences (Martinsried, Germany).

Supplementary material available online at

<http://jcs.biologists.org/lookup/suppl/doi:10.1242/jcs.099887/-/DC1>

References

- Anisimova, M. and Gascuel, O. (2006). Approximate likelihood-ratio test for branches: A fast, accurate, and powerful alternative. *Syst. Biol.* **55**, 539–552.
- Aplan, P. D., Lombardi, D. P. and Kirsch, I. R. (1991). Structural characterization of SIL, a gene frequently disrupted in T-cell acute lymphoblastic leukemia. *Mol. Cell. Biol.* **11**, 5462–5469.
- Azimzadeh, J. and Marshall, W. F. (2010). Building the centriole. *Curr. Biol.* **20**, R816–825.
- Bettencourt-Dias, M. and Glover, D. M. (2007). Centrosome biogenesis and function: centrosomes brings new understanding. *Nat. Rev. Mol. Cell Biol.* **8**, 451–463.
- Bettencourt-Dias, M., Rodrigues-Martins, A., Carpenter, L., Riparbelli, M., Lehmann, L., Gatt, M. K., Carmo, N., Balloux, F., Callaini, G. and Glover, D. M. (2005). SAK/PLK4 is required for centriole duplication and flagella development. *Curr. Biol.* **15**, 2199–2207.
- Bettencourt-Dias, M., Hildebrandt, F., Pellman, D., Woods, G. and Godinho, S. A. (2011). Centrosomes and cilia in human disease. *Trends Genet.* **27**, 307–315.
- Bornens, M. (2002). Centrosome composition and microtubule anchoring mechanisms. *Curr. Opin. Cell Biol.* **14**, 25–34.
- Campaner, S., Kaldis, P., Izraeli, S. and Kirsch, I. R. (2005). Sil phosphorylation in a Pin1 binding domain affects the duration of the spindle checkpoint. *Mol. Cell. Biol.* **25**, 6660–6672.
- Castiel, A., Danieli, M. M., David, A., Moshkovitz, S., Aplan, P. D., Kirsch, I. R., Brandeis, M., Kramer, A. and Izraeli, S. (2011). The Stil protein regulates centrosome integrity and mitosis through suppression of Chfr. *J. Cell Sci.* **124**, 532–539.
- Castresana, J. (2000). Selection of conserved blocks from multiple alignments for their use in phylogenetic analysis. *Mol. Biol. Evol.* **17**, 540–552.
- Chan, Y. W., Fava, L. L., Uldschmid, A., Schmitz, M. H., Gerlich, D. W., Nigg, E. A. and Santamaria, A. (2009). Mitotic control of kinetochore-associated dynein and spindle orientation by human Spindly. *J. Cell Biol.* **185**, 859–874.
- Chen, Z., Indjeian, V. B., McManus, M., Wang, L. and Dynlacht, B. D. (2002). CP110, a cell cycle-dependent CDK substrate, regulates centrosome duplication in human cells. *Dev. Cell* **3**, 339–350.
- Chevenet, F., Brun, C., Banuls, A. L., Jacq, B. and Christen, R. (2006). TreeDyn: towards dynamic graphics and annotations for analyses of trees. *BMC Bioinformatics* **7**, 439.
- Cunha-Ferreira, I., Rodrigues-Martins, A., Bento, I., Riparbelli, M., Zhang, W., Laue, E., Callaini, G., Glover, D. M. and Bettencourt-Dias, M. (2009). The SCF/Slimb ubiquitin ligase limits centrosome amplification through degradation of SAK/PLK4. *Curr. Biol.* **19**, 43–49.
- Delattre, M., Leidel, S., Wani, K., Baumer, K., Bamat, J., Schnabel, H., Feichtinger, R., Schnabel, R. and Goczny, P. (2004). Centriolar SAS-5 is required for centrosome duplication in *C. elegans*. *Nat. Cell Biol.* **6**, 656–664.
- Dereeper, A., Guignon, V., Blanc, G., Audic, S., Buffet, S., Chevenet, F., Dufayard, J. F., Guindon, S., Lefort, V., Lescot, M. et al. (2008). Phylogeny.fr: robust phylogenetic analysis for the non-specialist. *Nucleic Acids Res.* **36**, W465–W469.
- Doxsey, S., McCollum, D. and Theurkauf, W. (2005). Centrosomes in cellular regulation. *Annu. Rev. Cell Dev. Biol.* **21**, 411–434.
- Duensing, A., Liu, Y., Perdreau, S. A., Kleylein-Sohn, J., Nigg, E. A. and Duensing, S. (2007). Centriole overduplication through the concurrent formation of multiple daughter centrioles at single maternal templates. *Oncogene* **26**, 6280–6288.
- Edgar, R. C. (2004). MUSCLE: a multiple sequence alignment method with reduced time and space complexity. *BMC Bioinformatics* **5**, 113.
- Elbashir, S. M., Harborth, J., Lendeckel, W., Yalcin, A., Weber, K. and Tuschl, T. (2001). Duplexes of 21-nucleotide RNAs mediate RNA interference in cultured mammalian cells. *Nature* **411**, 494–498.
- Erez, A., Perelman, M., Hewitt, S. M., Cojocar, G., Goldberg, I., Shahar, I., Yaron, P., Muler, I., Campaner, S., Amariglio, N. et al. (2004). Sil overexpression in lung cancer characterizes tumors with increased mitotic activity. *Oncogene* **23**, 5371–5377.
- Erez, A., Castiel, A., Trakhtenbrot, L., Perelman, M., Rosenthal, E., Goldstein, I., Stettner, N., Harmelin, A., Eldar-Finkelman, H., Campaner, S. et al. (2007). The SIL gene is essential for mitotic entry and survival of cancer cells. *Cancer Res.* **67**, 4022–4027.
- Erez, A., Chaussepied, M., Castiel, A., Colaizzo-Anas, T., Aplan, P. D., Ginsberg, D. and Izraeli, S. (2008). The mitotic checkpoint gene, SIL is regulated by E2F1. *Int. J. Cancer* **123**, 1721–1725.

- Evan, G. I., Lewis, G. K., Ramsay, G. and Bishop, J. M. (1985). Isolation of monoclonal antibodies specific for human c-myc proto-oncogene product. *Mol. Cell Biol.* **5**, 3610-3616.
- Fry, A. M., Meraldi, P. and Nigg, E. A. (1998). A centrosomal function for the human Nek2 protein kinase, a member of the NIMA family of cell cycle regulators. *EMBO J.* **17**, 470-481.
- Goetz, S. C. and Anderson, K. V. (2010). The primary cilium: a signalling centre during vertebrate development. *Nat. Rev. Genet.* **11**, 331-344.
- Golling, G., Amsterdam, A., Sun, Z., Antonelli, M., Maldonado, E., Chen, W., Burgess, S., Haldi, M., Artzt, K., Farrington, S. et al. (2002). Insertional mutagenesis in zebrafish rapidly identifies genes essential for early vertebrate development. *Nat. Genet.* **31**, 135-140.
- Graser, S., Stierhof, Y. D., Lavoie, S. B., Gassner, O. S., Lamla, S., Le Clech, M. and Nigg, E. A. (2007). Cep164, a novel centriole appendage protein required for primary cilium formation. *J. Cell Biol.* **179**, 321-330.
- Guderian, G., Westendorf, J., Uldschmid, A. and Nigg, E. A. (2010). Plk4 trans-autophosphorylation regulates centriole number by controlling betaTrCP-mediated degradation. *J. Cell Sci.* **123**, 2163-2169.
- Guindon, S. and Gascuel, O. (2003). A simple, fast, and accurate algorithm to estimate large phylogenies by maximum likelihood. *Syst. Biol.* **52**, 696-704.
- Habedanck, R., Stierhof, Y. D., Wilkinson, C. J. and Nigg, E. A. (2005). The Polo kinase Plk4 functions in centriole duplication. *Nat. Cell Biol.* **7**, 1140-1146.
- Izraeli, S., Colaizzo-Anas, T., Bertness, V. L., Mani, K., Aplan, P. D. and Kirsch, I. R. (1997). Expression of the SIL gene is correlated with growth induction and cellular proliferation. *Cell Growth Differ.* **8**, 1171-1179.
- Izraeli, S., Lowe, L. A., Bertness, V. L., Good, D. J., Dorward, D. W., Kirsch, I. R. and Kuehn, M. R. (1999). The SIL gene is required for mouse embryonic axial development and left-right specification. *Nature* **399**, 691-694.
- Kitagawa, D., Vakonakis, I., Olieric, N., Hilbert, M., Keller, D., Olieric, V., Bortfeld, M., Erat, M. C., Fluckiger, I., Gonczy, P. et al. (2011). Structural basis of the 9-fold symmetry of centrioles. *Cell* **144**, 364-375.
- Kleylein-Sohn, J., Westendorf, J., Le Clech, M., Habedanck, R., Stierhof, Y.-D. and Nigg, E. A. (2007). Plk4-Induced Centriole Biogenesis in Human Cells. *Dev. Cell* **13**, 190-202.
- Kumar, A., Girimaji, S. C., Duvvari, M. R. and Blanton, S. H. (2009). Mutations in STIL, encoding a pericentriolar and centrosomal protein, cause primary microcephaly. *Am. J. Hum. Genet.* **84**, 286-290.
- Leidel, S., Delattre, M., Cerutti, L., Baumer, K. and Gonczy, P. (2005). SAS-6 defines a protein family required for centrosome duplication in *C. elegans* and in human cells. *Nat. Cell Biol.* **7**, 115-125.
- Luders, J. and Stearns, T. (2007). Microtubule-organizing centres: a re-evaluation. *Nat. Rev. Mol. Cell Biol.* **8**, 161-167.
- Meraldi, P., Lukas, J., Fry, A. M., Bartek, J. and Nigg, E. A. (1999). Centrosome duplication in mammalian somatic cells requires E2F and Cdk2-cyclin A. *Nat. Cell Biol.* **1**, 88-93.
- Nakazawa, Y., Hiraki, M., Kamiya, R. and Hirono, M. (2007). SAS-6 is a cartwheel protein that establishes the 9-fold symmetry of the centriole. *Curr. Biol.* **17**, 2169-2174.
- Nigg, E. A. (2002). Centrosome aberrations: cause or consequence of cancer progression? *Nat. Rev. Cancer* **2**, 815-825.
- Nigg, E. A. and Raff, J. W. (2009). Centrioles, centrosomes, and cilia in health and disease. *Cell* **139**, 663-678.
- Peel, N., Stevens, N. R., Basto, R. and Raff, J. W. (2007). Overexpressing centriole-replication proteins in vivo induces centriole overduplication and de novo formation. *Curr. Biol.* **17**, 834-843.
- Pelletier, L., O'Toole, E., Schwager, A., Hyman, A. A. and Muller-Reichert, T. (2006). Centriole assembly in *Caenorhabditis elegans*. *Nature* **444**, 619-623.
- Peters, J. M. (2006). The anaphase promoting complex/cyclosome: a machine designed to destroy. *Nat. Rev. Mol. Cell Biol.* **7**, 644-656.
- Pfaff, K. L., Straub, C. T., Chiang, K., Bear, D. M., Zhou, Y. and Zon, L. I. (2007). The zebra fish *cassiopia* mutant reveals that SIL is required for mitotic spindle organization. *Mol. Cell Biol.* **27**, 5887-5897.
- Rogers, G. C., Rusan, N. M., Roberts, D. M., Peifer, M. and Rogers, S. L. (2009). The SCF Slimb ubiquitin ligase regulates Plk4/Sak levels to block centriole reduplication. *J. Cell Biol.* **184**, 225-239.
- Schmidt, T. I., Kleylein-Sohn, J., Westendorf, J., Le Clech, M., Lavoie, S. B., Stierhof, Y. D. and Nigg, E. A. (2009). Control of Centriole Length by CPAP and CP110. *Curr. Biol.* **19**, 1005-1011.
- Stevens, N. R., Dobbelaere, J., Brunk, K., Franz, A. and Raff, J. W. (2010). *Drosophila* Ana2 is a conserved centriole duplication factor. *J. Cell Biol.* **188**, 313-323.
- Strnad, P. and Gonczy, P. (2008). Mechanisms of procentriole formation. *Trends Cell Biol.* **18**, 389-396.
- Strnad, P., Leidel, S., Vinogradova, T., Euteneuer, U., Khodjakov, A. and Gonczy, P. (2007). Regulated HsSAS-6 levels ensure formation of a single procentriole per centriole during the centrosome duplication cycle. *Dev. Cell* **13**, 203-213.
- Tang, C.-J. C., Lin S.-Y., Hsu, W.-B., Lin, Y.-N., Wu, C.-T., Lin, Y.-C., Chang, C.-W., Wu, H.-S. and Tang, T. K. (2011). The human microcephaly protein STIL interacts with CPAP and is required for procentriole formation. *EMBO J.* **30**, 4790-4804.
- Thornton, G. K. and Woods, C. G. (2009). Primary microcephaly: do all roads lead to Rome? *Trends Genet.* **25**, 501-510.
- Tsou, M. F. B. and Stearns, T. (2006a). Mechanism limiting centrosome duplication to once per cell cycle. *Nature* **442**, 947-951.
- Tsou, M. F. and Stearns, T. (2006b). Controlling centrosome number: licenses and blocks. *Curr. Opin. Cell Biol.* **18**, 74-78.
- Tsou, M. F., Wang, W. J., George, K. A., Uryu, K., Stearns, T. and Jallepalli, P. V. (2009). Polo kinase and separate regulate the mitotic licensing of centriole duplication in human cells. *Dev. Cell* **17**, 344-354.
- van Breugel, M., Hirono, M., Andreeva, A., Yanagisawa, H. A., Yamaguchi, S., Nakazawa, Y., Morgner, N., Petrovich, M., Ebong, I. O., Robinson, C. V. et al. (2011). Structures of SAS-6 suggest its organization in centrioles. *Science* **331**, 1196-1199.
- Wang, W. J., Soni, R. K., Uryu, K. and Bryan Tsou, M. F. (2011). The conversion of centrioles to centrosomes: essential coupling of duplication with segregation. *J. Cell Biol.* **193**, 727-739.
- Waterhouse, A. M., Procter, J. B., Martin, D. M., Clamp, M. and Barton, G. J. (2009). Jalview Version 2—a multiple sequence alignment editor and analysis workbench. *Bioinformatics* **25**, 1189-1191.
- Wong, S. Y. and Reiter, J. F. (2008). The primary cilium at the crossroads of mammalian hedgehog signaling. *Curr. Top Dev. Biol.* **85**, 225-260.
- Zyss, D. and Gergely, F. (2009). Centrosome function in cancer: guilty or innocent? *Trends Cell Biol.* **19**, 334-346.

Supplemental Information

Cell-Cycle-Regulated Expression of STIL Controls Centriole Number in Human Cells

Christian Arquint, Katharina F. Sonnen, York-Dieter Stierhof and Erich A. Nigg

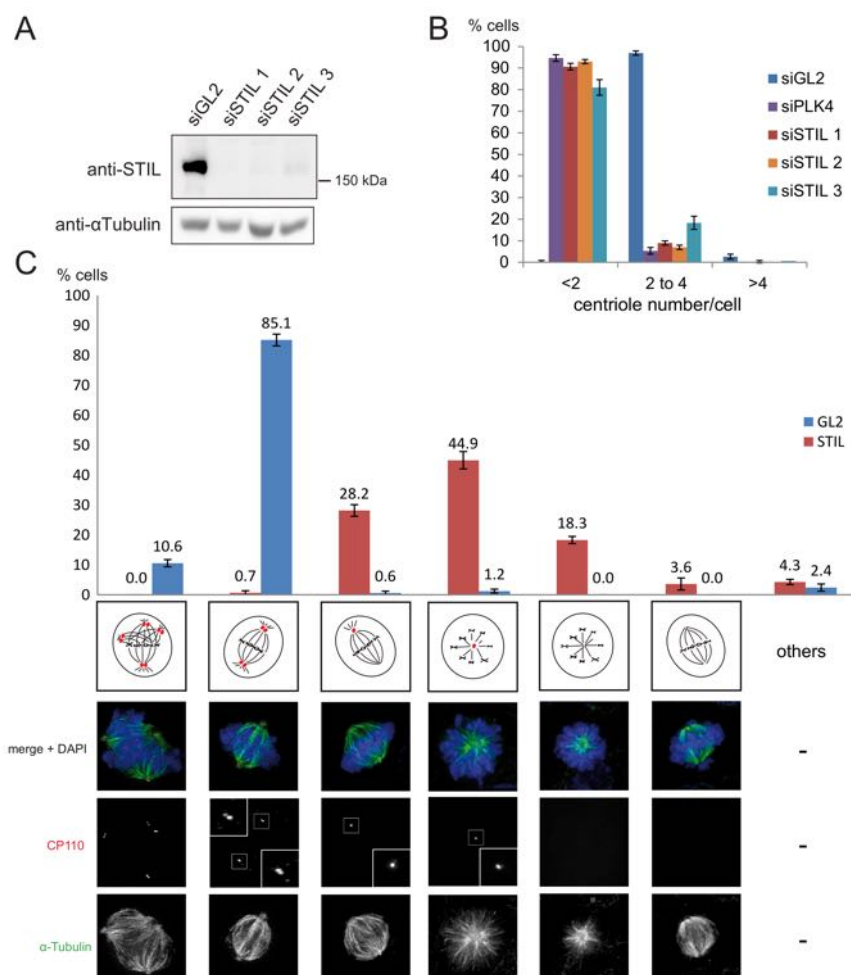
Published in Journal of Cell Science

Volume 125

Accepted 24 October 2011

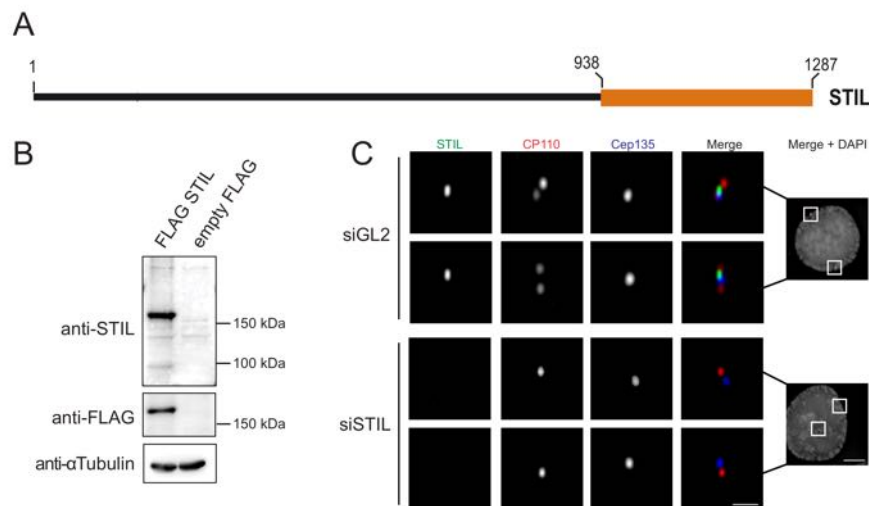
Published 01 March 2012

Fig. S1

**Fig. S1: STIL is required for centriole duplication in HeLa S3 cells**

Asynchronously growing HeLa S3 cells were transfected for 72 h with control siRNA (GL2), three different STIL siRNA (STIL 1-3) or PLK4 siRNA oligonucleotides. **(A)** Western Blot analysis of STIL protein levels in control- (GL2) and STIL-depleted U2OS cell lysates (STIL 1-3), probed with the STIL antibody ab89314 and an antibody against alpha-tubulin for loading control. **(B)** Control- (GL2), STIL- or PLK4-depleted cells were stained with antibodies against CP110 (red) and Cep135 (green) for immunofluorescence microscopy to determine centriolar numbers in each cell ($n=3$, 100 cells were analysed in each experiment, error bars denote SD). **(C)** Control- (GL2) and STIL- (STIL 1) depleted cells were fixed and stained for immunofluorescence microscopy with antibodies against CP110 (red) to visualize centrioles and alpha-tubulin (green) to visualize mitotic spindles. DNA was stained with DAPI (blue). Mitotic cells were then classified according to their spindle morphology and centriolar disposition ($n=3$, a minimum of 30 cells were analysed in each experiment; error bars denote SD). Schematic representations (top row) depicting spindle morphology (black lines) and centrioles (red dots) as well as representative images (bottom rows) are shown for each category (Scale bar 5 μm , insets represent threefold magnification).

Fig. S2

**Fig. S2: Characterization of STIL antibody ca66**

(A) Scheme of human STIL depicting the fragment (orange box) that was used for antibody production in rabbits. (B) HEK 293T cells were transfected with either FLAG-tagged STIL or an empty vector control. After 24 h the cells were lysed and the expression pattern analyzed by immunoblotting with the STIL antibody (ca66) and with antibodies against FLAG and alpha-tubulin (loading control). (C) Asynchronously growing U2OS cells were transfected with either control siRNA oligos (GL2) or STIL siRNA oligos for 72 h. Cells were then fixed and stained with antibodies against STIL (ca66, green), CP110 (red) and Cep135 (blue) for immunofluorescence microscopy; DAPI is shown in gray. Representative images of prophase cells are shown. Note that the centriolar staining by the STIL antibody ca66 in control-depleted cells is completely lost in STIL-depleted cells, demonstrating specificity of the antibody. Scale bars indicate 5 μ m (Merge + DAPI) and 1 μ m (higher magnifications).

Fig. S3

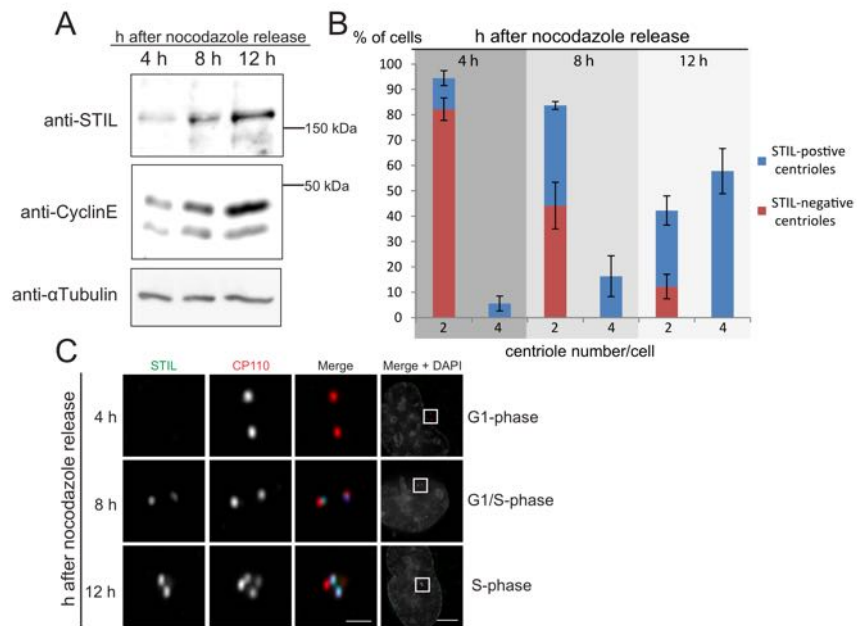
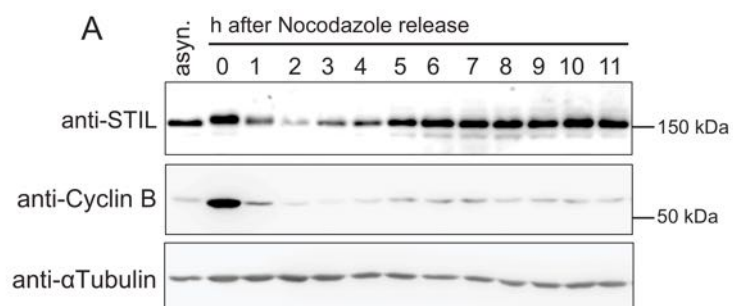


Fig. S3: STIL associates with nascent daughter centrioles at the G1/S-phase transition

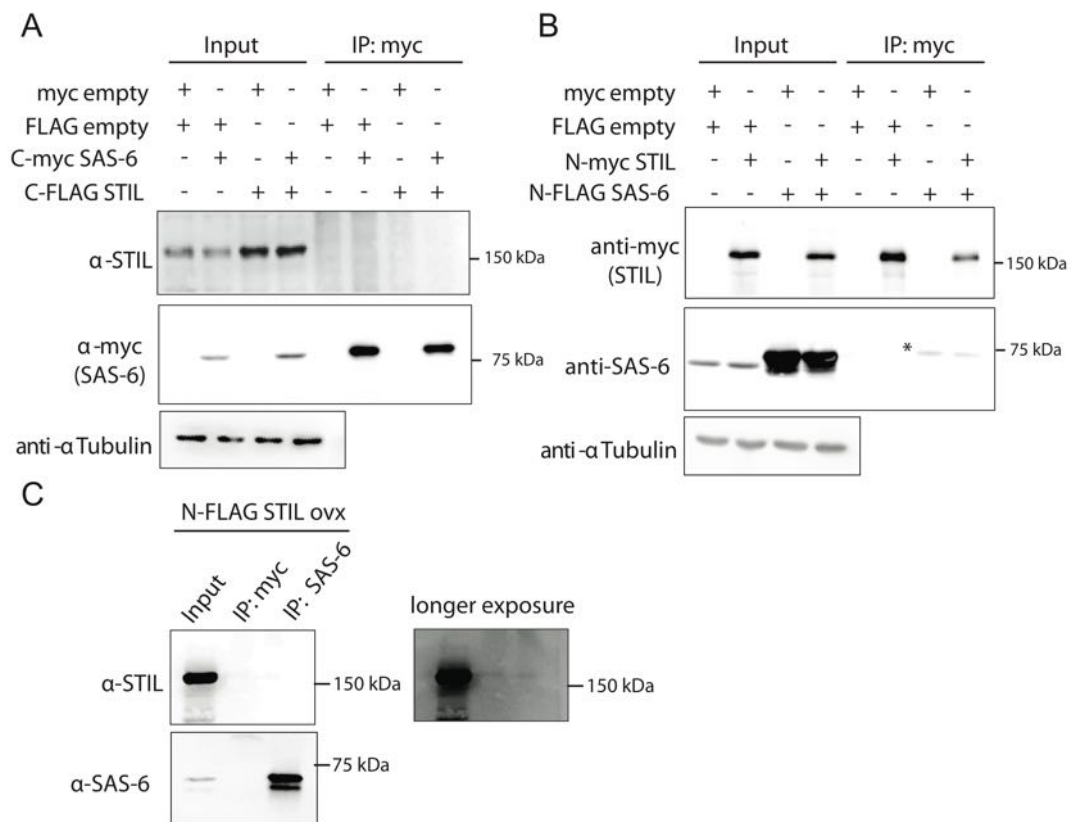
U2OS cells were released into G1-phase from a nocodazole arrest and analysed for the presence of STIL at successive time points after release. **(A)** U2OS cell lysates 4 h, 8 h and 12 h after release were probed with anti-STIL antibodies (ab89314), as well as antibodies against Cyclin E1 (to monitor the beginning of S-phase) and alpha-tubulin (loading control). **(B)** At the same time points as in (A), cells were fixed for immunofluorescence microscopy and stained with antibodies against STIL (ca66, green) and CP110 (red). Representative images for each time point are shown. Note that STIL gets recruited to preexisting centrioles 8 h after release. **(C)** Cells were processed as indicated in (B) and analysed for the presence of STIL at centrosomes at each time point. Centrosomes were further classified into unduplicated (2 centrioles per cell) and duplicated (4 centrioles per cell). (n = 3, 50 cells were analysed for each time point, error bars denote SD). Scale bars indicate 5 μ m (Merge + DAPI) and 1 μ m (higher magnifications).

Fig. S4

**Fig. S4: STIL is degraded upon progression through mitosis**

HeLa S3 cells were lysed at the indicated time points after release from a nocodazole arrest. Total cell lysates were probed with anti-STIL antibodies (ab89314), as well as antibodies against Cyclin B1 (to monitor the metaphase-to-anaphase transition) and alpha-tubulin (loading control).

Fig S5

**Fig. S5: Search for STIL-SAS-6 complexes by immunoprecipitation experiments**

(A) C-myc SAS-6 and C-FLAG STIL were transiently overexpressed in HEK293T cells and cell lysates were subjected to immunoprecipitation using anti-myc antibodies. Bound proteins were separated on SDS-PAGE and analysed by Western blotting using antibodies against STIL (ab89314) and antibodies against the myc tag to visualize SAS-6 (alpha-tubulin was used for loading control). (B) N-myc STIL and N-FLAG SAS-6 were transiently overexpressed in HEK293T cells and cell lysates were subjected to immunoprecipitation using anti-myc antibodies. Bound proteins were separated on SDS-PAGE and analysed by Western blotting using antibodies against the myc tag (to visualize STIL) and antibodies against SAS-6 (alpha-tubulin was used for loading control). Note that trace amounts of SAS-6 co-precipitate unspecifically with protein A beads, regardless of the presence or absence of STIL (asterisk). (C) Lysates from HEK293T cells overexpressing FLAG-STIL were used to immunoprecipitate endogenous SAS-6 and then probed by Western blotting with antibodies against STIL and SAS-6. Parallel immunoprecipitations were carried out using anti-myc antibodies for control. Short and long exposures of the anti-STIL Western blot are shown, illustrating that neither endogenous nor overexpressed STIL can be detected in SAS-6 immunoprecipitates.

4.2 STIL Microcephaly Mutations Interfere with APC/C-Mediated Degradation and Cause Centriole Amplification

Christian Arquint and Erich A. Nigg

Published in Current Biology

Volume 24

Accepted 09 December 2013

Published 30 January 2014

Article

STIL Microcephaly Mutations Interfere with APC/C-Mediated Degradation and Cause Centriole Amplification

Christian Arquint¹ and Erich A. Nigg^{1,*}¹Biozentrum, University of Basel, Klingelbergstrasse 50/70, 4056 Basel, Switzerland

Summary

Background: STIL is a centriole duplication factor that localizes to the procentriolar cartwheel region, and mutations in STIL are associated with autosomal recessive primary microcephaly (MCPH). Excess STIL triggers centriole amplification, raising the question of how STIL levels are regulated.

Results: Using fluorescence time-lapse imaging, we identified a two-step process that culminates in the elimination of STIL at the end of mitosis. First, at nuclear envelope breakdown, Cdk1 triggers the translocation of STIL from centrosomes to the cytoplasm. Subsequently, the cytoplasmic bulk of STIL is degraded via the anaphase-promoting complex/cyclosome (APC/C)-proteasome pathway. We identify a C-terminal KEN box as critical for STIL degradation. Remarkably, this KEN box is deleted in MCPH mutants of STIL, rendering STIL resistant to proteasomal degradation and causing centriole amplification.

Conclusions: Our results reveal a role for Cdk1 in STIL dissociation from centrosomes during early mitosis, with implications for the timing of cartwheel disassembly. Additionally, we propose that centriole amplification triggered by STIL stabilization is the underlying cause of microcephaly in human patients with corresponding STIL mutations.

Introduction

The *STIL* gene (or *SIL*; *SCL/TAL1* interrupting locus) was initially cloned in studies of a chromosomal rearrangement causing T cell acute lymphoblastic leukemia [1] and was subsequently shown to be essential for vertebrate embryonic development [2, 3]. Early studies emphasized a role in mitotic regulation [4, 5], but when the STIL protein was discovered to share localized sequence similarity with *Drosophila* Ana2 and *Caenorhabditis elegans* SAS-5 [6], attention was focused on a possible role of STIL in centriole duplication [7–9]. Indeed, STIL depletion completely blocks centriole formation, whereas STIL overexpression results in extensive centriole amplification. Furthermore, STIL colocalizes with SAS-6 at the procentriolar cartwheel [8, 9], a key structure in procentriole assembly (for review, see [10]).

Mutations in *STIL* cause autosomal recessive primary microcephaly (MCPH), a neurodevelopmental disorder characterized by reduced brain size. The disease is genetically heterogeneous, with at least ten causative loci identified (MCPH1–MCPH10), and remarkably, nearly all mutated genes code for centrosome-related proteins [11, 12]. Defects in spindle positioning [13, 14], cell-cycle progression [15], or DNA repair [16, 17] have been considered as root causes for MCPH. To date, four different STIL mutations have been

identified in microcephaly patients [18, 19], but how these interfere with human brain development is unknown.

In normal cells, levels of STIL need to be precisely controlled in order to prevent abnormal centriole numbers, raising the question of how STIL protein levels are regulated. Previous studies have revealed a proteasome-dependent decline of STIL at mitotic exit [8, 9, 20]. Here we have dissected the mechanisms underlying cell-cycle regulation of STIL at subcellular level, focusing on distinct centrosomal and cytoplasmic protein pools.

Results

Differential Regulation of Cytoplasmic and Centrosomal STIL Pools

To precisely monitor cell-cycle regulation of STIL at the single-cell level, we established a real-time assay based on time-lapse fluorescence microscopy. EGFP-tagged STIL was expressed in a U2OS Flp-In T-REX cell line, under control of a tetracycline-inducible promoter. After tetracycline addition for 12 to 24 hr, EGFP-STIL was expressed at near physiological levels (see [Figure S1A](#) available online). Immunofluorescence microscopy showed that EGFP-STIL was localized to centrioles ([Figure S1B](#)), and costaining for SAS-6 confirmed extensive colocalization, in line with previous results [8, 9, 21, 22]. In addition, EGFP-STIL was detectable throughout the cytoplasm. Surprisingly, even prolonged induction of EGFP-STIL expression failed to cause centriole amplification ([Figure S1C](#)), although transient overexpression of EGFP-STIL (estimated to produce an approximately 15-fold excess) caused supernumerary centrioles in more than 50% of transfected cells, including 20% with flower-like arrangements ([Figures S1D–S1F](#)). These results indicate that EGFP-STIL is functional in the tetracycline-inducible U2OS cell line but that its expression occurs at sufficiently low levels to escape centriole amplification. This implies that mild overexpression of STIL (an approximate doubling of levels) is tolerated, at least in these cells ([Figures S1A and S1C](#)).

Use of a spinning-disk confocal microscope allowed us to monitor both centrosomal and cytoplasmic EGFP-STIL levels for an entire cell cycle ([Figure 1](#); [Movie S1](#)). These measurements revealed that the cytoplasmic EGFP-STIL signal increased steadily toward mitosis and remained stable throughout prophase, prometaphase, and metaphase but dropped sharply after anaphase onset ([Figures 1A and 1C](#)). In the next cell cycle, cytoplasmic EGFP-STIL levels remained low in early G1 before they began to rise again 3–4 hr later. A strikingly different pattern was seen when analyzing EGFP-STIL intensity at the centrosome ([Figures 1B and 1C](#)). Although the centrosomal EGFP signal also increased toward mitosis, it rapidly disappeared from early mitotic centrosomes immediately after nuclear envelope breakdown (NEBD). No centriolar signal was detected in late mitosis and early G1, and relocalization of EGFP-STIL to centrioles was observed only when the cytoplasmic levels began to rise in late G1 and early S phase. Thus, whereas cytoplasmic STIL remains high until anaphase onset, centriolar STIL begins to disappear as early as NEBD, indicating

*Correspondence: erich.nigg@unibas.ch

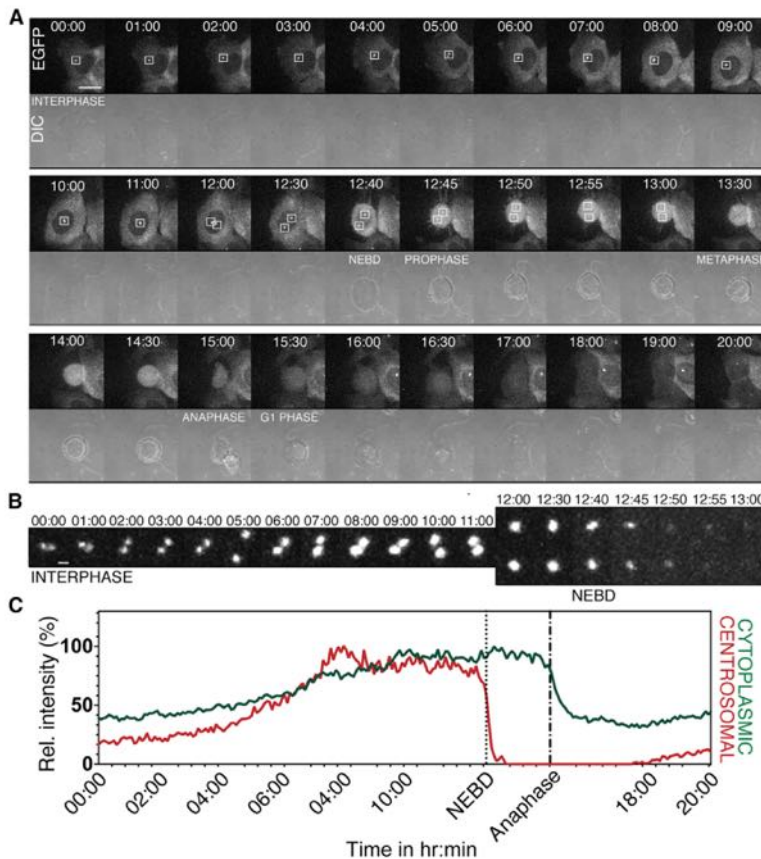


Figure 1. Cytoplasmic and Centrosomal STIL Pools Are Differentially Regulated

(A and B) Real-time visualization of EGFP-STIL in a U2OS Flp-In T-REx cell monitored for 20 hr (Movie S1).

(A) Stills from Movie S1 showing EGFP fluorescence (upper panels) and differential interference contrast (DIC; lower panels). Centrosomal EGFP-STIL signal is marked by white boxes. Time stamps show hours and minutes. Scale bar, 20 μ m.

(B) Magnification of the centrosomal EGFP-STIL signal, with adjusted intensity scale. Scale bar, 1 μ m.

(C) Line graphs showing the EGFP-STIL signal intensity over time measured in the cytoplasmic (green) or centrosomal (red) regions.

NEBD might influence centrosomal association of SAS-6 and thereby affect cartwheel stability. Immunofluorescence microscopy was used to carefully compare centrosomal levels of endogenous SAS-6 and STIL in fixed U2OS cells (Figure 3). Centrosomal SAS-6 levels decreased significantly already upon transit from prophase to metaphase, suggesting that SAS-6 also dissociates from centrosomes at these early stages, albeit with slower kinetics than STIL. Interestingly, STIL-negative metaphase centrosomes contained significantly less SAS-6 than those on which traces of STIL could be detected. In early G1 phase, STIL and SAS-6 were undetectable on virtually all centrosomes, as expected [7–9, 24].

that centrosomal and cytoplasmic STIL pools are differentially regulated.

Cdk1 Triggers Removal of Centrosomal STIL

To explore the mechanism underlying loss of STIL from early mitotic centrosomes, we filmed cells from NEBD into metaphase (Figure 2; Movies S2 and S3). Consistent with the above results, centrosomal STIL signals began to decrease at NEBD, reaching undetectable levels 15–30 min later, while cytoplasmic STIL intensity remained steady (Figures 2A and 2D). This loss of centrosomal STIL was not dependent on proteasome activity, as it was not impaired by addition of the proteasome inhibitor MG132 (Figures 2B and 2D; Figure S2). It follows that loss of centrosomal STIL reflects relocalization to the cytoplasm, most likely in response to posttranslational modification. As STIL dissociates from centrosomes at the time when Cdk1 is first activated, we explored a role for this key regulatory kinase in controlling STIL localization. Indeed, when two distinct Cdk1 inhibitors, RO-3306 or roscovitine, were added to cells shortly after entry into mitosis, the centrosomal STIL signal was completely stabilized (Figures 2C and 2E; Figure S3), indicating that activation of Cdk1 at the onset of mitosis triggers dissociation of STIL from centrosomes.

STIL and SAS-6 colocalize at newly forming procentrioles and depend partly on each other for localization [7–9], suggesting that both proteins interact at the cartwheel. Thus, we asked whether dissociation of STIL from centrosomes at

Collectively, these data indicate that STIL stabilizes SAS-6 association with centrosomes or vice versa.

The above results raised the possibility that cartwheel disassembly begins already during early mitosis. Thus, we analyzed centriolar STIL and SAS-6 levels in nocodazole-arrested prometaphase cells. Compared to prophase cells, which showed high levels of STIL and SAS-6 at centrosomes, the arrested cells showed reduced levels (Figures S4A and S4B), including 24% of centrosomes on which neither STIL nor SAS-6 could be detected. This suggests that complete loss of the cartwheel can occur as early as prior to spindle checkpoint silencing. Western blotting of cells arrested in nocodazole readily revealed a Cdk1-dependent upshift in STIL, but not SAS-6, pointing to STIL as a likely downstream target (Figure S4C).

The C-Terminal KEN Box Mediates Degradation of STIL by APC/C

To determine whether proteasome activity was required for loss of cytoplasmic STIL in later mitosis, we performed live-cell imaging on cells transiting from anaphase onset into G1 phase in the presence or absence of MG132 (Figures 4A and 4B; Movie S4). Proteasome inhibition clearly abolished the decrease in cytoplasmic STIL levels, in line with previous results [8, 9]. To provide direct evidence for degradation of STIL by the anaphase-promoting complex/cyclosome (APC/C), we took advantage of the observation that APC/C

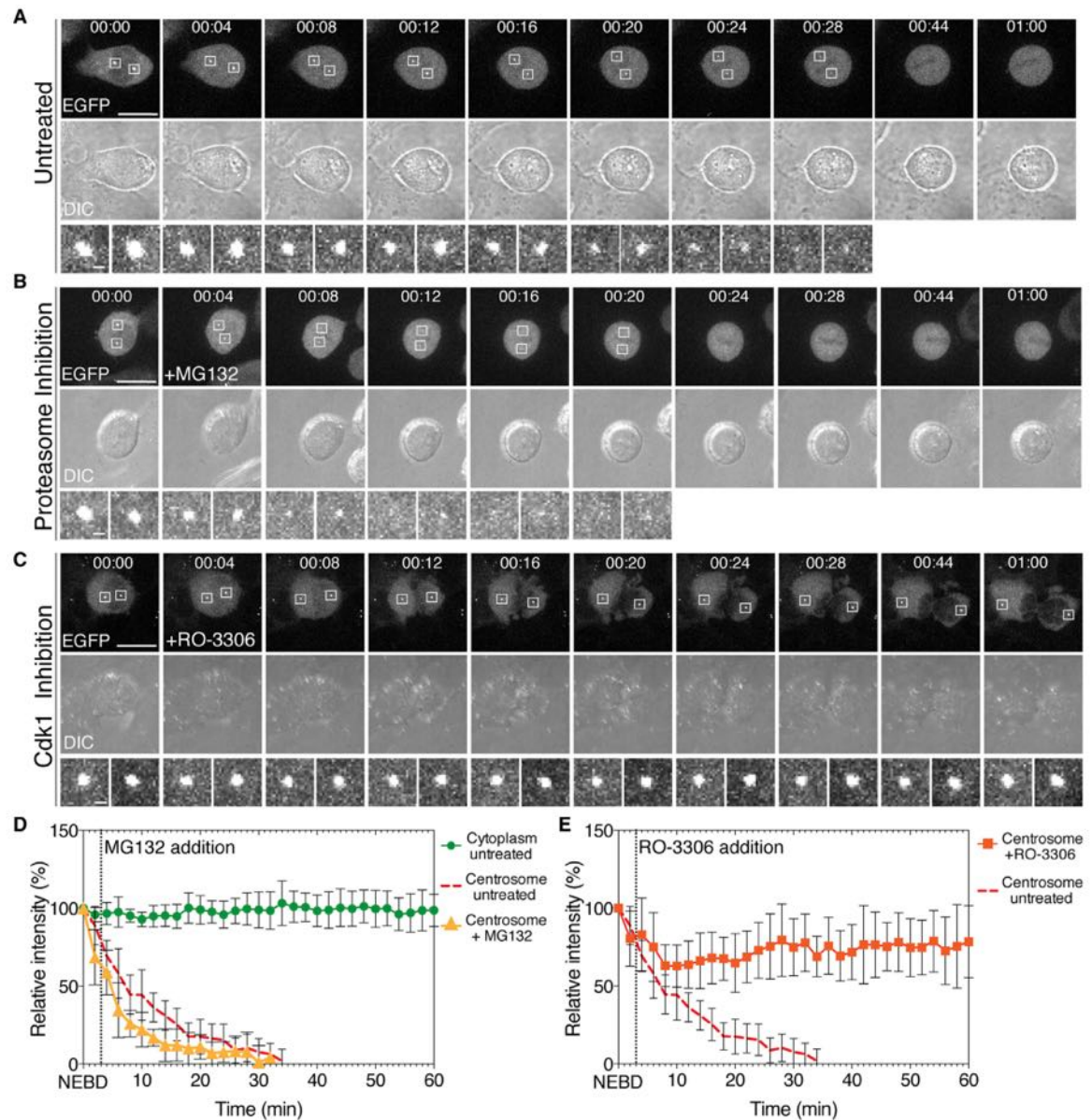
STIL MCPH Mutations Cause Centriole Amplification
 353


Figure 2. Cdk1 Triggers STIL Removal from Early Mitotic Centrosomes

(A–C) U2OS Flp-In T-REx:EGFP-STIL WT cells were filmed for 1 hr from NEBD to metaphase (Movies S2 and S3).

(A) Stills showing EGFP fluorescence (upper panels) and DIC (middle panels). Centrosomal EGFP-STIL signal is surrounded by white boxes, shown magnified in lower panels. Scale bars, 20 μ m (upper panels) and 1 μ m (lower panels).

(B) As in (A), except that 200 μ M MG132 was added after first image acquisition. (Note that under similar conditions, the APC/C^{Cdc20} substrate Nek2 was stabilized [23].)

(C) As above, except that 10 μ M RO-3306 was added after first image acquisition.

(D) Line graphs showing mean EGFP signal intensity for the experiments described in (A) and (B). Measurements were made in untreated cells, both in the cytoplasm (green circles; $n = 5$ cells, five experiments) and the centrosomal region (dashed red line; $n = 10$ centrosomes, five experiments) or in the centrosomal region of MG132-treated cells (yellow triangles; $n = 10$ centrosomes, five experiments). Dotted line marks time point of MG132 addition. Interestingly, STIL disappeared with slightly faster kinetics in MG132-treated cells, possibly reflecting enhanced Cdk1 activity in response to stabilization of cyclin A (see text). In (D) and (E), error bars represent \pm SD.

(E) Line graphs showing the mean EGFP signal intensity for the experiment described in (C); measurements were made in the centrosomal regions (orange squares; $n = 10$ centrosomes, five experiments). For comparison, the dashed red line shows data from untreated cells as in (D). Dotted line marks time point of RO-3306 addition.

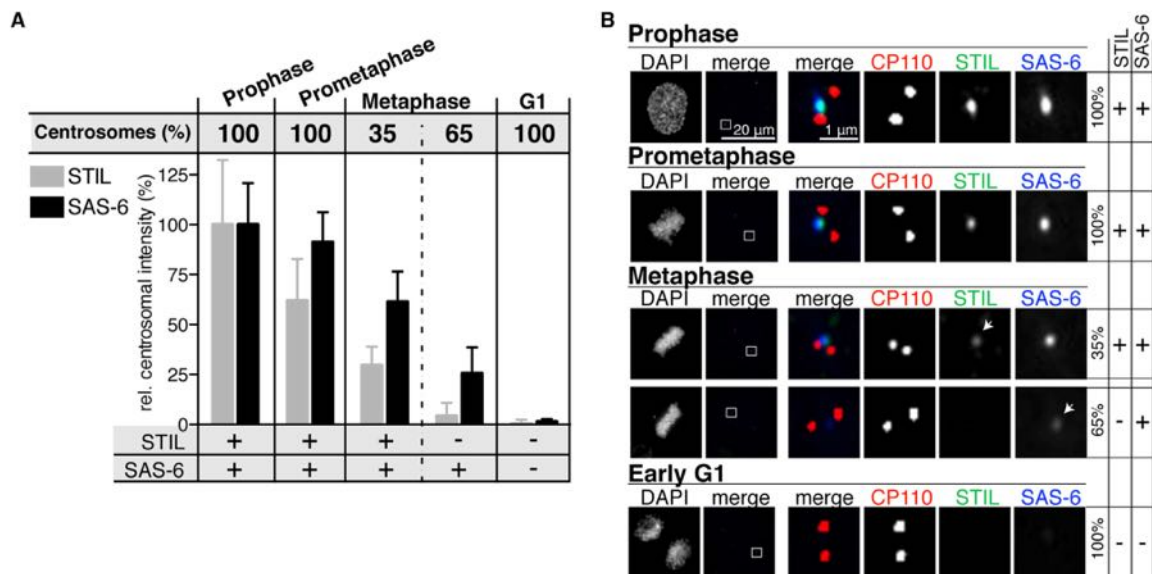


Figure 3. Dissociation of SAS-6 and STIL from Mitotic Centrosomes

(A) Graph showing relative fluorescence intensities of centrosomal STIL and SAS-6 staining in U2OS cells at the indicated stages (distinguished by DAPI). For each stage, 40 centrosomes were imaged and grouped into subcategories depending on STIL and SAS-6 signals, as indicated at the bottom of the graph. Staining intensities were quantified and background subtracted using ImageJ. Bars depict relative mean fluorescence intensities for centrosomal STIL (gray) and SAS-6 (black), after setting prophase intensities to 100%. The percentage of centrosomes within each subcategory is shown above the graph. Error bars represent \pm SD of individual intensity measurements.

(B) Representative images for each mitotic stage and each subcategory shown in (A), with percentages of centrosomes in each subcategory indicated on the right. White arrowheads point to centrosomal regions (in case of low signal intensity).

can be activated by exogenous expression of its coactivator Cdh1 [25]. We coexpressed FLAG-STIL with increasing amounts of myc-Cdh1 in human embryonic kidney (HEK) 293T cells and subsequently analyzed FLAG-STIL levels by western blotting. Myc-Cdh1 indeed triggered a drastic decrease in FLAG-STIL levels (Figure 4C), confirming that STIL is an APC/C target [9]. A strong effect of Cdh1 was also observed on FLAG-SAS-6, a known substrate of the APC/C [24] (Figure 4D), but not on EGFP (Figure 4E), confirming the specificity of this assay. Next, we used coexpression of Cdh1 with STIL truncations to map the part of STIL that mediates destruction by APC/C. Both the N-terminal and central parts of STIL resisted Cdh1 overexpression, whereas the C-terminal part was degraded (Figure 4F). This indicated that the C terminus of STIL harbors a signal for APC/C-mediated degradation, which was corroborated by analysis of STIL mutants lacking either the C or N terminus (Figure 4G).

APC/C-mediated degradation of substrate proteins depends on motifs, known as D boxes or KEN boxes, that allow recognition by the APC/C coactivators Cdc20 and Cdh1 [26]. A motif search identified five putative D boxes (RXXL) and one putative KEN box (KEN) within STIL (Figure 4H). Alanine substitutions of all potential degradation motifs and coexpression of the mutants with Cdh1 revealed that only mutation of the KEN box conferred significant stabilization (Figures 4I and 4J). The KEN box lies within the C terminus of STIL, in line with our mapping results (Figures 4F and 4G), indicating that it is the critical motif mediating APC/C-dependent degradation of human STIL during mitotic exit. Alignment of STIL sequences from different species revealed strong conservation of the KEN box among vertebrates, except for chicken,

suggesting utilization of another APC/C degradation motif in this species (Figure S5).

The KEN Box Is Lost in STIL Truncations of Microcephaly Patients

Mutations in the *STIL* gene have been linked to autosomal recessive primary microcephaly [19]. However, the molecular and cellular defects caused by these mutations are not understood. Given that two truncating mutations seen in patients (p.Gln1239X and p.Val1219X) cause loss of only 49 and 69 amino acids, respectively, from the C terminus of STIL [19], we were intrigued to find that these truncations remove the KEN box that we have identified here as critical for regulation of STIL stability (Figure 5A). This raised the possibility that development of primary microcephaly results from deregulation of STIL protein levels. To explore this provocative link, we first examined the response of the p.Gln1239X and p.Val1219X mutants to coexpression with Cdh1. As expected, both truncations showed substantial resistance to APC/C-mediated degradation (Figure 5B). Next, we analyzed the impact of these MCPH mutations on STIL localization and centriole duplication. Much like wild-type STIL, both mutants localized in a ring-like pattern around the central mother centriole, surrounded by an outer ring of the distal protein CP110 associated with multiple daughter centrioles (Figure 5C). In fact, transient overexpression of both MCPH mutants in U2OS cells promoted centriole amplification to an extent similar to overexpression of wild-type STIL (Figure 5D). Together, these results indicate that STIL truncations seen in microcephaly patients do not interfere with either correct localization or functionality of the STIL protein, in line with

STIL MCPH Mutations Cause Centriole Amplification
355

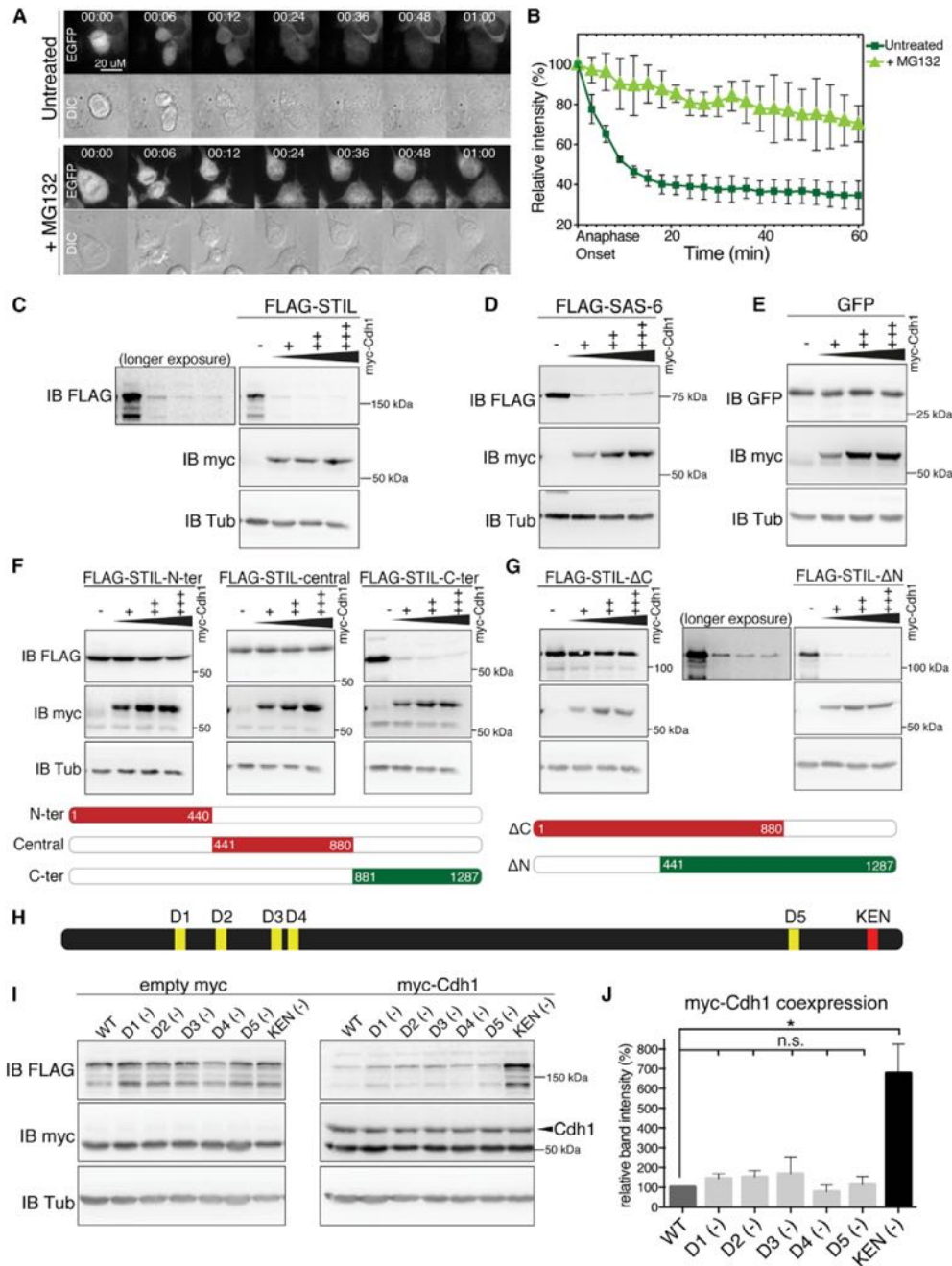


Figure 4. APC/C-Mediated Degradation of STIL Requires the C-Terminal KEN Box

(A) U2OS Fip-In T-REx:EGFP-STIL WT cells were filmed for 1 hr, from anaphase into G1, in the absence or presence of 100 μ M MG132 (Movie S4). Stills show EGFP fluorescence (upper panels) and DIC (lower panels).

(B) Line graphs representing mean cytoplasmic STIL WT signal intensity over time, as measured in three independent movies in the absence (dark green squares) or presence (light green triangles) of MG132. Error bars represent \pm SD.

(C) FLAG-STIL WT and increasing amounts of myc-Cdh1 (0, 2, 4, and 6 μ g) were coexpressed for 36 hr in HEK 293T cells before lysates were analyzed by western blotting using indicated antibodies. Empty myc vector was used to equal total amounts of DNA for each transfection, and α -tubulin was analyzed as loading control.

(D–G) Experiment as described in (C), except that myc-Cdh1 was coexpressed with FLAG-SAS-6 (D); EGFP (E); FLAG-STIL N terminus (aa 1–440), FLAG-STIL central part (aa 441–880), or FLAG-STIL C terminus (aa 881–1,287) (F); or FLAG-STIL Δ C terminus (aa 1–880) or FLAG-STIL Δ N terminus

(legend continued on next page)

previous results [7]. Further examination of various deletion mutants revealed that removal of up to 132 amino acids from the STIL C terminus did not detectably interfere with protein localization or potency to trigger centriole amplification (Figures 5E–5G). In contrast, partial or complete removal of the STAN motif, an evolutionarily conserved region [6], strongly interfered with correct localization and centriole amplification.

STIL p.Val1219X Causes Centriole Amplification

Having established that STIL mutations seen in microcephaly patients affect cell-cycle regulation of STIL expression, we carried out experiments aimed at uncovering the cellular consequences of STIL deregulation in microcephaly. As no patient material was available, we constructed a U2OS Flp-In T-REx cell line stably expressing EGFP-STIL p.Val1219X and compared its properties to the line expressing STIL WT (Figures 6A and 6B; Movie S5). STIL p.Val1219X (originally designated as p.Leu1218X) represents a mutation described in two unrelated Indian families [19]. We filmed cells for 5 hr, covering passage from metaphase into the next cell cycle (Figures 6A and 6B). Within minutes, STIL WT levels fell to around 30%–40% of preanaphase values and then remained low for about 3 hr, before rising again as cells entered late G1/early S phase (see also Figures 1A and 1C). In stark contrast, cytoplasmic levels of the truncated EGFP-STIL p.Val1219X remained stable throughout the experiment (Figures 6A and 6B). This demonstrates that EGFP-STIL p.Val1219X resists APC/C-mediated degradation, in line with deletion of the KEN box. On the other hand, filming of cells transiting from NEBD to metaphase showed that STIL p.Val1219X dissociates from early mitotic centrosomes (Figure S6; Movie S6), much like wild-type STIL (Figures 2A and 2D). We conclude that removal of 69 amino acids from the STIL C terminus in the microcephaly mutant p.Val1219X does not impair Cdk1-regulated dissociation of STIL from early mitotic centrosomes but completely abolishes its degradation in late mitosis. To corroborate the latter conclusion, we compared levels of wild-type and truncated STIL in U2OS Flp-In T-REx cell lines by western blotting. After induction of protein expression by tetracycline for 24, 48, or 72 hr, levels of truncated STIL were significantly higher than those of wild-type STIL at all time points (Figure 6C). As both EGFP-STIL WT and EGFP-STIL p.Val1219X are inserted into the same genomic locus, positional effects on protein expression can be largely excluded. Instead, our data indicate that deletion of the KEN box from the p.Val1219X microcephaly version of STIL causes a strong accumulation of this mutant protein.

Finally, and most importantly, the above results raised the question of whether the stabilization of microcephaly mutant STIL might trigger centriole amplification. Having established that expression of wild-type EGFP-STIL in our U2OS Flp-In T-REx model does not cause centriole amplification, because APC/C-mediated degradation limits its accumulation (Figure 1C; Figure S1C), we were in a position to ask whether truncation of the KEN box might cause an accumulation of EGFP-STIL p.Val1219X sufficient to trigger centriole

amplification. Thus, both wild-type and mutant STIL proteins were expressed for 24, 48, or 72 hr before cells were stained with anti-CP110 antibodies and centriole numbers counted (Figures 6D and 6E). Expression of EGFP-STIL WT did not produce any centriole amplification above background levels, in line with data shown above (Figure S1C). In stark contrast, expression of STIL p.Val1219X caused a marked increase in centriole numbers (Figure 6D). These results indicate that removal of the KEN box from the p.Val1219X microcephaly mutant version of STIL confers sufficient stabilization to trigger centriole amplification. This invites the attractive hypothesis that microcephaly in human patients carrying the p.Val1219X mutation is caused by the abrogation of STIL cell-cycle regulation.

Discussion

Here we have used time-lapse imaging to analyze the regulation of STIL levels and localization at the single-cell level, with a special focus on traverse of mitosis. Our results lead to two important conclusions. First, we have identified a role for Cdk1 in STIL dissociation from centrosomes during early mitosis, a finding that bears on the cell-cycle regulation of cartwheel disassembly. Second, we have uncovered a provocative mechanistic link to primary microcephaly. We show that a KEN box destruction motif is critical for STIL proteolysis and control of centriole numbers. This motif is deleted in STIL microcephaly truncations, which highlights the importance of orderly STIL cell-cycle regulation and suggests that deregulation of STIL turnover and ensuing centriole amplification constitute the underlying cause of MCPH in the corresponding patients.

A Role for CDK1 in Triggering Cartwheel Disassembly

The cartwheel is a key structural element conferring 9-fold symmetry to nascent centrioles [10]. It is thought to be assembled and disassembled in every cell cycle, but neither the exact timing nor the mechanism underlying cartwheel disassembly is well understood. Here we show that the activation of Cdk1 triggers progressive dissociation of STIL from early mitotic centrosomes. Thus, STIL is likely to be a direct substrate of Cdk1 [4], although indirect mechanisms are not excluded. We also find that the major cartwheel component SAS-6 is progressively lost from centrosomes upon NEBD, albeit with slower kinetics than STIL. Collectively, our data indicate that Cdk1 activation at NEBD initiates cartwheel disassembly, possibly by phosphorylation of STIL, and that release of both STIL and SAS-6 from mitotic centrosomes precedes their APC/C-dependent degradation at mitotic exit. This proposed two-step mechanism contributes to coordinate cartwheel disassembly with cell-cycle progression.

STIL Is Degraded after Anaphase Onset by the APC/C

Here, we show that STIL is a target of the APC/C, extending our previous observations [9]. By mutational inactivation of all putative D boxes and KEN boxes, we identify the KEN box as the critical degradation motif, indicating that APC/C^{Cdh1} is

(aa 441–1,287) (G). Schematic representations of STIL truncations used in (F) and (G) are shown below. Constructs depicted in red resisted myc-Cdh1 coexpression; constructs shown in green were degraded.

(H) Schematic representation of five putative D boxes (yellow) and one putative KEN box (red).

(I) FLAG-STIL constructs carrying alanine-substituted D boxes or KEN boxes were coexpressed in HEK 293T cells with empty myc vector or myc-Cdh1 (2 μ g). After 36 hr, lysates were analyzed by western blotting using the indicated antibodies. α -tubulin was analyzed as loading control.

(J) Graph depicting band intensities from western blots, as shown in (I). $n = 3$ independent experiments; error bars represent \pm SD; n.s., not significant; * $p < 0.05$.

STIL MCPH Mutations Cause Centriole Amplification
357

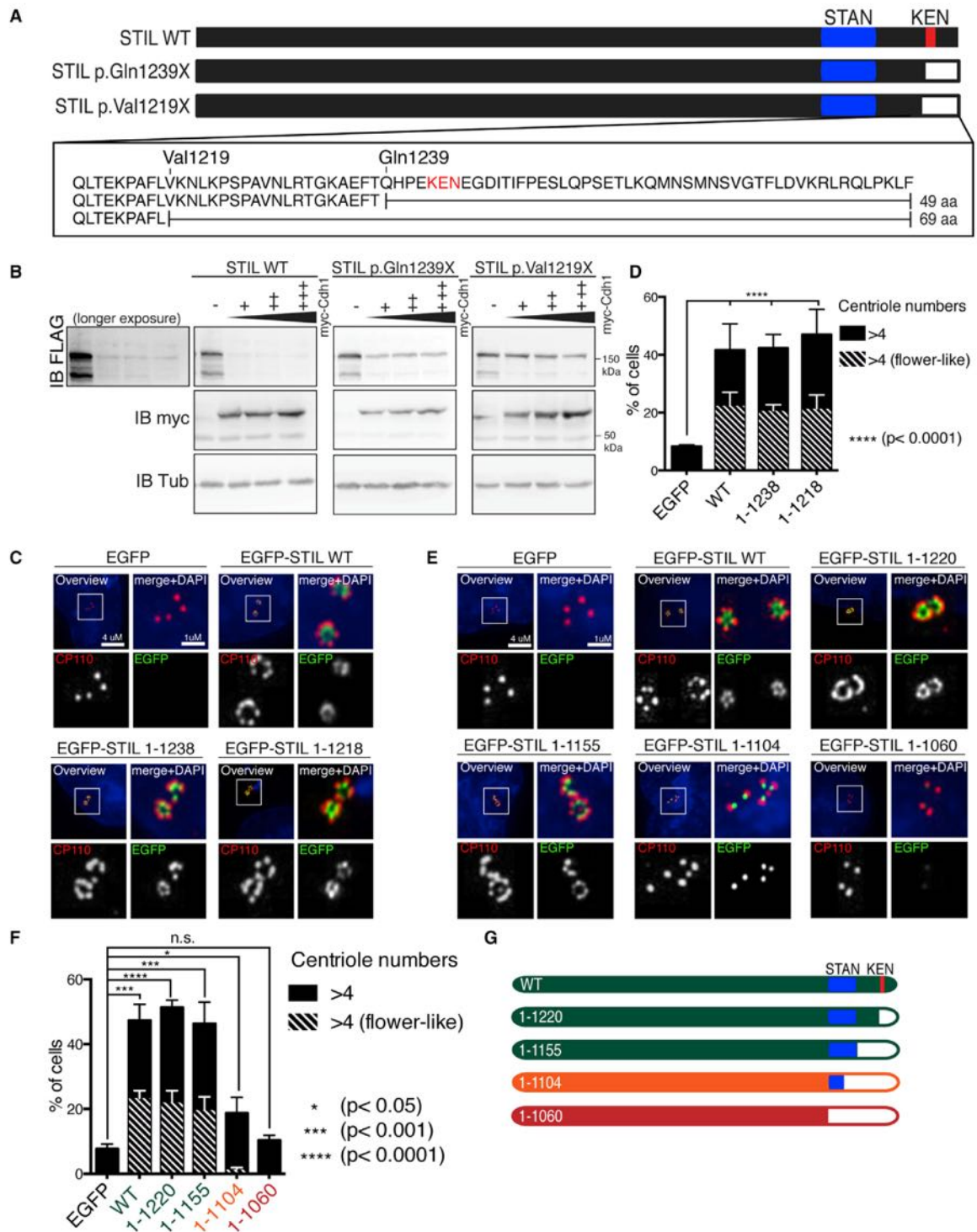


Figure 5. STIL Microcephaly Truncations Are Functional but Lack the KEN Box

(A) Schematic representations of STIL WT and STIL microcephaly truncations. The STAN motif (blue) and KEN box (red) are indicated.
 (B) The indicated FLAG-STIL constructs and increasing amounts of myc-Cdh1 (0, 2, 4, and 6 μ g) were coexpressed for 36 hr in HEK 293T cells before lysates were analyzed by western blotting using indicated antibodies. Empty myc vector was used to equal total amounts of DNA; α -tubulin was analyzed as loading control.
 (legend continued on next page)

the key driver behind STIL destruction. As single depletion of Cdh1 failed to stabilize STIL [9], it seems likely that Cdc20 can compensate for the absence of Cdh1, as observed previously for other KEN box-containing Cdh1 substrates [27]. Furthermore, it remains possible that Cdc20 contributes to STIL degradation early after anaphase onset [9].

STIL Truncations in MCPH Patients Cause Centriole Amplification

Many mutations in genes associated with MCPH are thought to functionally inactivate the corresponding proteins [12]. However, this is not the case for the MCPH-related STIL mutations examined in this study. When transiently overexpressed in U2OS cells, two different MCPH STIL truncations (p.Val1219X and p.Gln1239X) promoted centriole amplification to the same extent as wild-type STIL, attesting to their functionality in centriole biogenesis (see also [7]). Similar results were obtained (data not shown) with a recently identified MCPH missense mutation termed p.L798W [18]. Thus, we conclude that centriole formation is not fundamentally impaired in the corresponding microcephaly patients. One described MCPH mutation (IVS16DS, G-A, +1) has been proposed to truncate STIL upstream of the STAN motif [19], but alternative interpretations have not been excluded. As disruption of the STAN motif clearly interferes with STIL function (this study, [7]), it would be important to examine the functionality of STIL in the corresponding patients. Considering that genetic knockouts of *STIL* cause embryonic lethality in both mouse and zebrafish [2, 3], it seems unlikely that complete loss of STIL function would be compatible with life in humans. Instead of causing loss of function, our study reveals that at least two STIL MCPH mutations result in a gain of function. Specifically, these truncations delete a critical KEN box from the C-terminal region of STIL, which leads to STIL stabilization and triggers centriole amplification.

Centriole Amplification, a Root Cause of Microcephaly?

Centriole amplification has attracted great interest from the perspective of genome instability and cancer [28–31] but has not generally been considered a likely mechanism for causing MCPH. Yet, supernumerary centrosomes have been noted in patients or mouse models with mutations in microcephalin (MCPH1), Cep135 (MCPH8), or Cdk5rap2 (MCHP3) [15, 32, 33]. Moreover, a recent study on a mouse model of centriole amplification directly demonstrates that supernumerary centrosomes are able to impair brain development. In this study [34], centriole amplification was induced in the developing mouse brain by overexpression of *Plk4* and was found to result in significantly smaller brains. Interestingly, spindle orientation was not significantly disturbed in *Plk4*-overexpressing neuroprogenitors. Instead, a high proportion of neuroprogenitors exhibited aneuploidy and underwent apoptosis, providing an attractive alternative explanation for depletion of the neuroprogenitor pool.

Our present data establish a direct link between centriole amplification and STIL mutations in MCPH patients. It will

be interesting in future studies to explore whether MCPH mutations in other centriole duplication factors, notably CPAP, Cep135, and Cep152, also affect centriole numbers. Of particular interest in this context is the finding that CPAP interacts with STIL [7, 8]. Moreover, recent studies on the structure of CPAP-STIL complexes suggest that CPAP mutations interfere with STIL binding and centriole biogenesis [35, 36].

Experimental Procedures

Generation of U2OS Flp-In T-REx Cell Lines

U2OS Flp-In T-REx cells were generated according to manufacturer protocols (Invitrogen). To select for transgene integration, we used complete Dulbecco's modified Eagle's medium with 10% tetracycline-free fetal bovine serum (PAA), 5% PenStrep (Invitrogen), 100 μ g/ml hygromycin (Invitrogen), and 15 μ g/ml blasticidine (Invitrogen).

Cell Culture and Transfections

U2OS and HEK 293T cells were grown under standard conditions. Transient transfections were performed with TransIT-LT1 (MirusBio).

Cell Extracts and Western Blots

Cells were lysed in Tris lysis buffer (20 mM Tris-HCl [pH 7.4], 150 mM NaCl, 0.5% IGEPAL CA-630) with protease and phosphatase inhibitors. Polyclonal anti-STIL (Abcam), polyclonal anti-GFP (Abcam), monoclonal anti-myc (Millipore), monoclonal anti-Flag (Sigma), monoclonal anti-hSAS-6 [37], and mouse anti- α -tubulin (Sigma) were used for western blotting.

Statistical Analysis

All p values were derived from unpaired two-tailed t tests.

Supplemental Information

Supplemental Information includes six figures, Supplemental Experimental Procedures, and six movies and can be found with this article online at <http://dx.doi.org/10.1016/j.cub.2013.12.016>.

Acknowledgments

We are grateful to Stephen C. Blacklow (Harvard Medical School), Jeff Parvin (Ohio State University Medical Center), and Peter Jackson (Genentech) for sharing cell lines and reagents. We thank Alexia Ferrand, Niko Ehrenfeuchter, and Oliver Biehler (Imaging Core Facility, Biozentrum, University of Basel) for assistance with microscopy and Thorsten Schmidt, Elisabeth Bürgelt, and Elena Nigg for providing anti-CP110 monoclonal antibodies. We further thank Elena Nigg for technical assistance and Alwin Krämer (DKFZ, Heidelberg) as well as members of the Krämer and Nigg laboratories for helpful discussions. This work was supported by the Swiss National Science Foundation (grant 310030B_149641/1). C.A. was funded by a PhD fellowship from the Werner Siemens-Foundation (Zug, Switzerland).

Received: August 27, 2013

Revised: November 20, 2013

Accepted: December 9, 2013

Published: January 30, 2014

References

1. Aplan, P.D., Lombardi, D.P., and Kirsch, I.R. (1991). Structural characterization of SIL, a gene frequently disrupted in T-cell acute lymphoblastic leukemia. *Mol. Cell. Biol.* 11, 5462–5469.

(C) The indicated microcephaly-related STIL constructs were transiently overexpressed in U2OS cells for 48 hr before cells were fixed and centrioles stained with anti-CP110 antibodies (red). EGFP is shown in green; DNA was stained with DAPI (blue).

(D) Graph representing percentages of cells with multiple centrioles (>4; black bars) and the fraction thereof bearing flower-like arrangements (hashed bars) (see C). A total of 300 cells were analyzed in three independent experiments. In (D) and (F), error bars represent \pm SD.

(E and F) Experiment as described in (C) and (D), except that systematic STIL deletion constructs were analyzed.

(G) Schematic representation of STIL versions used for transfections in (E). Truncations that support centriole amplification are shown in green; partially functional or nonfunctional truncations are depicted in orange and red, respectively.

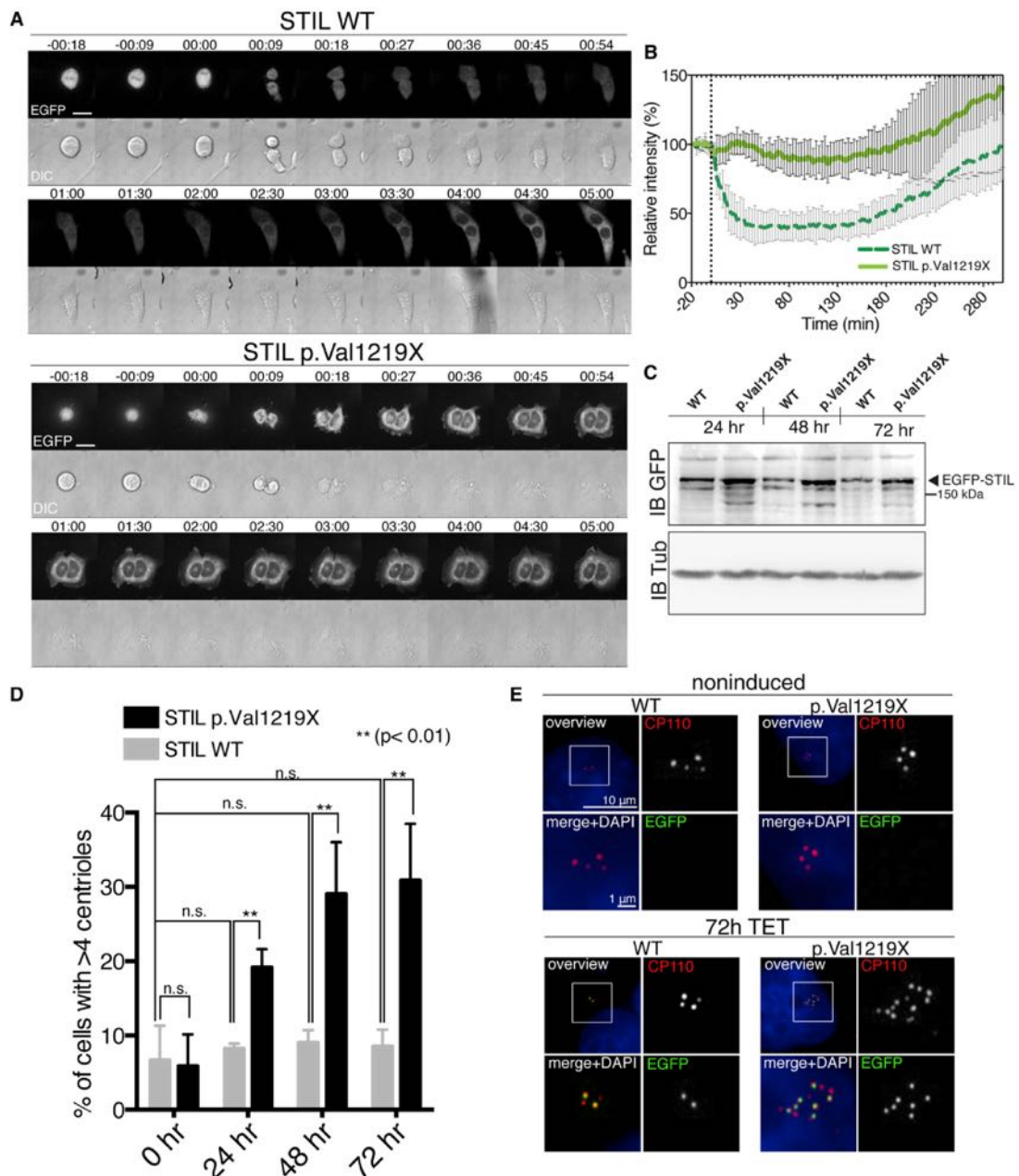
STIL MCPH Mutations Cause Centriole Amplification
 359


Figure 6. STIL p.Val1219X Resists APC/C-Mediated Degradation and Causes Centriole Amplification

(A) Real-time visualization of cytoplasmic EGFP-STIL WT and EGFP-STIL p.Val1219X in U2OS Flp-In T-REx cells filmed from metaphase into the next cell cycle (see *Movie S5*). Stills show EGFP fluorescence (upper panels) and DIC (lower panels). Scale bar, 20 μ m.

(B) Line graphs representing mean signal intensity over time for cytoplasmic STIL WT (dark green dashed line) or STIL p.Val1219X (light green line), measured in movies from (A) ($n = 5$). Error bars represent \pm SD for each time point.

(C) Western blot analysis of EGFP-STIL WT and EGFP-STIL p.Val1219X after 24, 48, or 72 hr of expression in U2OS Flp-In T-REx cells. Blots were probed with antibodies against EGFP and α -tubulin (loading control).

(D) Graph representing the percentage of cells with more than four centrioles after expression of EGFP-STIL WT (gray bars) or EGFP-STIL p.Val1219X (black bars) in U2OS Flp-In T-REx cells for 0, 24, 48, or 72 hr. Centrioles were counted by fluorescence microscopy after CP110 staining. A total of 600 cells were analyzed in three independent experiments. Error bars represent \pm SD. Note that 5%–10% of all U2OS Flp-In T-REx cells display multiple centrioles prior to any treatment.

(E) Representative images for cells analyzed in (D). Fixed cells were stained with antibodies against CP110 (red), and DAPI was used to stain DNA (blue). EGFP is shown in green.

2. Izraeli, S., Lowe, L.A., Bertness, V.L., Good, D.J., Dorward, D.W., Kirsch, I.R., and Kuehn, M.R. (1999). The SIL gene is required for mouse embryonic axial development and left-right specification. *Nature* 399, 691–694.
3. Pfaff, K.L., Straub, C.T., Chiang, K., Bear, D.M., Zhou, Y., and Zon, L.I. (2007). The zebra fish *cassiopia* mutant reveals that SIL is required for mitotic spindle organization. *Mol. Cell. Biol.* 27, 5887–5897.
4. Campaner, S., Kaldis, P., Izraeli, S., and Kirsch, I.R. (2005). Sil phosphorylation in a Pin1 binding domain affects the duration of the spindle checkpoint. *Mol. Cell. Biol.* 25, 6660–6672.
5. Erez, A., Castiel, A., Trakhtenbrot, L., Perelman, M., Rosenthal, E., Goldstein, I., Stettner, N., Harmelin, A., Eldar-Finkelman, H., Campaner, S., et al. (2007). The SIL gene is essential for mitotic entry and survival of cancer cells. *Cancer Res.* 67, 4022–4027.
6. Stevens, N.R., Dobbelaere, J., Brunk, K., Franz, A., and Raff, J.W. (2010). *Drosophila* Ana2 is a conserved centriole duplication factor. *J. Cell Biol.* 188, 313–323.
7. Vulprecht, J., David, A., Tibelius, A., Castiel, A., Konotop, G., Liu, F., Bestvater, F., Raab, M.S., Zentgraf, H., Izraeli, S., and Krämer, A. (2012). STIL is required for centriole duplication in human cells. *J. Cell Sci.* 125, 1353–1362.
8. Tang, C.-J.C., Lin, S.-Y., Hsu, W.-B., Lin, Y.-N., Wu, C.-T., Lin, Y.-C., Chang, C.-W., Wu, K.-S., and Tang, T.K. (2011). The human microcephaly protein STIL interacts with CPAP and is required for procentriole formation. *EMBO J.* 30, 4790–4804.
9. Arquint, C., Sonnen, K.F., Stierhof, Y.-D., and Nigg, E.A. (2012). Cell-cycle-regulated expression of STIL controls centriole number in human cells. *J. Cell Sci.* 125, 1342–1352.
10. Gönczy, P. (2012). Towards a molecular architecture of centriole assembly. *Nat. Rev. Mol. Cell Biol.* 13, 425–435.
11. Kaindl, A.M., Passemard, S., Kumar, P., Kraemer, N., Issa, L., Zwirner, A., Gerard, B., Verloes, A., Mani, S., and Gressens, P. (2010). Many roads lead to primary autosomal recessive microcephaly. *Prog. Neurobiol.* 90, 363–383.
12. Thornton, G.K., and Woods, C.G. (2009). Primary microcephaly: do all roads lead to Rome? *Trends Genet.* 25, 501–510.
13. Kitagawa, D., Kohimaier, G., Keller, D., Strnad, P., Balestra, F.R., Flücker, I., and Gönczy, P. (2011). Spindle positioning in human cells relies on proper centriole formation and on the microcephaly proteins CPAP and STIL. *J. Cell Sci.* 124, 3884–3893.
14. Fish, J.L., Kosodo, Y., Enard, W., Pääbo, S., and Huttner, W.B. (2006). Aspm specifically maintains symmetric proliferative divisions of neuroepithelial cells. *Proc. Natl. Acad. Sci. USA* 103, 10438–10443.
15. Alderton, G.K., Galbiati, L., Griffith, E., Surinya, K.H., Neitzel, H., Jackson, A.P., Jeggo, P.A., and O'Driscoll, M. (2006). Regulation of mitotic entry by microcephalin and its overlap with ATR signalling. *Nat. Cell Biol.* 8, 725–733.
16. Barr, A.R., Kilmartin, J.V., and Gergely, F. (2010). CDK5RAP2 functions in centrosome to spindle pole attachment and DNA damage response. *J. Cell Biol.* 189, 23–39.
17. Yang, S.-Z., Lin, F.-T., and Lin, W.-C. (2008). MCPH1/BRIT1 cooperates with E2F1 in the activation of checkpoint, DNA repair and apoptosis. *EMBO Rep.* 9, 907–915.
18. Papari, E., Bastami, M., Farhadi, A., Abedini, S.S., Hosseini, M., Bahman, I., Mohseni, M., Garshasbi, M., Moheb, L.A., Behjati, F., et al. (2013). Investigation of primary microcephaly in Bushehr province of Iran: novel STIL and ASPM mutations. *Clin. Genet.* 83, 488–490.
19. Kumar, A., Girimaji, S.C., Duvvari, M.R., and Blanton, S.H. (2009). Mutations in STIL, encoding a pericentriolar and centrosomal protein, cause primary microcephaly. *Am. J. Hum. Genet.* 84, 286–290.
20. Izraeli, S., Colaizzo-Anas, T., Bertness, V.L., Mani, K., Aplan, P.D., and Kirsch, I.R. (1997). Expression of the SIL gene is correlated with growth induction and cellular proliferation. *Cell Growth Differ.* 8, 1171–1179.
21. Sonnen, K.F., Schermelleh, L., Leonhardt, H., and Nigg, E.A. (2012). 3D-structured illumination microscopy provides novel insight into architecture of human centrosomes. *Biol. Open* 1, 965–976.
22. Lukinavičius, G., Lavogina, D., Orpinell, M., Umezawa, K., Raymond, L., Garin, N., Gönczy, P., and Johnsson, K. (2013). Selective chemical crosslinking reveals a Cep57-Cep63-Cep152 centrosomal complex. *Curr. Biol.* 23, 265–270.
23. Hayes, M.J., Kimata, Y., Wattam, S.L., Lindon, C., Mao, G., Yamano, H., and Fry, A.M. (2006). Early mitotic degradation of Nek2A depends on Cdc20-independent interaction with the APC/C. *Nat. Cell Biol.* 8, 607–614.
24. Strnad, P., Leidel, S., Vinogradova, T., Euteneuer, U., Khodjakov, A., and Gönczy, P. (2007). Regulated HsSAS-6 levels ensure formation of a single procentriole per centriole during the centrosome duplication cycle. *Dev. Cell* 13, 203–213.
25. Kramer, E.R., Scheuringer, N., Podtelejnikov, A.V., Mann, M., and Peters, J.M. (2000). Mitotic regulation of the APC activator proteins CDC20 and CDH1. *Mol. Biol. Cell* 11, 1555–1569.
26. Peters, J.-M. (2006). The anaphase promoting complex/cyclosome: a machine designed to destroy. *Nat. Rev. Mol. Cell Biol.* 7, 644–656.
27. Gurden, M.D.J.M., Holland, A.J.A., van Zon, W.W., Tighe, A.A., Vergnolle, M.A.M., Andres, D.A.D., Spielmann, H.P.H., Malumbres, M.M., Wolthuis, R.M.F.R., Cleveland, D.W.D., and Taylor, S.S. (2010). Cdc20 is required for the post-anaphase, KEN-dependent degradation of centromere protein F. *J. Cell Sci.* 123, 321–330.
28. Basto, R., Brunk, K., Vinadogrova, T., Peel, N., Franz, A., Khodjakov, A., and Raff, J.W. (2008). Centrosome amplification can initiate tumorigenesis in flies. *Cell* 133, 1032–1042.
29. Ganem, N.J., Godinho, S.A., and Pellman, D. (2009). A mechanism linking extra centrosomes to chromosomal instability. *Nature* 460, 278–282.
30. Zys, D., and Gergely, F. (2009). Centrosome function in cancer: guilty or innocent? *Trends Cell Biol.* 19, 334–346.
31. Nigg, E.A. (2006). Origins and consequences of centrosome aberrations in human cancers. *Int. J. Cancer* 119, 2717–2723.
32. Hussain, M.S., Baig, S.M., Neumann, S., Nürnberg, G., Farooq, M., Ahmad, I., Alef, T., Hennies, H.C., Technau, M., Altmüller, J., et al. (2012). A truncating mutation of CEP135 causes primary microcephaly and disturbed centrosomal function. *Am. J. Hum. Genet.* 90, 871–878.
33. Barrera, J.A., Kao, L.-R., Hammer, R.E., Seemann, J., Fuchs, J.L., and Megraw, T.L. (2010). CDK5RAP2 regulates centriole engagement and cohesion in mice. *Dev. Cell* 18, 913–926.
34. Marthiens, V., Rujano, M.A., Pennetier, C., Tessier, S., Paul-Gilloteaux, P., and Basto, R. (2013). Centrosome amplification causes microcephaly. *Nat. Cell Biol.* 15, 731–740.
35. Cottee, M.A., Muschalik, N., Wong, Y.L., Johnson, C.M., Johnson, S., Andreeva, A., Oegema, K., Lea, S.M., Raff, J.W., and van Breugel, M. (2013). Crystal structures of the CPAP/STIL complex reveal its role in centriole assembly and human microcephaly. *Elife* 2, e01071.
36. Hatzopoulos, G.N., Erat, M.C., Cutts, E., Rogala, K.B., Slater, L.M., Stansfeld, P.J., and Vakonakis, I. (2013). Structural analysis of the G-box domain of the microcephaly protein CPAP suggests a role in centriole architecture. *Structure* 21, 2069–2077.
37. Kleylein-Sohn, J., Westendorf, J., Le Clech, M., Habedanck, R., Stierhof, Y.-D., and Nigg, E.A. (2007). Plk4-induced centriole biogenesis in human cells. *Dev. Cell* 13, 190–202.

Supplemental Information

STIL Microcephaly Mutations Interfere with APC/C-Mediated Degradation and Cause Centriole Amplification

Christian Arquint and Erich A. Nigg

Published in Current Biology

Volume 24

Accepted 09 December 2013

Published 30 January 2014

Figure S1

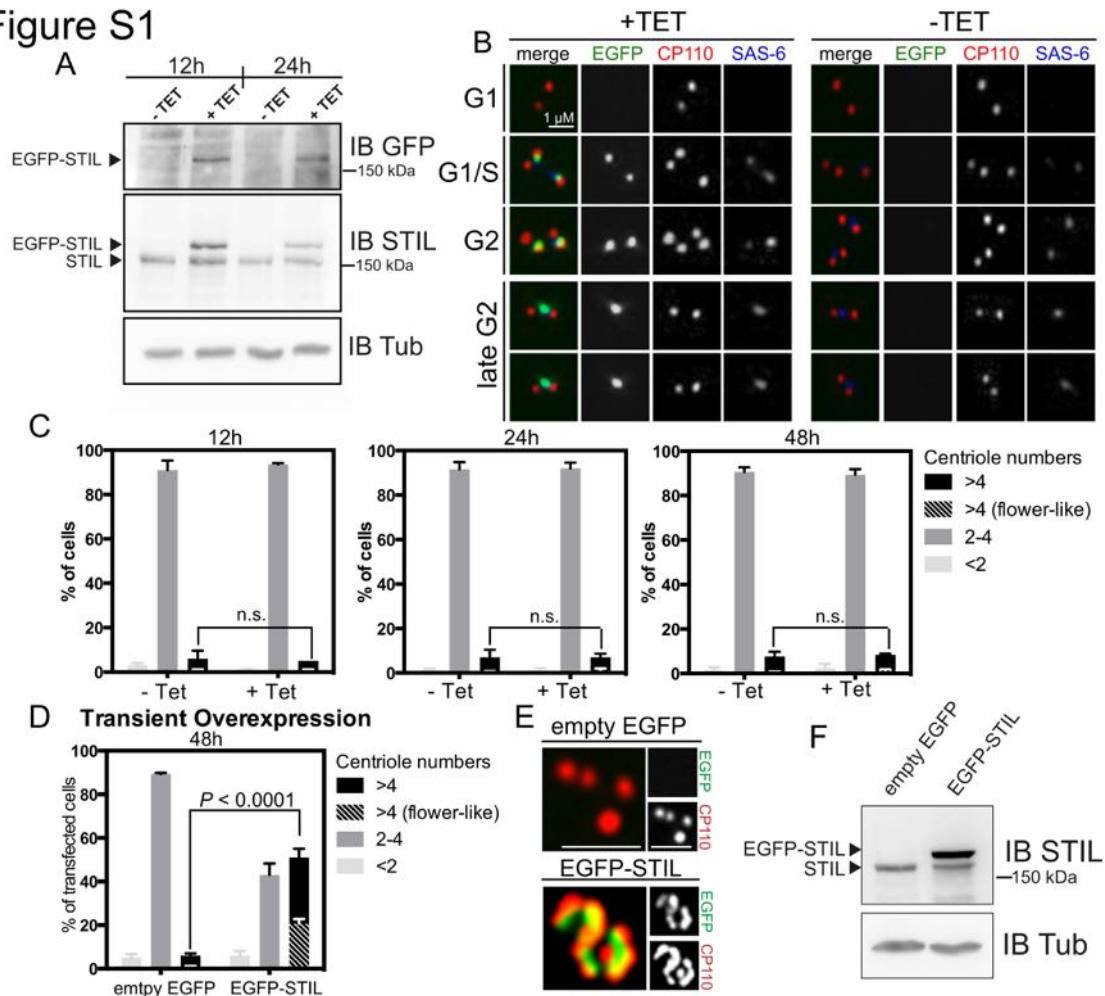


Fig. S1: U2OS Flp-In T-REx cells expressing EGFP-STIL WT at near-endogenous levels. Related to Figure 1.

A Western blot analysis was used to compare the expression of EGFP-STIL and endogenous STIL in a U2OS Flp-In T-REx:EGFP-STIL WT cell line. Transgene expression was induced for 12 or 24 hours and blots were probed with antibodies against EGFP, STIL or alpha-tubulin (loading control). **B** Analysis of EGFP-STIL localization to centrosomes in fixed U2OS Flp-In T-REx:EGFP-STIL WT cells by immunofluorescence microscopy. Antibodies targeting CP110 (red) and SAS-6 (blue) were used for immunostaining of fixed cells. EGFP is shown in green. Representative images are shown for the different cell cycle stages (determined by the number of centrioles). Note that CP110 localizes at the distal tips of all centrioles, whereas SAS-6 and STIL co-localize only in the proximal regions of newly forming daughter centrioles. **C** Graphs representing centriole numbers in U2OS Flp-In T-REx cells expressing EGFP-STIL WT for 12, 24 or 48 hours. Centriole numbers were determined by fluorescence microscopy after CP110 staining. Percentages of cells having multiple centrioles (>4; black bars) and the fraction thereof bearing multiple centrioles arranged around one parental centriole (flower-like arrangements; black white striped bars) are shown. A total of 300 cells were analyzed in 3 different experiments. N.s. denotes P value > 0.05 **D** Graph representing centriole numbers after transient overexpression of EGFP or EGFP-STIL WT in U2OS cells for 48 hours. Cells were fixed and immunostained with anti-CP110 antibodies before counting centrioles by fluorescence microscopy. Percentage of cells having multiple centrioles (>4; black bars) and the fraction thereof bearing multiple centrioles arranged around one parental centriole (flower-like; black white striped bars) are shown. A total of 300 cells were analyzed in 3 independent experiments. **E** Representative images of U2OS cells transiently expressing EGFP or EGFP-STIL WT, fixed and stained with anti-CP110 antibodies (red) for immunofluorescence microscopy. EGFP is shown in green. Both scale bars indicate 1 μ m. **F** Western blot analysis of transient EGFP-STIL and endogenous STIL expression in U2OS cells, after transfection for 48 hours. Antibodies targeting STIL or alpha-tubulin were used for probing. Alpha-tubulin was used as loading control. In C-D, error bars denote \pm -SD.

Figure S2

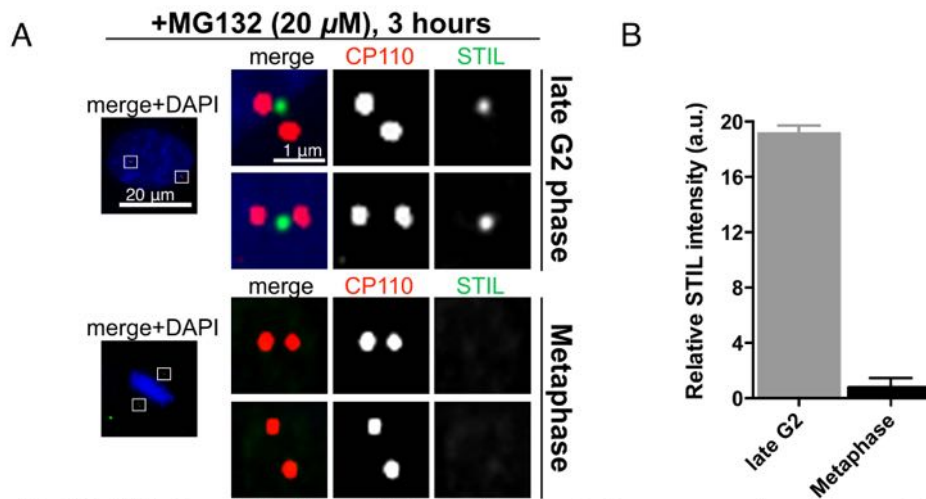


Fig. S2: STIL dissociation from mitotic centrosomes in the presence of proteasome inhibition. Related to Figure 2B.

A After treating U2OS cells with the proteasome inhibitor MG132 (20 μ M) for 3 hours, cells were fixed and stained with antibodies against STIL (green) and CP110 (red). DAPI is depicted in blue. Representative images of late G2 and metaphase cells are shown. **B** Graph representing relative mean fluorescence intensities of STIL stainings at late G2 (grey bar) and metaphase (black bar) centrosomes, as measured in MG132-treated U2OS cells from A. A total of 180 centrosomes (90 late G2 and 90 metaphase) were analyzed. Error bars denote +/-SD (3 independent experiments).

Figure S3

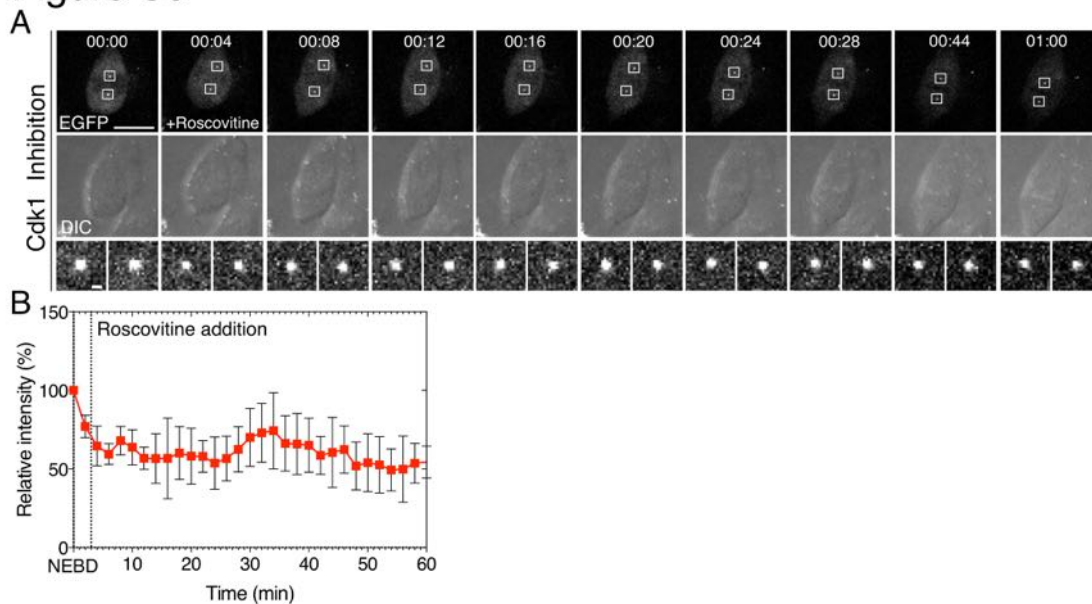


Fig. S3: Roscovitine treatment does stabilize STIL at mitotic centrosomes. Related to Figure 2C.

Real time visualization of EGFP-STIL distribution in U2OS Flp-In T-REx:EGFP-STIL WT cells filmed for 1 hour from NEBD to metaphase (see movie S3B) in the presence of $100\mu\text{M}$ roscovitine. **A** Stills show EGFP fluorescence (EGFP; upper panels) and differential interference contrast microscopy (DIC; middle panels). Centrosomal EGFP-STIL signal is surrounded by white boxes and shown with 10x magnification in lower panels. Scale bars indicate $20\mu\text{m}$ (upper panels) or $1\mu\text{m}$ (lower panels). **B** Line graph showing mean EGFP intensity over time measured in the centrosomal regions ($n=6$ centrosomes, 3 independent experiments). Timepoint of roscovitine addition is indicated by a vertical dotted line. Error bars denote \pm SD.

Figure S4

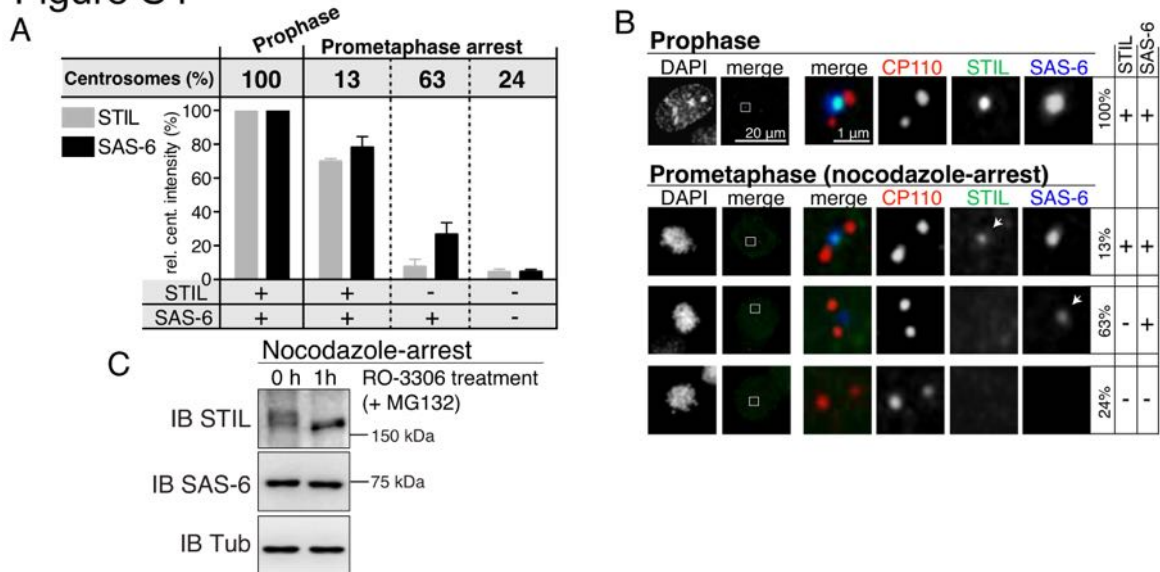


Fig. S4: Dissociation of SAS-6 and STIL from centrosomes in nocodazole-arrested prometaphase cells. Related to Figure 3.

A Graph representing relative mean fluorescence intensities of STIL (grey bars) and SAS-6 (black bars) stainings at centrosomes in prophase and nocodazole-arrested prometaphase U2OS cells. After nocodazole treatment (50 ng ml⁻¹ nocodazole; 12 hours), cells were fixed and stained with indicated antibodies. A total of 300 prophase and 300 prometaphase centrosomes were imaged and grouped into subcategories depending on whether they were positive (+) or negative (-) for STIL and SAS-6 (bottom of the graph). For each subcategory, 60 centrosomes were used to measure the respective STIL and SAS-6 intensities. Intensity values of prophase cells were set to 100%. Error bars denote +/-SD (3 independent experiments). **B** Representative images are shown for each subcategory defined in **A**. **C** Nocodazole-arrested U2OS cells (50 ng ml⁻¹ nocodazole; 12 hours) were treated for 1 h with RO-3306 (10 μM) in the presence of MG132 (10 μM; to prevent STIL degradation) and samples were subjected to Western blot analysis, using indicated antibodies. Antibodies against alpha-tubulin were used as a loading control. Note upshift of STIL in prometaphase-arrested cells (0h). As shown previously [S1], this upshift is sensitive to phosphatase treatment and thus almost certainly reflects phosphorylation.

Figure S6

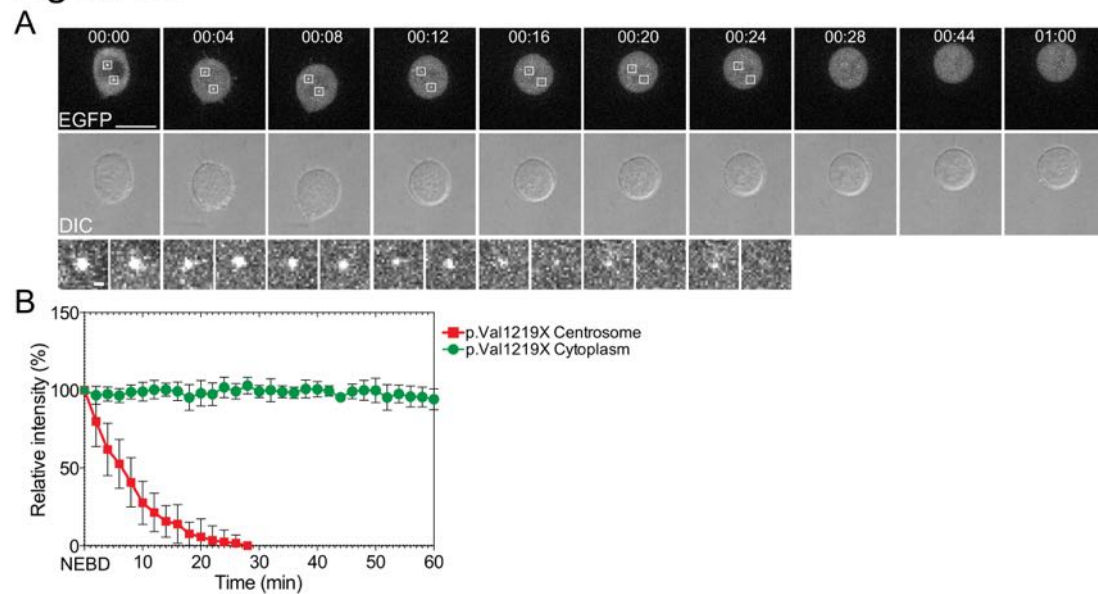


Fig. S6: STIL p.Val1219X disappears from mitotic centrosomes. Related to Figure 6.

A Real time visualization of EGFP-STIL p.Val1219X distribution in U2OS Flp-In T-REx:EGFP-STIL p.Val1219X cells filmed for 1 hour during transit from nuclear envelope breakdown (NEBD) into metaphase (see movie S6). EGFP fluorescence (EGFP; upper panels) and differential interference contrast microscopy (DIC; middle panels) are shown. Centrosomal EGFP-STIL signal is surrounded by white rectangles and shown with 10x magnification in lower panels. Scale bars indicate 20 μm (upper panels) or 1 μm (lower panels). **B** Line graph showing the mean EGFP intensity over time measured in the cytoplasmic (green circles, $n=5$ cells from 5 independent experiments) or in the centrosomal region (red squares, $n = 10$ centrosomes from 5 independent experiments). Error bars denote \pm -SD.

Supplemental Experimental Procedures

SPINNING DISK TIME-LAPSE IMAGING

Movies were acquired via a 3i Marianas spinning disk confocal microscopy setup (Intelligent Imaging Innovations) mounted on an inverted microscope (Axio Observer, Zeiss), equipped with a 60x 1.4 NA Plan Apo objective and an EMCCD camera (Photometrics Evolve 512). U2OS Flp-In T-REx cells were seeded onto 35 mm μ -Dishes (Ibidi) containing DMEM^{GFP} (Evrogen) and transgene expression was induced with 1 μ g/mL tetracycline 24 hours before imaging. EGFP signal intensities were measured in the centrosomal and cytoplasmic regions of filmed cells using ImageJ, background signal intensities were subtracted for all measurements. A table with acquisition and measurement details is shown below:

Movies	Length (hours)	Interval (min)	No of z-Stacks	Step Size (μ M)	Projection	Intensity Measurements	
						Cytoplasmic Intensity	Centrosomal Intensity
S1	20	5	30	0.7	Maximum intensity	Measured on 3 different z-stacks and averaged	Measured on max. intensity projections.
S2	1	2	26	0.6	Maximum intensity	Measured on max. intensity projections	Measured on max. intensity projections
S3	1	2	30	0.6	Maximum intensity	-	Measured on max. intensity projections
S4	1	3	22	0.7	Average intensity	Measured on 3 different z-stacks and averaged	-
S5	5	3	22	0.7	Average intensity	Measured on 3 different z-stacks and averaged	-
S6	1	2	26	0.6	Maximum intensity	Measured on max. intensity projections	Measured on max. intensity projections

IMMUNOFLUORESCENCE MICROSCOPY

Anti-STIL[S2] and anti-SAS-6[S3] antibodies were described previously. A monoclonal mouse antibody of the IgG1 subtype was raised against CP110 (aa1-149). Anti-CP110 and anti-SAS-6 antibodies were directly coupled to AlexaRed-555 and AlexaFar-Red647 using labeling kits (Invitrogen). AlexaGreen-488 labeled secondary anti-rabbit antibodies were from Invitrogen. U2OS cells were fixed in methanol for 5 minutes at -20°C , U2OS Flp-In T-REx cells were fixed in 3% paraformaldehyde for 15 minutes followed by permeabilisation with 0.5% Triton X-100 for 2 minutes. Stainings were analyzed using a DeltaVision microscope on a Nikon TE200 base (Applied Precision), equipped with a 60x 1.4 NA plan Apo objective and 1.6x auxiliary magnification. Serial optical z-sections were collected, deconvoluted and maximum intensity projected using Softworx (Applied Precision). STIL and SAS-6 centrosomal signal intensities were measured on deconvoluted and maximum intensity projected images in ImageJ, background signal intensities were subtracted for all measurements. Identical image acquisition and image processing conditions were applied whenever measurements were compared.

CLONING PROCEDURES

The pENTR/D-TOPO Cloning Kit (Invitrogen) was used to ligate blunt-ended PCR products into the pENTR/D-TOPO vector (Invitrogen), thereby generating entry vectors for use with the Gateway cloning system (Invitrogen). The QuikChange II XL Site-Directed Mutagenesis Kit (Agilent Technologies) was used for site-specific mutagenesis, with pENTR/D-TOPO_STIL_1-1287 as template. Expression vectors were generated by recombination of entry vectors and destination vectors with Gateway LR Clonase Enzyme mix (Invitrogen). SAS-6 cDNA was cloned into pcDNA5/FRT/TO (Invitrogen), which was modified to encode a FLAG tag. Cdh1 cDNA was amplified by PCR from a HeLa cDNA library and cloned into pcDNA3.1/3xmyc-A (Invitrogen).

Entry vectors, generated via TOPO cloning

Entry Vector	Template	Primer A	Primer B
pENTR/D-TOPO_STIL_1-1287	cDNA STIL (ImaGenes; IRCMp5012H1125D)	CACCGAGCCTATATATCCTTTTG	TTAAAATAATTTGGTAACTGTCTG
pENTR/D-TOPO_STIL N-ter_1-440	cDNA STIL (ImaGenes; IRCMp5012H1125D)	CACCGAGCCTATATATCCTTTTG	TTAAGGGTTTGATCTATGA
pENTR/D-TOPO_Stil central_441-880	cDNA STIL (ImaGenes; IRCMp5012H1125D)	CACCTGCTACTCCAATTGGAA	TTATCTTTTTCACAACTA
pENTR/D-TOPO_STIL C-ter_881-1287	cDNA STIL (ImaGenes; IRCMp5012H1125D)	CACCCCTGATGTACCTGTGTTT	TTAAAATAATTTGGTAACTGTCTG
pENTR/D-TOPO_STIL del C_1-880	cDNA STIL (ImaGenes; IRCMp5012H1125D)	CACCGAGCCTATATATCCTTTTG	TTATCTTTTTCACAACTA
pENTR/D-TOPO_STIL delN_441-1287	cDNA STIL (ImaGenes; IRCMp5012H1125D)	CACCTGCTACTCCAATTGGAA	TTAAAATAATTTGGTAACTGTCTG
pENTR/D-TOPO_STIL_1-1238	cDNA STIL (ImaGenes; IRCMp5012H1125D)	CACCGAGCCTATATATCCTTTTG	TTAAGTGAACCTGTCTTCCCG
pENTR/D-TOPO_STIL_1-1218	cDNA STIL (ImaGenes; IRCMp5012H1125D)	CACCGAGCCTATATATCCTTTTG	TTATAAGAAAGCTGGCT
pENTR/D-TOPO_STIL_1-1220	cDNA STIL (ImaGenes; IRCMp5012H1125D)	CACCGAGCCTATATATCCTTTTG	TTACTTACTAAGAAAGCTGGCTTTTCA
pENTR/D-TOPO_STIL_1-1155	cDNA STIL (ImaGenes; IRCMp5012H1125D)	CACCGAGCCTATATATCCTTTTG	TTACTGATCAATAAATTAATCACTCTGTACTCT
pENTR/D-TOPO_STIL_1-1104	cDNA STIL (ImaGenes; IRCMp5012H1125D)	CACCGAGCCTATATATCCTTTTG	TTATGTCTTCTGTCTATTAATATG
pENTR/D-TOPO_STIL_1-1060	cDNA STIL (ImaGenes; IRCMp5012H1125D)	CACCGAGCCTATATATCCTTTTG	TTACAAATCCACCACTGGGGCTTA

Entry vectors, generated via site-directed mutagenesis

Entry Vector	Template	Primers
pENTR/D-TOPO_STIL D1-	pENTR/D-TOPO_STIL_1-1287	CCTAAGAGTTCATATCACTTCCGCGGAGAGTGCCGACAGTGTGGAATTTGACTTG CAAGTCAAATTCACACTGTCCGCACTTCCGCGGAAGTGATATGAACCTTAGG
pENTR/D-TOPO_STIL D2-	pENTR/D-TOPO_STIL_1-1287	GGGACTTATAAATATGGATATCTTACCATGGATGAAACAGCAAATTTGGCACTTTTGTGGAACTGTATC GATCAGATCCCAAAAAGTGCCTAATTTGGCTGTTTCAATCCATGGTAAGATATCCATATTTATAAGTCCC
pENTR/D-TOPO_STIL D3-	pENTR/D-TOPO_STIL_1-1287	CCTTGATGCGCAAGATACCTGACTTTGCGTTTCAGGCGCTAACCCAGTAAGGA TCCTTACTGTTTAGCGCTGAAACGCAAAAGTCAGGATCTTGCATCACAAGG
pENTR/D-TOPO_STIL D4-	pENTR/D-TOPO_STIL_1-1287	CCTCCTGACAAAAATCCAATCGCTTGTGAAGCGAGCGCTGAAAGCCAAAATG CATTGTTGGCTTTCAGCGCTCGCTTCAAGCGATTGGATTTTGTGAGGAGG
pENTR/D-TOPO_STIL D5-	pENTR/D-TOPO_STIL_1-1287	CATGCAATTTGCAACCAAAAATATATGAAGCATATGGAGCCCTACAAAGCAGTGACAATATGTAAG CTTCAATTTGCACTGTCTTGTAGGGCTCCATATGCCTCATATATTTTTGGTGCAAAATGACATG GGAAAGCAGAGTTCACCAATCTGAGGCGAGCTGAAGGGGACATTAATTTTTCTGTGAAA TTTCAGGAAAAATGTAATGTCCCTTCAGCTGCTGCTCAGGATGTTGAGTGAACCTGTCTTCC

Expression vectors, generated via LR reactions

Expression Vector	Entry Vector	Dest Vector
pDEST_pcDNA3.1_N3xFLAG_STIL_1-1287	pENTR/D-TOPO_STIL_1-1287	pDEST_pcDNA3.1_N3xFLAG
pDEST_pcDNA3.1_N3xFLAG_STIL N-ter_1-440	pENTR/D-TOPO_STIL N-ter_1-440	pDEST_pcDNA3.1_N3xFLAG
pDEST_pcDNA3.1_N3xFLAG_STIL central_441-880	pENTR/D-TOPO_Stil central_441-880	pDEST_pcDNA3.1_N3xFLAG
pDEST_pcDNA3.1_N3xFLAG_STIL C-ter_881-1287	pENTR/D-TOPO_STIL C-ter_881-1287	pDEST_pcDNA3.1_N3xFLAG
pDEST_pcDNA3.1_N3xFLAG_STIL del C_1-880	pENTR/D-TOPO_STIL del C_1-880	pDEST_pcDNA3.1_N3xFLAG
pDEST_pcDNA3.1_N3xFLAG_STIL delN_441-1287	pENTR/D-TOPO_STIL delN_441-1287	pDEST_pcDNA3.1_N3xFLAG
pDEST_pcDNA3.1_N3xFLAG_STIL_1-1238	pENTR/D-TOPO_STIL_1-1238	pDEST_pcDNA3.1_N3xFLAG
pDEST_pcDNA3.1_N3xFLAG_STIL_1-1218	pENTR/D-TOPO_STIL_1-1218	pDEST_pcDNA3.1_N3xFLAG
pDEST_pcDNA3.1_N3xFLAG_STIL D1 -	pENTR/D-TOPO_STIL D1 -	pDEST_pcDNA3.1_N3xFLAG
pDEST_pcDNA3.1_N3xFLAG_STIL D2 -	pENTR/D-TOPO_STIL D2 -	pDEST_pcDNA3.1_N3xFLAG
pDEST_pcDNA3.1_N3xFLAG_STIL D3 -	pENTR/D-TOPO_STIL D3 -	pDEST_pcDNA3.1_N3xFLAG
pDEST_pcDNA3.1_N3xFLAG_STIL D4 -	pENTR/D-TOPO_STIL D4 -	pDEST_pcDNA3.1_N3xFLAG
pDEST_pcDNA3.1_N3xFLAG_STIL D5 -	pENTR/D-TOPO_STIL D5 -	pDEST_pcDNA3.1_N3xFLAG
pDEST_pcDNA3.1_N3xFLAG_STIL KEN -	pENTR/D-TOPO_STIL KEN -	pDEST_pcDNA3.1_N3xFLAG
pExp_pcDNA5_FRT_TO_EGFP_S_STIL_1-1287	pENTR/D-TOPO_STIL_1-1287	pgLAP1 (Addgene plasmid 19702)
pExp_pcDNA5_FRT_TO_EGFP_S_1-1218	pENTR/D-TOPO_STIL_1-1218	pgLAP1 (Addgene plasmid 19702)
pExp_pcDNA3.1_EGFP_STIL_1-1287	pENTR/D-TOPO_STIL_1-1287	pDEST/pcDNA3.1_NEGFP
pExp_pcDNA3.1_EGFP_STIL_1-1238	pENTR/D-TOPO_STIL_1-1238	pDEST/pcDNA3.1_NEGFP
pExp_pcDNA3.1_EGFP_STIL_1-1218	pENTR/D-TOPO_STIL_1-1218	pDEST/pcDNA3.1_NEGFP
pExp_pcDNA3.1_EGFP_STIL_1-1220	pENTR/D-TOPO_STIL_1-1220	pDEST/pcDNA3.1_NEGFP
pExp_pcDNA3.1_EGFP_STIL_1-1155	pENTR/D-TOPO_STIL_1-1155	pDEST/pcDNA3.1_NEGFP
pExp_pcDNA3.1_EGFP_STIL_1-1104	pENTR/D-TOPO_STIL_1-1104	pDEST/pcDNA3.1_NEGFP
pExp_pcDNA3.1_EGFP_STIL_1-1060	pENTR/D-TOPO_STIL_1-1060	pDEST/pcDNA3.1_NEGFP

SUPPLEMENTAL REFERECES

- S1. Tang, C.-J. C., Lin, S.-Y., Hsu, W.-B., Lin, Y.-N., Wu, C.-T., Lin, Y.-C., Chang, C.-W., Wu, K.-S., and Tang, T. K. (2011). The human microcephaly protein STIL interacts with CPAP and is required for procentriole formation. *EMBO J* 30, 4790–4804.
- S2. Arquint, C., Sonnen, K. F., Stierhof, Y.-D., and Nigg, E. A. (2012). Cell-cycle-regulated expression of STIL controls centriole number in human cells. *J. Cell. Sci.* 125, 1342–1352.
- S3. Kleylein-Sohn, J., Westendorf, J., Le Clech, M., Habedanck, R., Stierhof, Y.-D., and Nigg, E. A. (2007). Plk4-induced centriole biogenesis in human cells. *Dev. Cell* 13, 190–202.

5. DISCUSSION

5.1 On the Relation between SAS-5, Ana2 and STIL

The centriole duplication machinery was highly conserved in evolution. Components that are required to form a new centriole have initially been identified by genetic screens in *C. elegans* (Leidel and Gönczy, 2005). Whereas only five proteins are necessary to form a centriole in this organism, additional duplication factors are required to build a centriole in human cells (Nigg and Stearns, 2011). This suggests the process in human cells to be more complex, but the basic principles of centriole formation have been conserved, as most of the centriole duplication factors from *C. elegans* are also present in human cells. However, one centriole duplication factor, named SAS-5, has long been lacking any obvious counterpart outside of *C. elegans*. Elegant work in *Drosophila* then revealed that a protein named Ana2 constitutes the SAS-5 homolog in flies, and it has furthermore been proposed that a protein called STIL might be the respective candidate in human cells (Stevens et al., 2010a).

We and others therefore started to investigate whether STIL is implicated in centriole biogenesis of proliferating human cells, with a special focus on a possible relation between STIL, Ana2 and SAS-5 (Arquint et al., 2012; Tang et al., 2011; Vulprecht et al., 2012). Indeed, depletion of STIL from cells completely abrogated centriole duplication, whereas STIL overexpression triggered the near-simultaneous formation of multiple daughter centrioles around each pre-existing centriole (Figure 10). The same phenotype can be observed for two major centriole duplication factors, Plk4 and HsSAS-6 (Habedanck et al., 2005; Kleylein-Sohn et al., 2007; Strnad et al., 2007), which suggests that STIL has adopted a key function in assembly of human centrioles. Furthermore, by immunofluorescence and electron microscopy, we and others observed localization of STIL to the proximal procentriole region (Arquint et al., 2012; Lukinavičius et al., 2013; Tang et al., 2011). This part of the centriole contains the cartwheel structure, a template for centriole assembly that is formed by 9-fold oligomerization of HsSAS-6 homodimers (Gönczy, 2012). The localization of STIL to the cartwheel region has furthermore been confirmed by prominent HsSAS-6 and STIL co-localization (Arquint et al., 2012; Lukinavičius et al., 2013). We therefore suggest that STIL constitutes a key centriole duplication factor in human cells that cooperates with Plk4 and HsSAS-6 in cartwheel formation.

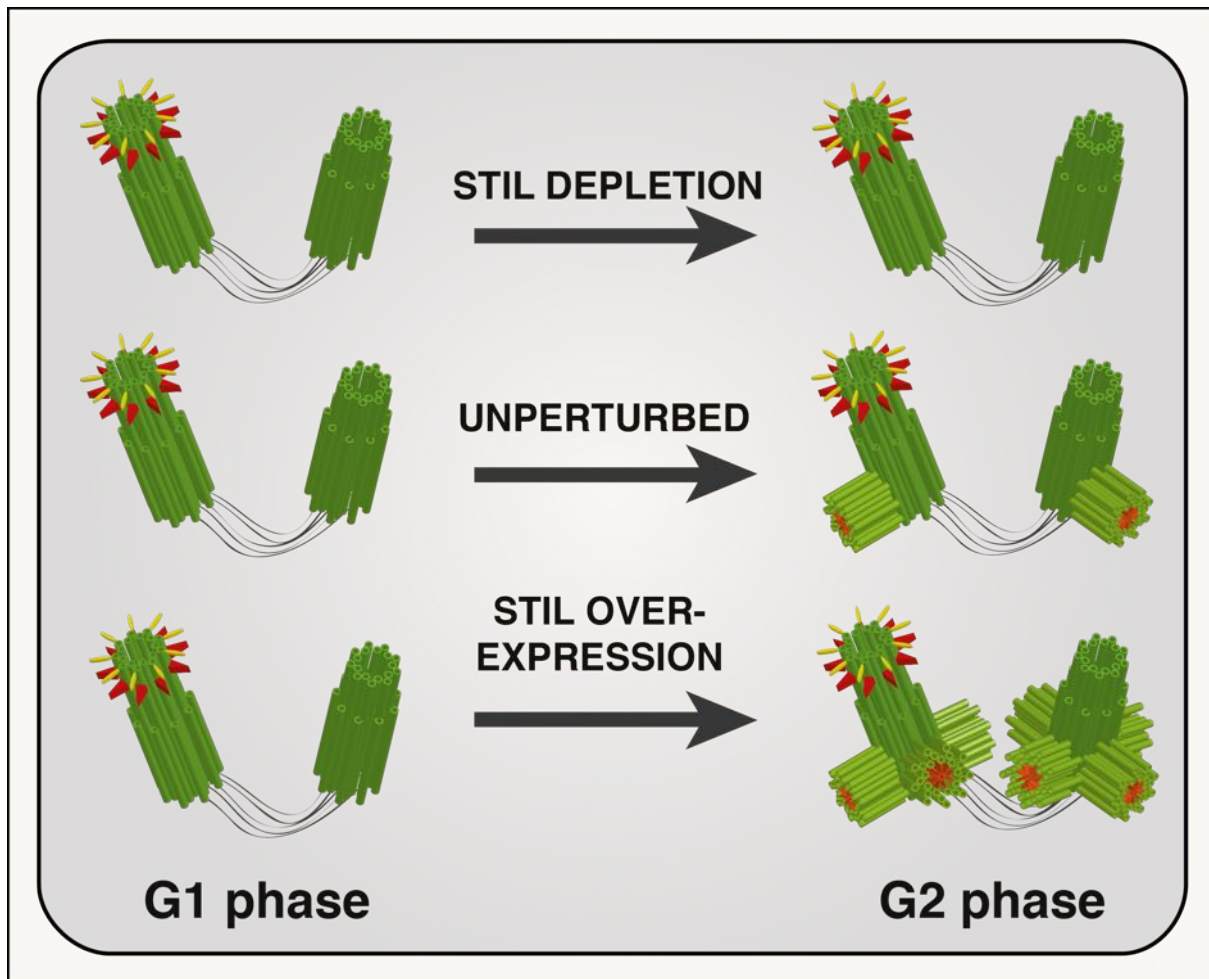


Figure 10: STIL Depletion and Overexpression Phenotypes Schematic illustrations showing the effects on centriole duplication in STIL depleted (top), unperturbed (middle) or STIL overexpressing cells (bottom). After centriole duplication (G2 phase, right side) new daughter centrioles were formed in orthogonal orientation to preexisting centrioles in unperturbed cells (right side, middle). In STIL depleted G2 phase cells (right side, top), daughter centrioles did not form. In STIL overexpressing G2 phase cells (right side, bottom), several daughter centrioles formed simultaneously around both preexisting centrioles.

In contrast, two studies localized STIL to the PCM region of centrosomes (Pfaff et al., 2007; Vulprecht et al., 2012), a finding that could not be reproduced in our hands (Arquint et al., 2012). However, antibody specificity issues have not been completely ruled out, which would be necessary before drawing definitive conclusions. Furthermore, a localization of exogenous STIL to the PCM region was not observed when ectopically expressing GFP-tagged STIL, which localizes as a ring around pre-

existing centrioles to trigger the near-simultaneous formation of multiple daughter centrioles (Arquint et al., 2012; Tang et al., 2011). We therefore suggest that STIL is an integral part of newly formed centrioles, rather than a PCM component (Arquint et al., 2012; Lukinavičius et al., 2013; Tang et al., 2011).

In summary, the above results confirm a relation between STIL, Ana2 and SAS-5 in centriole formation. We suggest that the key functions of SAS-5, the assembly of centriole scaffolds (central tube in *C. elegans* or cartwheel in *Drosophila* and human cells), have been conserved in STIL. This also fits with results obtained for *Drosophila* Ana2, which does specifically localize to daughter centrioles and triggers the *de novo* formation of centriole-like structures, when overexpressed in unfertilized *Drosophila* eggs (Stevens et al., 2010a).

However, not all the functions that have been described for *C. elegans* SAS-5 seem to be conserved in human STIL. For example, previous studies emphasized that SAS-5 and SAS-6 are forming a stable complex in the cytoplasm of *C. elegans*, which gets recruited to the site of procentriole formation at the G1/S phase transition to form the central tube (Leidel et al., 2005). A similar, direct interaction was observed for Ana2 and DSAS-6 (Stevens et al., 2010a). We therefore conducted a series of co-immunoprecipitation experiments in HEK 293T cells in order to check for an interaction between STIL and HsSAS-6. However, we were not able to detect such an interaction (Arquint et al., 2012). Also, neither endogenous nor overexpressed STIL was detected in endogenous SAS-6 immunoprecipitates (Arquint et al., 2012). This makes it unlikely that STIL and HsSAS-6 form a stable complex in the cytoplasm. STIL and HsSAS-6 might well interact at the cartwheel region, but such a localized (and perhaps transient) interaction would be difficult to detect by co-immunoprecipitation experiments. One study nevertheless managed to demonstrate an interaction, albeit weak, in co-immunoprecipitation experiments, but contrary to what has been shown in *C. elegans* or *Drosophila*, a direct interaction between the two proteins was not observed (Tang et al., 2011). Furthermore, two studies have revealed an interaction between STIL and CPAP (Tang et al., 2011; Vulprecht et al., 2012), which has been confirmed to be of direct nature (Cottee et al., 2013; Hatzopoulos et al., 2013; Tang et al., 2011). This latter interaction is evolutionarily conserved and has also been observed between SAS-4 and *Drosophila* Ana2 and *C. elegans* SAS-5. Furthermore, the interaction has been shown to be essential for

centriole formation in *Drosophila* (Cottee et al., 2013) and in human cells (Kitagawa et al., 2011a). Interestingly, a mutation in CPAP (E1235V) that is associated with MCPH in humans interferes with binding to STIL (Tang et al., 2011), suggesting that centriole duplication might be partially impaired in those patients (Kitagawa et al., 2011a).

Also, *C. elegans* SAS-5 and SAS-6 mutually depend on each other for centriolar localization (Leidel et al., 2005). Such a co-dependency on localization could not be fully reproduced in our hands (Arquint et al., 2012). Even though STIL was not localizing to centrioles in the absence of HsSAS-6, reduced levels of HsSAS-6 were consistently detected at centrioles in STIL depleted cells. As HsSAS-6 disappears from centrioles at the end of mitosis and gets newly recruited to centrioles at each G1/S phase transition, we are confident that this does not reflect remaining HsSAS-6 that has been present at centrioles prior to depletion. This rather suggests that cartwheels might be partially assembled in the absence of STIL, but stable integration into procentrioles does not take place. However, this result is controversial and has not been observed by others, which rather revealed a complete mutual dependency for both HsSAS-6 and STIL on centriolar targeting (Tang et al., 2011; Vulprecht et al., 2012). Therefore, this will need further experimentation.

Furthermore, there are prominent differences in the localization patterns of STIL/Ana2 and SAS-5. Unlike Ana2 or STIL, that both localize specifically to daughter centrioles, SAS-5 is present at daughter and mother centrioles. These discrepancies could reflect differences in cartwheel and central tube stability. Whereas the cartwheel (at least in vertebrate cells) is known to disassemble each cell cycle transition and therefore is daughter centriole specific, the central tube (or at least some components of it) might persist stably integrated into mother centrioles of *C. elegans*.

5.2 Do STIL and E2F Cooperate in Control of Centriole Duplication?

Two years before STIL has been implicated in centriole biogenesis, it has been revealed that STIL transcriptional expression is under tight control of the E2F1 transcription factor (Erez et al., 2008). Intriguingly, E2F transcription factors are, in conjunction with Cdk2 Cyclin A or E, important controls that determine the timepoint of centriole duplication as well as DNA replication towards the G1/S phase transition (Meraldi et al., 1999). Therefore, STIL might provide an interesting link between activation of E2F transcription factors and onset of centriole duplication.

5.3 Is STIL a Genuine Cartwheel Protein?

Our results, as well as those of others, unequivocally show that STIL localizes to the cartwheel region of human centrioles (Arquint et al., 2012; Lukinavičius et al., 2013; Tang et al., 2011). Furthermore, STIL is amongst the first components that get recruited to the site of centriole formation, suggesting that it assists early on in cartwheel assembly (Arquint et al., 2012). After its recruitment, STIL co-localizes with HsSAS-6 to the proximal part of newly forming centrioles. Both STIL and HsSAS-6 centriolar levels increase towards mitosis (Arquint et al., 2012; Tang et al., 2011), suggesting that cartwheel assembly continues in parallel to centriole elongation. Finally, STIL and HsSAS-6 both disappear from centrioles in mitosis (Arquint and Nigg, 2014; Arquint et al., 2012; Strnad et al., 2007), which is the time when cartwheels disassemble. All these data are in line with STIL being a genuine cartwheel component in human cells. Similar conclusions have been reached in *Drosophila*, where ectopic Ana2 and DSAS-6 coassembled into tubules that resembled the inner cartwheel structure (Stevens et al., 2010b).

From an evolutionary perspective, however, it seems possible that cartwheels can form in the absence of STIL. STIL is highly conserved in vertebrates and is also

found in some other metazoa, but it can not be readily identified in unicellular organisms that use centrioles to build flagella, such as *Trypanosomas* or *Chlamydomonas* (unpublished data). SAS-6, in contrast, is thought to be present in any organism that forms centrioles. Also Cep135 or SAS-4 are highly conserved in many unicellular organisms (Hodges et al., 2010). This suggests that STIL probably evolved as an additional cartwheel component in metazoan organisms that assists with SAS-6, CPAP and Plk4 in centriole formation.

5.4 Is STIL Required for Cartwheel Stability?

Both STIL and HsSAS-6 are completely removed from cells by proteasomal degradation at the end of mitosis (Arquint et al., 2012; Izraeli et al., 1997; Strnad et al., 2007; Tang et al., 2011), and the APC/C has been implicated in degradation of both proteins (Arquint and Nigg, 2014; Arquint et al., 2012; Strnad et al., 2007). While using a real-time based assay to monitor cell cycle regulation of GFP-STIL in a U2OS Flp-In T-Rex cell line, we were surprised to see that STIL disappears from centrioles already in early mitosis (upon nuclear envelope breakdown), before it gets removed by the APC/C (Arquint and Nigg, 2014). We first checked whether removal of centriolar STIL would reflect proteasomal degradation, which was not the case. We therefore suspected that posttranslational modifications might be involved in this process. A prominent kinase that gets activated at this time in the cell cycle is Cdk1/CyclinB. Indeed, several Cdk1 inhibitors potently blocked STIL removal from centrioles (Arquint and Nigg, 2014). Although in a different context, previous studies had already linked Cdk1 to STIL phosphorylation (Campaner et al., 2005). The release of STIL from mitotic centrioles into the cytoplasm upon Cdk1 phosphorylation is therefore the most likely scenario (Arquint and Nigg, 2014). However, we can not exclude an indirect mechanism, and future work will have to reveal the exact mechanism.

Importantly, these findings bear on our understanding of cartwheel disassembly. The cartwheel of vertebrate centrioles is known to disassemble in mitosis, but the exact timing and the underlying mechanisms are unknown. On the

basis of our results, we propose that the translocation of STIL from centrioles into the cytoplasm initiates cartwheel disassembly in early mitosis. SAS-6 is a major cartwheel protein. We therefore carefully assessed HsSAS-6 centriolar levels at all stages of mitosis. In line with our hypothesis, HsSAS-6 levels at centrioles gradually decreased already upon mitotic entry and HsSAS-6 was completely lost from centrioles in anaphase. We therefore propose that STIL removal from centrioles destabilizes the cartwheel, which then disassembles throughout the rest of mitosis. Cdk1 therefore allows for tight coupling of cartwheel disassembly with mitotic progression, since this kinase is required for initiation of both processes.

In summary, all these data support a model according to which STIL is a factor that positively regulates cartwheel stability, most probably in cooperation with HsSAS-6, CPAP and Plk4. STIL is one of the first components to localize to the site where cartwheels assemble and it might be required for stable integration of HsSAS-6 into the proximal part of newly forming centrioles. Finally, dissociation of STIL from mitotic centrioles, which is followed by release of centriolar HsSAS-6, might initiate cartwheel disassembly.

5.5 APC/C-Mediated Degradation of STIL

Centriole amplification is a widespread characteristic of cancer cells where it is predicted to promote genetic instability (Lingle et al., 2002; Nigg, 2002; 2006). Extra centrosomes interfere with important cellular processes, such as MT organisation, mitotic spindle formation or spindle orientation. Therefore, tight control over centriole duplication is fundamental for cellular integrity.

Fluctuations of STIL protein levels in proliferating cells have been described as early as 15 years ago (Izraeli et al., 1997) and levels of STIL are critical for maintenance of correct centriole numbers (Arquint et al., 2012; Tang et al., 2009; Vulprecht et al., 2012). We therefore analyzed the subcellular distribution of STIL throughout the cell cycle. We found that STIL is completely absent in G1 phase cells but gradually accumulates both in the cytoplasm and at centrioles from the G1/S

phase transition to early mitosis (Arquint et al., 2014). At nuclear envelope breakdown, STIL disappears from centrioles, whereas cytoplasmic STIL persists until late anaphase, when it is subject to complete proteasomal degradation (Arquint et al., 2012; Tang et al., 2011). A prominent ubiquitin ligase complex activated at this cell cycle stage is the APC/C. RNAi experiments suggested that both APC/C activator proteins Cdc20 and Cdh1 might contribute to STIL degradation (Arquint et al., 2012). Activator proteins associate with the APC/C and bind respective substrate proteins via short amino acid sequences, called D- or KEN boxes, to bring the E3 ubiquitin ligase close to its substrates (Peters, 2006). Mutational analysis of five putative D- and one putative KEN box revealed that only the KEN box was functional in terms of STIL degradation (Arquint et al., 2012). Since KEN boxes are primarily targeted by Cdh1, we propose that APC/C^{Cdh1} is the major mediator of STIL degradation, but initial contribution of the APC/C^{Cdc20} can not be fully excluded (Arquint et al., 2012). Complete degradation of STIL (Arquint and Nigg, 2014; Arquint et al., 2012; Tang et al., 2011), HsSAS-6 (Strnad et al., 2007) or CPAP (Tang et al., 2009) at the end of mitosis might act as a reset mechanism to set levels of respective centriole duplication factors to zero before a new round of centriole duplication is initiated. As levels of all those duplication factors are critical to maintain correct centriole numbers, this might prevent aberrant centriole formation.

Intriguingly, two nonsense mutations in STIL that are associated with MCPH (p.Val1219X and p.Gln1239X) remove only a small part of the protein's C-terminus (Kumar et al., 2009), which includes the KEN box (Arquint et al., 2014). We thus hypothesized that abrogation of STIL cell-cycle regulation could account for the reduced brain size in corresponding patients via STIL stabilization and centriole amplification (Figure 11). In line with this hypothesis, centriole amplification is indeed sufficient to trigger microcephaly, as has been shown by overexpression of Plk4 in the developing mouse central nervous system (Marthiens et al., 2013). We therefore set out to experimentally test our hypothesis.

5.6 STIL Microcephaly Mutations are Gain-of-Function

If our above hypothesis was true, the respective microcephaly mutations (p.Val1219X, p.Gln1239X) should not abrogate the ability of STIL to function in centriole duplication. We therefore checked whether removal of 49 or 69 amino acids from the STIL C-terminus would interfere with its ability to trigger centriole amplification. Overexpression of both truncations resulted in centriole amplification, and we found that removal of up to 132 amino acids from the STIL C-terminus is well tolerated in regard to centriole duplication (Arquint and Nigg, 2014). This suggests that STIL microcephaly truncations retain functionality in centriole duplication, as has also been observed by others (Vulprecht et al., 2012).

As a next step, it was important to assess *in vivo* whether STIL protein truncations would sufficiently accumulate to trigger centriole amplification. Unfortunately, we had no patient material available to check for STIL protein stabilization or centriole amplification, but we emphasize that it will be of importance to confirm our findings with patient material in future studies. We therefore generated a U2OS Flp-In T-Rex cell line expressing a truncated version of STIL (p.Val1219X) and compared it to a cell line expressing wild type STIL. Clearly, mutant STIL accumulated to sufficiently high levels to trigger robust centriole amplification, whereas wild type STIL did not. Thus, removal of the KEN box from STIL in proliferating cells does indeed result in centriole amplification (Arquint and Nigg, 2014).

Overall, the STIL mutations described here are not loss-, but rather gain-of-function. At first glance, this result seems surprising, as most of the mutations that occur in MCPH associated genes result in a loss-of-function phenotype, as is typical of recessive diseases. In contrast, gain-of-function mutations are predicted to act in a dominant fashion, because one copy of the mutated allele is often sufficient to trigger a phenotype in heterozygous patients. Therefore, why would the disease phenotype (microcephaly) not be visible in heterozygote individuals in our case? One possibility is that one copy of mutated STIL is not enough to trigger STIL accumulation and centriole amplification (partial dominance). Also, it has been shown that STIL forms

dimers or higher order oligomers *in vivo* (Tang et al., 2011). Therefore, mutant and wild-type STIL are most likely in a complex if both copies are present in an organism. Wild type STIL might therefore provide its KEN box for degradation of the whole complex, thereby rescue accumulation of mutant STIL. Only complete loss of the KEN box in both alleles might therefore be sufficient to trigger robust centriole amplification.

Besides the two STIL mutations analyzed here, two additional mutations have been described in the literature (Kumar et al., 2009; Papari et al., 2013). Kumar and co-workers described a third STIL mutation that is predicted to interfere with mRNA splicing, but the consequences of this mutation are not easy to predict without experimental verification. It was suggested that this splice site mutation would result in a larger truncation from the STIL C-terminus, which, according to our experiments, would abrogate the function of STIL in centriole duplication (Arquint and Nigg, 2014). However, complete loss of STIL function in humans is likely to be fatal, as elimination of STIL in both zebrafish and mice results in embryonic lethality (Izraeli et al., 1999; Pfaff et al., 2007) Before reaching further conclusions, the exact outcome of this mutation on mRNA splicing therefore will have to be experimentally tested. Also, a missense mutation termed p.L798W has been described in another study (Papari et al., 2013). This mutation does not delete the KEN box, which implies that loss of the KEN box is probably not the only cause for microcephaly in STIL-related MCPH patients. However, it could be that this mutation does trigger centriole amplification or interfere with STIL degradation by other means.

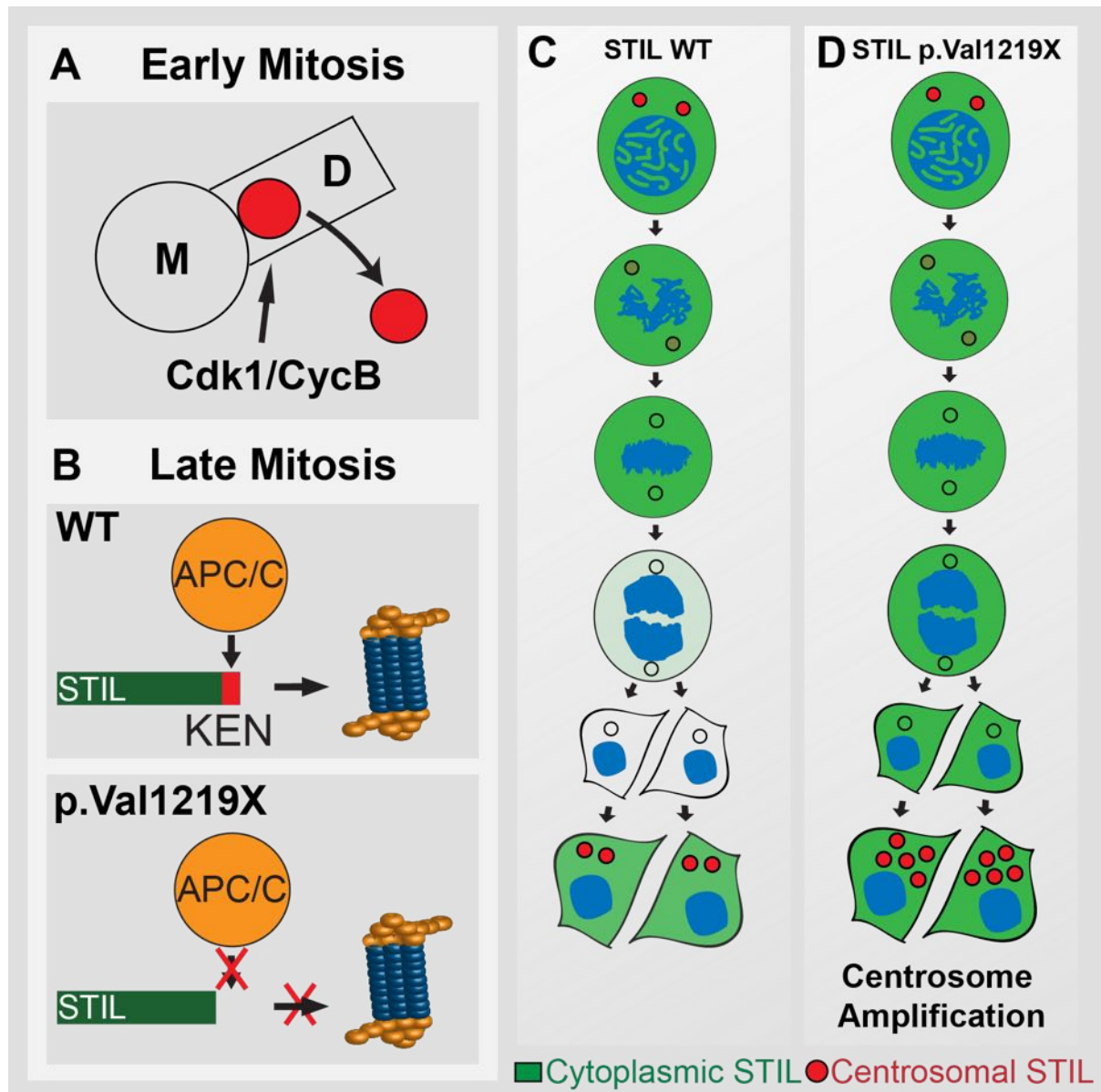


Figure 11: A Two Step Mechanism Results in Late Mitotic Degradation of STIL, which is Abrogated by STIL MCPH Mutations (A) In early mitosis, Cdk1/Cyclin B drives translocation of centrosomal STIL (red) into the cytoplasm. (B) In late mitosis, the APC/C recognizes a KEN box on the C-terminus of STIL, which results in proteasomal degradation. A STIL MCPH mutation (p.Val1219X) deletes the KEN box and renders STIL resistant to degradation. (C) Schematic illustration depicting the early mitotic translocation of centrosomal STIL (red) into the cytoplasm, followed by degradation of cytoplasmic STIL (green) at the end of mitosis. (D) STIL p.Val1219X does also translocate from early mitotic centrosomes into the cytoplasm, but is not degraded at mitotic exit. This results in centriole amplification. Figure adapted from (Arquint and Nigg, 2014).

5.7 Is Centriole Amplification a Root Cause of Microcephaly?

So, how could centriole amplification caused by STIL mutations mechanistically result in microcephaly? In our opinion, there are at least two possible explanations for how such a phenotype could arise via centriole amplification. First, extra centrosomes in neuroprogenitors are likely to interfere with mitotic spindle orientation, which is important to keep the ratio between stem cells and differentiated cells in balance. Therefore, spindle misorientation does reduce the neuroprogenitor pool (Noatynska et al., 2012). Surprisingly, spindle misorientation was not evident in a developing mouse brain overexpressing Plk4, which induced microcephaly via massive centriole amplification (Marthiens et al., 2013). Instead, neuroprogenitors underwent extensive cell death. Apoptosis is therefore an alternative explanation for how the neuroprogenitor pool could be reduced. Apoptosis is likely to be triggered by defects in bipolar spindle formation, which cause chromosome missegregation (Ganem et al., 2009). In this regard, it is interesting to mention that mutations in a prominent kinetochore protein, called CASC5 (KNL1), were also linked to MCPH (Genin et al., 2012). Abrogation of kinetochore function is predicted to interfere with MT-kinetochore attachments, which also results in genetic instability (Foley and Kapoor, 2013).

Therefore, both spindle misorientation and chromosome missegregation are likely defects in a developing brain with extra centrosomes. However, at least in the case described here (Arquint and Nigg, 2014), centriole amplification is predicted to occur in cells throughout the body, and not only within the brain region. But why is only the brain affected, whereas other parts of the body remain normal? Probably, the answer to this question lies in the extraordinary ability of cells to cluster extra centrioles, which allows for bipolar spindle formation in such contexts (Gergely and Basto, 2008; Kwon et al., 2008; Ring et al., 1982). The ability of organisms to withstand centriole amplification has been convincingly demonstrated in flies overexpressing Plk4. Even though a majority of their cells harbored supernumerary centrioles, these flies maintained a stable diploid genome over many generations,

and only the asymmetric divisions of neuroprogenitors were compromised (Basto et al., 2008). Therefore, in comparison to other cell types, neuroprogenitors might be inefficient in centrosome clustering, which would render them especially susceptible to perturbations in centriole numbers. However, results from *Drosophila* can not be directly applied to vertebrates. Therefore, it will be interesting to check in future whether centriole amplification in vertebrates might only affect brain development, or also other organs.

Here, we demonstrate that primary microcephaly in patients with mutations in STIL might likely underlie a centriole amplification phenotype (Arquint and Nigg, 2014), and centriole amplification in the mouse brain has been shown to be sufficient to trigger microcephaly (Marthiens et al., 2013). However, it is clear that centriole amplification is not the only cause of MCPH, and defects in other cellular pathways, such as centriole maturation, cell cycle progression or DNA damage responses, have all been linked to this disease (Kaindl et al., 2010; Thornton and Woods, 2009). Finally, defects in completely different pathways might have a similar outcome. For example, perturbation of DNA damage signaling has also been shown to cause centriole amplification (Bourke et al., 2007). Regarding the growing list of mutated genes involved in MCPH and the diversity of defects they might cause in affected patients, it will be of great interest in future studies to define the underlying mechanisms that might explain how all these defects converge into one common phenotype.

6. ABBREVIATIONS

APC/C: anaphase-promoting complex/cyclosome
Ana2: anastral spindle 2
ASPM: abnormal spindle-like, microcephaly-associated
ATR: ataxia telangiectasia and Rad3-related
ATRIP: ATR interacting protein
Bld10: basal body protein 10
CASC5: cancer susceptibility candidate 5
CCDC78: coiled-coil domain containing 78
CDC: cell division cycle
Cdh1: CDC20 homolog 1
Cdk: cyclin-dependent kinase
Cdk5rap2: CDK5 regulatory subunit-associated protein 2
CDT1: chromatin licensing and DNA replication factor 1
Cep/CP: centrosomal protein
CPAP: centrosomal P4.1-associated protein
CTL: cytotoxic T lymphocytes
C-Nap1: centrosomal Nek2-associated protein 1
Deup1: deuterosome protein 1
FBF1: fas-binding factor 1
FBXW5: F-box/WD repeat-containing protein 5
HEK: human embryonic kidney
Kif24: kinesin family member 24
KNL-1: kinetochore-null protein 1
MCPH: autosomal recessive primary microcephaly
MOPDI: microcephalic osteodysplastic primordial dwarfism type I
MOPDII: microcephalic osteodysplastic primordial dwarfism type II
MPS1: monopolar spindle protein 1
MT: microtubule
Nedd1: neural precursor cell expressed developmentally down-regulated protein 1
Nek2: never in mitosis A-related kinase 2
ODF2: outer dense fiber protein 2
ORC: origin recognition complex
PCM: pericentriolar material
PD: primordial dwarfism
PHC1: polyhomeotic-like 1
Pin1: peptidyl-prolyl cis-trans isomerase NIMA-interacting 1
Plk: polo-like kinase
PLP: pericentrin-like-protein
POC: protein of centriole
PP: protein phosphatase
RBBP8: retinoblastoma-binding protein 8
RNU4ATAC: RNA, U4atac small nuclear
SAS: spindle assembly abnormal
SCF: Skp, Cullin, F-box containing complex
SCL: stem cell leukemia
SCLT1: sodium channel and clathrin linker 1
Sfi1: suppressor of fermentation induced loss of stress resistance protein 1
Shh: sonic hedgehog
Slimb: supernumerary limbs

snRNA: small nuclear ribonucleic acid
SPB: spindle pole body
SPD-2: spindle-defective protein 2
SPICE1: spindle and centriole-associated protein 1
STAN: STIL/Ana2 motif
STIL: SCL/TAL1 interrupting locus
Stu2: suppressor of tubulin 2
TAL1: T-cell acute lymphocytic leukemia protein 1
USP33: ubiquitin carboxyl-terminal hydrolase 33
WDR62: WD repeat domain 62
XMAP215: microtubule associated protein 215 kDa
ZNF335: zinc finger protein 335
ZYG-1: zygote defective protein 1
 β -TrcP: beta-transducin repeat containing
 γ -TuRC: gamma tubulin ring complex

7. REFERENCES

-
- Alderton, G.K., Galbiati, L., Griffith, E., Surinya, K.H., Neitzel, H., Jackson, A.P., Jeggo, P.A., and O'Driscoll, M. (2006). Regulation of mitotic entry by microcephalin and its overlap with ATR signalling. *Nature Cell Biology* 8, 725–733.
- Andersen, J.S., Wilkinson, C.J., Mayor, T., Mortensen, P., Nigg, E.A., and Mann, M. (2003). Proteomic characterization of the human centrosome by protein correlation profiling. *Nature* 426, 570–574.
- Angus, K.L., and Griffiths, G.M. (2013). Cell polarisation and the immunological synapse. *Curr Opin Cell Biol* 25, 85–91.
- Aplan, P.D., Lombardi, D.P., and Kirsch, I.R. (1991). Structural characterization of SIL, a gene frequently disrupted in T-cell acute lymphoblastic leukemia. *Mol Cell Biol* 11, 5462–5469.
- Aplan, P.D., Lombardi, D.P., Ginsberg, A.M., Cossman, J., Bertness, V.L., and Kirsch, I.R. (1990). Disruption of the human SCL locus by “illegitimate” V-(D)-J recombinase activity. *Science* 250, 1426–1429.
- Arquint, C., and Nigg, E.A. (2014). STIL microcephaly mutations interfere with APC/C-mediated degradation and cause centriole amplification. *Curr. Biol.* 24, 351–360.
- Arquint, C., Gabryjonczyk, A.-M., and Nigg, E.A. (2014). Centrosomes as signaling centers. *Philosophical Transactions of the Royal Society B: Biological Sciences*, in Press.
- Arquint, C., Sonnen, K.F., Stierhof, Y.-D., and Nigg, E.A. (2012). Cell-cycle-regulated expression of STIL controls centriole number in human cells. *J. Cell. Sci.* 125, 1342–1352.
- Azimzadeh, J., and Bornens, M. (2007). Structure and duplication of the centrosome. *J. Cell. Sci.* 120, 2139–2142.
- Azimzadeh, J., and Marshall, W.F. (2010). Building the Centriole. *Current Biology* 20, R816–R825.
- Azimzadeh, J., Hergert, P., Delouvee, A., Euteneuer, U., Formstecher, E., Khodjakov, A., and Bornens, M. (2009). hPOC5 is a centrin-binding protein required for assembly of full-length centrioles. *The Journal of Cell Biology* 185, 101–114.
- Azimzadeh, J., Wong, M.L., Downhour, D.M., Sánchez Alvarado, A., and Marshall, W.F. (2012). Centrosome loss in the evolution of planarians. *Science* 335, 461–463.
- Bahe, S., Stierhof, Y.-D., Wilkinson, C.J., Leiss, F., and Nigg, E.A. (2005). Rootletin forms centriole-associated filaments and functions in centrosome cohesion. *The Journal of Cell Biology* 171, 27–33.
- Bahmanyar, S., Kaplan, D.D., DeLuca, J.G., Giddings, T.H., O'Toole, E.T., Winey, M., Salmon, E.D., Casey, P.J., Nelson, W.J., and Barth, A.I.M. (2008). -Catenin is a Nek2 substrate involved in centrosome separation. *Genes Dev.* 22, 91–105.
- Balczon, R., Bao, L., Zimmer, W.E., Brown, K., Zinkowski, R.P., and Brinkley, B.R. (1995). Dissociation of centrosome replication events from cycles of DNA synthesis and mitotic division in hydroxyurea-arrested Chinese hamster ovary cells. *The Journal of Cell*
-

Biology 130, 105–115.

Balestra, F.R., Strnad, P., Flückiger, I., and Gönczy, P. (2013). Discovering Regulators of Centriole Biogenesis through siRNA-Based Functional Genomics in Human Cells. *Dev. Cell* 25, 555–571.

Barr, A.R., Kilmartin, J.V., and Gergely, F. (2010). CDK5RAP2 functions in centrosome to spindle pole attachment and DNA damage response. *The Journal of Cell Biology* 189, 23–39.

Barrera, J.A., Kao, L.-R., Hammer, R.E., Seemann, J., Fuchs, J.L., and Megraw, T.L. (2010). CDK5RAP2 regulates centriole engagement and cohesion in mice. *Dev. Cell* 18, 913–926.

Basto, R., Brunk, K., Vinadogrova, T., Peel, N., Franz, A., Khodjakov, A., and Raff, J.W. (2008). Centrosome amplification can initiate tumorigenesis in flies. *Cell* 133, 1032–1042.

Basto, R., Lau, J., Vinogradova, T., Gardiol, A., Woods, C.G., Khodjakov, A., and Raff, J.W. (2006). Flies without centrioles. *Cell* 125, 1375–1386.

Berdnik, D., and Knoblich, J.A. (2002). Drosophila Aurora-A Is Required for Centrosome Maturation and Actin-Dependent Asymmetric Protein Localization during Mitosis. *Current Biology* 12, 640–647.

Bertran, M.T., Sdelci, S., Regué, L., Avruch, J., Caelles, C., and Roig, J. (2011). Nek9 is a Plk1-activated kinase that controls early centrosome separation through Nek6/7 and Eg5. *Embo J* 30, 2634–2647.

Bettencourt-Dias, M., Rodrigues-Martins, A., Carpenter, L., Riparbelli, M., Lehmann, L., Gatt, M.K., Carmo, N., Balloux, F., Callaini, G., and Glover, D.M. (2005). SAK/PLK4 is required for centriole duplication and flagella development. *Curr. Biol.* 15, 2199–2207.

Bettencourt-Dias, M., Hildebrandt, F., Pellman, D., Woods, G., and Godinho, S.A. (2011). Centrosomes and cilia in human disease. *Trends in Genetics* 27, 307–315.

Blachon, S., Cai, X., Roberts, K.A., Yang, K., Polyanovsky, A., Church, A., and Avidor-Reiss, T. (2009). A proximal centriole-like structure is present in Drosophila spermatids and can serve as a model to study centriole duplication. *Genetics* 182, 133–144.

Blachon, S., Gopalakrishnan, J., Omori, Y., Polyanovsky, A., Church, A., Nicastro, D., Malicki, J., and Avidor-Reiss, T. (2008). Drosophila asterless and vertebrate Cep152 Are orthologs essential for centriole duplication. *Genetics* 180, 2081–2094.

Blangy, A., Lane, H.A., d'Hérin, P., Harper, M., Kress, M., and Nigg, E.A. (1995). Phosphorylation by p34cdc2 regulates spindle association of human Eg5, a kinesin-related motor essential for bipolar spindle formation in vivo. *Cell* 83, 1159–1169.

Bobinnec, Y., Khodjakov, A., Mir, L.M., Rieder, C.L., Edde, B., and Bornens, M. (1998a). Centriole disassembly in vivo and its effect on centrosome structure and function in vertebrate cells. *The Journal of Cell Biology* 143, 1575–1589.

Bobinnec, Y., Moudjou, M., Fouquet, J.P., Desbruyeres, E., Edde, B., and Bornens, M.

- (1998b). Glutamylation of centriole and cytoplasmic tubulin in proliferating non-neuronal cells. *Cell Motil Cytoskeleton* 39, 223–232.
- Bogoyevitch, M.A., Yeap, Y.Y.C., Qu, Z., Ngoei, K.R., Yip, Y.Y., Zhao, T.T., Heng, J.I., and Ng, D.C.H. (2012). WD40-repeat protein 62 is a JNK-phosphorylated spindle pole protein required for spindle maintenance and timely mitotic progression. *J. Cell. Sci.* 125, 5096–5109.
- Bornens, M. (2012). The Centrosome in Cells and Organisms. *Science* 335, 422–426.
- Bornens, M., Paintrand, M., Berges, J., Marty, M.C., and Karsenti, E. (1987). Structural and chemical characterization of isolated centrosomes. *Cell Motil Cytoskeleton* 8, 238–249.
- Bornens, M. (2002). Centrosome composition and microtubule anchoring mechanisms. *Curr Opin Cell Biol* 14, 25–34.
- Bornens, M., and Azimzadeh, J. (2007). Origin and evolution of the centrosome. *Adv. Exp. Med. Biol.* 607, 119–129.
- Bourke, E., Dodson, H., Merdes, A., Cuffe, L., Zachos, G., Walker, M., Gillespie, D., and Morrison, C.G. (2007). DNA damage induces Chk1-dependent centrosome amplification. *EMBO Rep.* 8, 603–609.
- Boveri, T. (1887). Ueber die Befruchtung der Eier von *Ascaris megalcephala*. *Sitzungsberichte Der Gesellschaft Für Morphologie Und Physiologie in München* 3, 394–443.
- Boveri, T. (1914). Zur Frage der Entstehung maligner Tumore. (English Translation: The Origin of malignant Tumors, Williams and Wilkins, Baltimore, Maryland, 1929).
- Brown, N.J., Marjanović, M., Lüders, J., Stracker, T.H., and Costanzo, V. (2013). Cep63 and cep152 cooperate to ensure centriole duplication. *PLoS ONE* 8, e69986.
- Brownlee, C.W., and Rogers, G.C. (2013). Show me your license, please: deregulation of centriole duplication mechanisms that promote amplification. *Cell. Mol. Life Sci.* 70, 1021–1034.
- Brownlee, C.W., Klebba, J.E., Buster, D.W., and Rogers, G.C. (2011). The Protein Phosphatase 2A regulatory subunit Twins stabilizes Plk4 to induce centriole amplification. *The Journal of Cell Biology* 195, 231–243.
- Campaner, S., Kaldis, P., Izraeli, S., and Kirsch, I.R. (2005). Sil phosphorylation in a Pin1 binding domain affects the duration of the spindle checkpoint. *Mol Cell Biol* 25, 6660–6672.
- Carlotti, E., Pettenella, F., Amaru, R., Slater, S., Lister, T.A., Barbui, T., Basso, G., Cazzaniga, G., Rambaldi, A., and Biondi, A. (2002). Molecular characterization of a new recombination of the SIL/TAL-1 locus in a child with T-cell acute lymphoblastic leukaemia. *British Journal of Haematology* 118, 1011–1018.
- Carvalho-Santos, Z., Azimzadeh, J., Pereira-Leal, J.B., and Bettencourt-Dias, M. (2011). Evolution: Tracing the origins of centrioles, cilia, and flagella. *The Journal of Cell Biology*

194, 165–175.

Carvalho-Santos, Z., Machado, P., Alvarez-Martins, I., Gouveia, S.M., Jana, S.C., Duarte, P., Amado, T., Branco, P., Freitas, M.C., Silva, S.T., et al. (2012). BLD10/CEP135 Is a Microtubule-Associated Protein that Controls the Formation of the Flagellum Central Microtubule Pair. *Dev. Cell* 23, 412–424.

Castiel, A., Danieli, M.M., David, A., Moshkovitz, S., Aplan, P.D., Kirsch, I.R., Brandeis, M., Krämer, A., and Izraeli, S. (2011). The Stil protein regulates centrosome integrity and mitosis through suppression of Chfr. *J. Cell. Sci.* 124, 532–539.

Chang, J., Cizmecioglu, O., Hoffmann, I., and Rhee, K. (2010). PLK2 phosphorylation is critical for CPAP function in procentriole formation during the centrosome cycle. *Embo J* 29, 2395–2406.

Chen, Z., Indjeian, V.B., McManus, M., Wang, L., and Dynlacht, B.D. (2002). CP110, a cell cycle-dependent CDK substrate, regulates centrosome duplication in human cells. *Dev. Cell* 3, 339–350.

Ching, Y.-P., Pang, A.S.H., Lam, W.-H., Qi, R.Z., and Wang, J.H. (2002). Identification of a neuronal Cdk5 activator-binding protein as Cdk5 inhibitor. *J. Biol. Chem.* 277, 15237–15240.

Choi, Y.K., Liu, P., Sze, S.K., Dai, C., and Qi, R.Z. (2010). CDK5RAP2 stimulates microtubule nucleation by the γ -tubulin ring complex. *The Journal of Cell Biology* 191, 1089–1095.

Cizmecioglu, O., Arnold, M., Bahtz, R., Settele, F., Ehret, L., Haselmann-Weiß, U., Antony, C., and Hoffmann, I. (2010). Cep152 acts as a scaffold for recruitment of Plk4 and CPAP to the centrosome. *The Journal of Cell Biology* 191, 731–739.

Cizmecioglu, O., Krause, A., Bahtz, R., Ehret, L., Malek, N., and Hoffmann, I. (2012). Plk2 regulates centriole duplication through phosphorylation-mediated degradation of Fbxw7 (human Cdc4). *J. Cell. Sci.* 125, 981–992.

Comartin, D., Gupta, G.D., Fussner, E., Coyaud, É., Hasegan, M., Archinti, M., Cheung, S.W.T., Pinchev, D., Lawo, S., Raught, B., et al. (2013). CEP120 and SPICE1 cooperate with CPAP in centriole elongation. *Curr. Biol.* 23, 1360–1366.

Conduit, P.T., Feng, Z., Richens, J.H., and Baumbach, J. (2014). The Centrosome-Specific Phosphorylation of Cnn by Polo/Plk1 Drives Cnn Scaffold Assembly and Centrosome Maturation. *Dev. Cell.*

Cooper, J.A. (2013). Cell biology in neuroscience: mechanisms of cell migration in the nervous system. *The Journal of Cell Biology* 202, 725–734.

Cottee, M.A., Muschalik, N., Wong, Y.L., Johnson, C.M., Johnson, S., Andreeva, A., Oegema, K., Lea, S.M., Raff, J.W., and van Breugel, M. (2013). Crystal structures of the CPAP/STIL complex reveal its role in centriole assembly and human microcephaly. *Elife* 2, e01071.

Cunha-Ferreira, I., Bento, I., Pimenta-Marques, A., Jana, S.C., Lince-Faria, M., Duarte, P., Borrego-Pinto, J., Gilberto, S., Amado, T., Brito, D., et al. (2013). Regulation of Autophosphorylation Controls PLK4 Self-Destruction and Centriole Number. *Curr. Biol.*

23, 2245–2254.

Cunha-Ferreira, I., Rodrigues-Martins, A., Bento, I., Riparbelli, M., Zhang, W., Laue, E., Callaini, G., Glover, D.M., and Bettencourt-Dias, M. (2009). The SCF/Slimb ubiquitin ligase limits centrosome amplification through degradation of SAK/PLK4. *Curr. Biol.* *19*, 43–49.

Dammermann, A., Maddox, P.S., Desai, A., and Oegema, K. (2008). SAS-4 is recruited to a dynamic structure in newly forming centrioles that is stabilized by the gamma-tubulin-mediated addition of centriolar microtubules. *The Journal of Cell Biology* *180*, 771–785.

Dammermann, A., Müller-Reichert, T., Pelletier, L., Habermann, B., Desai, A., and Oegema, K. (2004). Centriole assembly requires both centriolar and pericentriolar material proteins. *Dev. Cell* *7*, 815–829.

Dantas, T.J.T., Wang, Y.Y., Lalor, P.P., Dockery, P.P., and Morrison, C.G.C. (2011). Defective nucleotide excision repair with normal centrosome structures and functions in the absence of all vertebrate centrin. *The Journal of Cell Biology* *193*, 307–318.

Delattre, M., Canard, C., and Gönczy, P. (2006). Sequential Protein Recruitment in *C. elegans* Centriole Formation. *Curr. Biol.* *16*, 1844–1849.

Delattre, M., Leidel, S., Wani, K., Baumer, K., Bamat, J., Schnabel, H., Feichtinger, R., Schnabel, R., and Gönczy, P. (2004). Centriolar SAS-5 is required for centrosome duplication in *C. elegans*. *Nature Cell Biology* *6*, 656–664.

Delgehyr, N., Rangone, H., Fu, J., Mao, G., Tom, B., Riparbelli, M.G., Callaini, G., and Glover, D.M. (2012). Klp10A, a Microtubule-Depolymerizing Kinesin-13, Cooperates with CP110 to Control *Drosophila* Centriole Length. *Curr. Biol.* *22*, 502–509.

Delgehyr, N., Sillibourne, J., and Bornens, M. (2005). Microtubule nucleation and anchoring at the centrosome are independent processes linked by ninein function. *J. Cell. Sci.* *118*, 1565–1575.

Dicthenberg, J.B., Zimmerman, W., Sparks, C.A., Young, A., Vidair, C., Zheng, Y., Carrington, W., Fay, F.S., and Doxsey, S.J. (1998). Pericentrin and gamma-tubulin form a protein complex and are organized into a novel lattice at the centrosome. *The Journal of Cell Biology* *141*, 163–174.

Dippell, R.V. (1968). The development of basal bodies in paramecium. *Proc. Natl. Acad. Sci. U.S.A.* *61*, 461–468.

Dix, C.I., and Raff, J.W. (2007). *Drosophila* Spd-2 recruits PCM to the sperm centriole, but is dispensable for centriole duplication. *Curr. Biol.* *17*, 1759–1764.

Dobbelaere, J., Josué, F., Suijkerbuijk, S., Baum, B., Tapon, N., and Raff, J. (2008). A genome-wide RNAi screen to dissect centriole duplication and centrosome maturation in *Drosophila*. *PLoS Biol.* *6*, e224.

Doxsey, S.J., Stein, P., Evans, L., Calarco, P.D., and Kirschner, M. (1994). Pericentrin, a highly conserved centrosome protein involved in microtubule organization. *Cell* *76*, 639–650.

-
- Doxsey, S., McCollum, D., and Theurkauf, W. (2005a). Centrosomes in cellular regulation. *Annu. Rev. Cell Dev. Biol.* *21*, 411–434.
- Doxsey, S., Zimmerman, W., and Mikule, K. (2005b). Centrosome control of the cell cycle. *Trends in Cell Biology* *15*, 303–311.
- Dzhindzhev, N.S., Yu, Q.D., Weiskopf, K., Tzolovsky, G., Cunha-Ferreira, I., Riparbelli, M., Rodrigues-Martins, A., Bettencourt-Dias, M., Callaini, G., and Glover, D.M. (2010). Asterless is a scaffold for the onset of centriole assembly. *Nature* *467*, 714–718.
- D’Angiolella, V., Donato, V., Vijayakumar, S., Saraf, A., Florens, L., Washburn, M.P., Dynlacht, B., and Pagano, M. (2010). SCF(Cyclin F) controls centrosome homeostasis and mitotic fidelity through CP110 degradation. *Nature* *466*, 138–142.
- Erez, A., Castiel, A., Trakhtenbrot, L., Perelman, M., Rosenthal, E., Goldstein, I., Stettner, N., Harmelin, A., Eldar-Finkelman, H., Campaner, S., et al. (2007). The SIL gene is essential for mitotic entry and survival of cancer cells. *Cancer Research* *67*, 4022–4027.
- Erez, A., Chaussepied, M., Castiel, A., Colaizzo-Anas, T., Aplan, P.D., Ginsberg, D., and Izraeli, S. (2008). The mitotic checkpoint gene, SIL is regulated by E2F1. *Int. J. Cancer* *123*, 1721–1725.
- Erez, A., Perelman, M., Hewitt, S.M., Cojocar, G., Goldberg, I., Shahar, I., Yaron, P., Muler, I., Campaner, S., Amariglio, N., et al. (2004). Sil overexpression in lung cancer characterizes tumors with increased mitotic activity. *Oncogene: an International Journal* *23*, 5371–5377.
- Farag, H.G., Froehler, S., Oexle, K., Ravindran, E., Schindler, D., Staab, T., Huebner, A., Kraemer, N., Chen, W., and Kaindl, A.M. (2013). Abnormal centrosome and spindle morphology in a patient with autosomal recessive primary microcephaly type 2 due to compound heterozygous WDR62 gene mutation. *Orphanet J Rare Dis* *8*, 178.
- Faragher, A.J., and Fry, A.M. (2003). Nek2A kinase stimulates centrosome disjunction and is required for formation of bipolar mitotic spindles. *Molecular Biology of the Cell* *14*, 2876–2889.
- Félix, M.A., Antony, C., Wright, M., and Maro, B. (1994). Centrosome assembly in vitro: role of gamma-tubulin recruitment in *Xenopus* sperm aster formation. *The Journal of Cell Biology* *124*, 19–31.
- Fish, J.L., Kosodo, Y., Enard, W., Pääbo, S., and Huttner, W.B. (2006). Aspm specifically maintains symmetric proliferative divisions of neuroepithelial cells. *Proc. Natl. Acad. Sci. U.S.A.* *103*, 10438–10443.
- Fisk, H.A., and Winey, M. (2001). The mouse Mps1p-like kinase regulates centrosome duplication. *Cell* *106*, 95–104.
- Foley, E.A., and Kapoor, T.M. (2013). Microtubule attachment and spindle assembly checkpoint signalling at the kinetochore. *Nat Rev Mol Cell Biol* *14*, 25–37.
- Fong, K.-W., Choi, Y.-K., Rattner, J.B., and Qi, R.Z. (2008). CDK5RAP2 is a pericentriolar protein that functions in centrosomal attachment of the gamma-tubulin ring complex.
-

Molecular Biology of the Cell 19, 115–125.

Fourrage, C., Chevalier, S., and Houliston, E. (2010). A highly conserved Poc1 protein characterized in embryos of the hydrozoan *Clytia hemisphaerica*: localization and functional studies. *PLoS ONE* 5, e13994.

Franz, A., Roque, H., Saurya, S., Dobbelaere, J., and Raff, J.W. (2013). CP110 exhibits novel regulatory activities during centriole assembly in *Drosophila*. *The Journal of Cell Biology* 203, 785–799.

Fraser, A.G., Kamath, R.S., Zipperlen, P., Martinez-Campos, M., Sohrmann, M., and Ahringer, J. (2000). Functional genomic analysis of *C. elegans* chromosome I by systematic RNA interference. *Nature* 408, 325–330.

Fry, A.M., Mayor, T., Meraldi, P., Stierhof, Y.D., Tanaka, K., and Nigg, E.A. (1998). C-Nap1, a novel centrosomal coiled-coil protein and candidate substrate of the cell cycle-regulated protein kinase Nek2. *The Journal of Cell Biology* 141, 1563–1574.

Fu, J., and Glover, D.M. (2012). Structured illumination of the interface between centriole and peri-centriolar material. *Open Biol* 2, 120104–120104.

Fuller, S.D., Gowen, B.E., Reinsch, S., Sawyer, A., Buendia, B., Wepf, R., and Karsenti, E. (1995). The core of the mammalian centriole contains gamma-tubulin. *Curr. Biol.* 5, 1384–1393.

Gadde, S., and Heald, R. (2004). Mechanisms and molecules of the mitotic spindle. *Curr. Biol.* 14, R797–R805.

Ganem, N.J., Godinho, S.A., and Pellman, D. (2009). A mechanism linking extra centrosomes to chromosomal instability. *Nature* 460, 278–282.

Genin, A., Desir, J., Lambert, N., Biervliet, M., Van Der Aa, N., Pierquin, G., Killian, A., Tosi, M., Urbina, M., Lefort, A., et al. (2012). Kinetochore KMN network gene CASC5 mutated in primary microcephaly. *Hum. Mol. Genet.* 21, 5306–5317.

Gergely, F., and Basto, R. (2008). Multiple centrosomes: together they stand, divided they fall. *Genes Dev.* 22, 2291–2296.

Giansanti, M.G., Bucciarelli, E., Bonaccorsi, S., and Gatti, M. (2008). *Drosophila* SPD-2 is an essential centriole component required for PCM recruitment and astral-microtubule nucleation. *Curr. Biol.* 18, 303–309.

Goetz, S.C., and Anderson, K.V. (2010). The primary cilium: a signalling centre during vertebrate development. *Nat. Rev. Genet.* 11, 331–344.

Gomez-Ferreria, M.A., Rath, U., Buster, D.W., Chanda, S.K., Caldwell, J.S., Rines, D.R., and Sharp, D.J. (2007). Human Cep192 is required for mitotic centrosome and spindle assembly. *Curr. Biol.* 17, 1960–1966.

Gonczy, P., Echeverri, C., Oegema, K., Coulson, A., Jones, S.J., Copley, R.R., Duperon, J., Oegema, J., Brehm, M., Cassin, E., et al. (2000). Functional genomic analysis of cell division in *C. elegans* using RNAi of genes on chromosome III. *Nature* 408, 331–336.

- Gopalakrishnan, J., Chim, Y.-C.F., Ha, A., Basiri, M.L., Lerit, D.A., Rusan, N.M., and Avidor-Reiss, T. (2012). Tubulin nucleotide status controls Sas-4-dependent pericentriolar material recruitment. *Nature Cell Biology* *14*, 865–873.
- Gopalakrishnan, J., Guichard, P., Smith, A.H., Schwarz, H., Agard, D.A., Marco, S., and Avidor-Reiss, T. (2010). Self-assembling SAS-6 multimer is a core centriole building block. *J Biol Chem* *285*, 8759–8770.
- Gopalakrishnan, J., Mennella, V., Blachon, S., Zhai, B., Smith, A.H., Megraw, T.L., Nicastro, D., Gygi, S.P., Agard, D.A., and Avidor-Reiss, T. (2011). Sas-4 provides a scaffold for cytoplasmic complexes and tethers them in a centrosome. *Nat Comms* *2*, 359.
- Goshima, G., Wollman, R., Goodwin, S.S., Zhang, N., Scholey, J.M., Vale, R.D., and Stuurman, N. (2007). Genes required for mitotic spindle assembly in *Drosophila* S2 cells. *Science* *316*, 417–421.
- Gould, R.R., and Borisy, G.G. (1977). The pericentriolar material in Chinese hamster ovary cells nucleates microtubule formation. *The Journal of Cell Biology* *73*, 601–615.
- Gönczy, P. (2012). Towards a molecular architecture of centriole assembly. *Nat Rev Mol Cell Biol* *13*, 425–435.
- Gönczy, P., and Rose, L.S. (2005). Asymmetric cell division and axis formation in the embryo. *WormBook* 1–20.
- Graser, S., Stierhof, Y.-D., and Nigg, E.A. (2007). Cep68 and Cep215 (Cdk5rap2) are required for centrosome cohesion. *J. Cell. Sci.* *120*, 4321–4331.
- Gruber, R., Zhou, Z., Sukchev, M., Joerss, T., Frappart, P.-O., and Wang, Z.-Q. (2011). MCPH1 regulates the neuroprogenitor division mode by coupling the centrosomal cycle with mitotic entry through the Chk1-Cdc25 pathway. *Nature Cell Biology* *13*, 1325–1334.
- Gruss, O.J., and Vernos, I. (2004). The mechanism of spindle assembly: functions of Ran and its target TPX2. *The Journal of Cell Biology* *166*, 949–955.
- Guderian, G., Westendorf, J., Uldschmid, A., and Nigg, E.A. (2010). Plk4 trans-autophosphorylation regulates centriole number by controlling betaTrCP-mediated degradation. *J. Cell. Sci.* *123*, 2163–2169.
- Gudi, R., Zou, C., Li, J., and Gao, Q. (2011). Centrobin-tubulin interaction is required for centriole elongation and stability. *The Journal of Cell Biology* *193*, 711–725.
- Guichard, P., Desfosses, A., Maheshwari, A., Hachet, V., Dietrich, C., Brune, A., Ishikawa, T., Sachse, C., and Gönczy, P. (2012). Cartwheel Architecture of *Trichonympha* Basal Body. *Science* *337*, 553–553.
- Guichard, P., Chrétien, D., Marco, S., and Tassin, A.-M. (2010). Procentriole assembly revealed by cryo-electron tomography. *Embo J* *29*, 1565–1572.
- Guichard, P., Hachet, V., Majubu, N., Neves, A., Demurtas, D., Olieric, N., Flückiger, I., Yamada, A., Kihara, K., Nishida, Y., et al. (2013). Native architecture of the centriole

- proximal region reveals features underlying its 9-fold radial symmetry. *Curr. Biol.* *23*, 1620–1628.
- Habedanck, R., Stierhof, Y.-D., Wilkinson, C.J., and Nigg, E.A. (2005). The Polo kinase Plk4 functions in centriole duplication. *Nature Cell Biology* *7*, 1140–1146.
- Hachet, V., Canard, C., and Gönczy, P. (2007). Centrosomes Promote Timely Mitotic Entry in *C. elegans* Embryos. *Dev. Cell* *12*, 531–541.
- Hannak, E., Kirkham, M., Hyman, A.A., and Oegema, K. (2001). Aurora-A kinase is required for centrosome maturation in *Caenorhabditis elegans*. *The Journal of Cell Biology* *155*, 1109–1116.
- Haren, L., Stearns, T., and Lüders, J. (2009). Plk1-dependent recruitment of gamma-tubulin complexes to mitotic centrosomes involves multiple PCM components. *PLoS ONE* *4*, e5976.
- Hatch, E.M., Kulukian, A., Holland, A.J., Cleveland, D.W., and Stearns, T. (2010). Cep152 interacts with Plk4 and is required for centriole duplication. *The Journal of Cell Biology* *191*, 721–729.
- Hatzopoulos, G.N., Erat, M.C., Cutts, E., Rogala, K.B., Slater, L.M., Stansfeld, P.J., and Vakonakis, I. (2013). Structural analysis of the G-box domain of the microcephaly protein CPAP suggests a role in centriole architecture. *Structure* *21*, 2069–2077.
- Heald, R., Tournebize, R., Blank, T., Sandaltzopoulos, R., Becker, P., Hyman, A., and Karsenti, E. (1996). Self-organization of microtubules into bipolar spindles around artificial chromosomes in *Xenopus* egg extracts. *Nature* *382*, 420–425.
- Helps, N.R., Luo, X., Barker, H.M., and Cohen, P.T. (2000). NIMA-related kinase 2 (Nek2), a cell-cycle-regulated protein kinase localized to centrosomes, is complexed to protein phosphatase 1. *Biochem. J.* *349*, 509–518.
- Higgins, J., Midgley, C., Bergh, A.-M., Bell, S.M., Askham, J.M., Roberts, E., Binns, R.K., Sharif, S.M., Bennett, C., Glover, D.M., et al. (2010). Human ASPM participates in spindle organisation, spindle orientation and cytokinesis. *BMC Cell Biol.* *11*, 85.
- Hilbert, M., Erat, M.C., Hachet, V., Guichard, P., Blank, I.D., Flückiger, I., Slater, L., Lowe, E.D., Hatzopoulos, G.N., Steinmetz, M.O., et al. (2013). *Caenorhabditis elegans* centriolar protein SAS-6 forms a spiral that is consistent with imparting a ninefold symmetry. *Proceedings of the National Academy of Sciences* *110*, 11373–11378.
- Hinchcliffe, E.H., Li, C., Thompson, E.A., Maller, J.L., and Sluder, G. (1999). Requirement of Cdk2-cyclin E activity for repeated centrosome reproduction in *Xenopus* egg extracts. *Science* *283*, 851–854.
- Hinchcliffe, E.H., Miller, F.J., Cham, M., Khodjakov, A., and Sluder, G. (2001). Requirement of a centrosomal activity for cell cycle progression through G1 into S phase. *Science* *291*, 1547–1550.
- Hiraki, M., Nakazawa, Y., Kamiya, R., and Hirono, M. (2007). Bld10p constitutes the cartwheel-spoke tip and stabilizes the 9-fold symmetry of the centriole. *Curr. Biol.* *17*,

1778–1783.

Hodges, M.E., Scheumann, N., Wickstead, B., Langdale, J.A., and Gull, K. (2010). Reconstructing the evolutionary history of the centriole from protein components. *J. Cell. Sci.* *123*, 1407–1413.

Holland, A.J., Fachinetti, D., Zhu, Q., Bauer, M., Verma, I.M., Nigg, E.A., and Cleveland, D.W. (2012). The autoregulated instability of Polo-like kinase 4 limits centrosome duplication to once per cell cycle. *Genes Dev.* *26*, 2684–2689.

Holland, A.J., Lan, W., Niessen, S., Hoover, H., and Cleveland, D.W. (2010). Polo-like kinase 4 kinase activity limits centrosome overduplication by autoregulating its own stability. *The Journal of Cell Biology* *188*, 191–198.

Horio, T., Uzawa, S., Jung, M.K., Oakley, B.R., Tanaka, K., and Yanagida, M. (1991). The fission yeast gamma-tubulin is essential for mitosis and is localized at microtubule organizing centers. *J. Cell. Sci.* *99 (Pt 4)*, 693–700.

Hudson, J.W., Kozarova, A., Cheung, P., Macmillan, J.C., Swallow, C.J., Cross, J.C., and Dennis, J.W. (2001). Late mitotic failure in mice lacking Sak, a polo-like kinase. *Curr. Biol.* *11*, 441–446.

Hung, L.Y., Tang, C.J., and Tang, T.K. (2000). Protein 4.1 R-135 interacts with a novel centrosomal protein (CPAP) which is associated with the gamma-tubulin complex. *Mol Cell Biol* *20*, 7813–7825.

Inanc, B., Dodson, H., and Morrison, C.G. (2010). A Centrosome-autonomous Signal That Involves Centriole Disengagement Permits Centrosome Duplication in G2 Phase after DNA Damage. *Molecular Biology of the Cell* *21*, 3866–3877.

Ishikawa, H., and Marshall, W.F. (2011). Ciliogenesis: building the cell's antenna. *Nat Rev Mol Cell Biol* *12*, 222–234.

Isono, K.-I., Fujimura, Y.-I., Shinga, J., Yamaki, M., O-Wang, J., Takihara, Y., Murahashi, Y., Takada, Y., Mizutani-Koseki, Y., and Koseki, H. (2005). Mammalian polyhomeotic homologues Phc2 and Phc1 act in synergy to mediate polycomb repression of Hox genes. *Mol Cell Biol* *25*, 6694–6706.

Izraeli, S., Colaizzo-Anas, T., Bertness, V.L., Mani, K., Aplan, P.D., and Kirsch, I.R. (1997). Expression of the SIL gene is correlated with growth induction and cellular proliferation. *Cell Growth Differ.* *8*, 1171–1179.

Izraeli, S., Lowe, L.A., Bertness, V.L., Campaner, S., Hahn, H., Kirsch, I.R., and Kuehn, M.R. (2001). Genetic evidence that Sil is required for the Sonic Hedgehog response pathway. *Genesis* *31*, 72–77.

Izraeli, S., Lowe, L.A., Bertness, V.L., Good, D.J., Dorward, D.W., Kirsch, I.R., and Kuehn, M.R. (1999). The SIL gene is required for mouse embryonic axial development and left-right specification. *Nature* *399*, 691–694.

Jakobsen, L., Vanselow, K., Skogs, M., Toyoda, Y., Lundberg, E., Poser, I., Falkenby, L.G., Bennetzen, M., Westendorf, J., Nigg, E.A., et al. (2011). Novel asymmetrically localizing

- components of human centrosomes identified by complementary proteomics methods. *Embo J* 30, 1520–1535.
- Januschke, J., Reina, J., Llamazares, S., Bertran, T., Rossi, F., Roig, J., and Gonzalez, C. (2013). Centrobin controls mother-daughter centriole asymmetry in *Drosophila* neuroblasts. *Nature Cell Biology* 15, 241–248.
- Januschke, J., Llamazares, S., Reina, J., and Gonzalez, C. (2011). *Drosophila* neuroblasts retain the daughter centrosome. *Nat Comms* 2, 243.
- Jaspersen, S.L., and Winey, M. (2004). The budding yeast spindle pole body: structure, duplication, and function. *Annu. Rev. Cell Dev. Biol.* 20, 1–28.
- Jerka-Dziadosz, M., Gogendeau, D., Klotz, C., Cohen, J., Beisson, J., and Koll, F. (2010). Basal body duplication in *Paramecium*: the key role of Bld10 in assembly and stability of the cartwheel. *Cytoskeleton (Hoboken)* 67, 161–171.
- Joukov, V., De Nicolo, A., Rodriguez, A., Walter, J.C., and Livingston, D.M. (2010). Centrosomal protein of 192 kDa (Cep192) promotes centrosome-driven spindle assembly by engaging in organelle-specific Aurora A activation. *Proc. Natl. Acad. Sci. U.S.a.* 107, 21022–21027.
- Kaindl, A.M., Passemard, S., Kumar, P., Kraemer, N., Issa, L., Zwirner, A., Gerard, B., Verloes, A., Mani, S., and Gressens, P. (2010). Many roads lead to primary autosomal recessive microcephaly. *Prog. Neurobiol.* 90, 363–383.
- Keller, L.C., Geimer, S., Romijn, E., Yates, J., Zamora, I., and Marshall, W.F. (2009). Molecular architecture of the centriole proteome: the conserved WD40 domain protein POC1 is required for centriole duplication and length control. *Molecular Biology of the Cell* 20, 1150–1166.
- Keller, L.C., Romijn, E.P., Zamora, I., Yates, J.R., and Marshall, W.F. (2005). Proteomic analysis of isolated *Chlamydomonas* centrioles reveals orthologs of ciliary-disease genes. *Curr. Biol.* 15, 1090–1098.
- Kemp, C.A., Kopish, K.R., Zipperlen, P., Ahringer, J., and O'Connell, K.F. (2004). Centrosome maturation and duplication in *C. elegans* require the coiled-coil protein SPD-2. *Dev. Cell* 6, 511–523.
- Khodjakov, A., and Rieder, C.L. (2001). Centrosomes enhance the fidelity of cytokinesis in vertebrates and are required for cell cycle progression. *The Journal of Cell Biology* 153, 237–242.
- Khodjakov, A., Rieder, C.L., Sluder, G., Cassels, G., Sibon, O., and Wang, C.-L. (2002). De novo formation of centrosomes in vertebrate cells arrested during S phase. *The Journal of Cell Biology* 158, 1171–1181.
- Kilburn, C.L., Pearson, C.G., Romijn, E.P., Meehl, J.B., Giddings, T.H., Culver, B.P., Yates, J.R., and Winey, M. (2007). New *Tetrahymena* basal body protein components identify basal body domain structure. *The Journal of Cell Biology* 178, 905–912.
- Kilmartin, J.V. (2003). Sfi1p has conserved centrin-binding sites and an essential

- function in budding yeast spindle pole body duplication. *The Journal of Cell Biology* *162*, 1211–1221.
- Kim, S., and Dynlacht, B.D. (2013). Assembling a primary cilium. *Curr Opin Cell Biol* *25*, 506–511.
- Kim, T.-S., Park, J.-E., Shukla, A., Choi, S., Murugan, R.N., Lee, J.H., Ahn, M., Rhee, K., Bang, J.K., Kim, B.Y., et al. (2013). Hierarchical recruitment of Plk4 and regulation of centriole biogenesis by two centrosomal scaffolds, Cep192 and Cep152. *Proceedings of the National Academy of Sciences* *110*, E4849–E4857.
- Kirkham, M., Müller-Reichert, T., Oegema, K., Grill, S., and Hyman, A.A. (2003). SAS-4 is a *C. elegans* centriolar protein that controls centrosome size. *Cell* *112*, 575–587.
- Kitagawa, D., Kohlmaier, G., Keller, D., Strnad, P., Balestra, F.R., Fluckiger, I., and Gonczy, P. (2011a). Spindle positioning in human cells relies on proper centriole formation and on the microcephaly proteins CPAP and STIL. *J. Cell. Sci.* *124*, 3884–3893.
- Kitagawa, D.D., Vakonakis, I.I., Olieric, N.N., Hilbert, M.M., Keller, D.D., Olieric, V.V., Bortfeld, M.M., Erat, M.C.M., Flückiger, I.I., Gönczy, P.P., et al. (2011b). Structural basis of the nine-fold symmetry of centrioles. *Cell* *144*, 12–12.
- Klebba, J.E., Buster, D.W., Nguyen, A.L., Swatkoski, S., Gucek, M., Rusan, N.M., and Rogers, G.C. (2013). Polo-like Kinase 4 Autodeconstructs by Generating Its Slimb-Binding Phosphodegron. *Curr. Biol.* *23*, 2255–2261.
- Kleylein-Sohn, J., Westendorf, J., Le Clech, M., Habedanck, R., Stierhof, Y.-D., and Nigg, E.A. (2007). Plk4-induced centriole biogenesis in human cells. *Dev. Cell* *13*, 190–202.
- Klingseisen, A., and Jackson, A.P. (2011). Mechanisms and pathways of growth failure in primordial dwarfism. *Genes Dev.* *25*, 2011–2024.
- Klos Dehring, D.A., Vldar, E.K., Werner, M.E., Mitchell, J.W., Hwang, P., and Mitchell, B.J. (2013). Deuterosome-mediated centriole biogenesis. *Dev. Cell* *27*, 103–112.
- Kobayashi, D., and Takeda, H. (2012). Ciliary motility: the components and cytoplasmic preassembly mechanisms of the axonemal dyneins. *Differentiation* *83*, S23–S29.
- Kohlmaier, G., Loncarek, J., Meng, X., McEwen, B.F., Mogensen, M.M., Spektor, A., Dynlacht, B.D., Khodjakov, A., and Gönczy, P. (2009). Overly long centrioles and defective cell division upon excess of the SAS-4-related protein CPAP. *Curr. Biol.* *19*, 1012–1018.
- Komada, M., Fujiyama, F., Yamada, S., Shiota, K., and Nagao, T. (2010). Methylnitrosourea induces neural progenitor cell apoptosis and microcephaly in mouse embryos. *Birth Defects Res. B Dev. Reprod. Toxicol.* *89*, 213–222.
- Kotak, S., and Gönczy, P. (2013). Mechanisms of spindle positioning: cortical force generators in the limelight. *Curr Opin Cell Biol* *25*, 741–748.
- Kubo, A., Sasaki, H., Yuba-Kubo, A., Tsukita, S., and Shiina, N. (1999). Centriolar satellites: molecular characterization, ATP-dependent movement toward centrioles and possible involvement in ciliogenesis. *The Journal of Cell Biology* *147*, 969–980.

-
- Kumar, A., Girimaji, S.C., Duvvari, M.R., and Blanton, S.H. (2009). Mutations in STIL, Encoding a Pericentriolar and Centrosomal Protein, Cause Primary Microcephaly. *The American Journal of Human Genetics* 84, 286–290.
- Kuriyama, R., and Borisy, G.G. (1981). Centriole cycle in Chinese hamster ovary cells as determined by whole-mount electron microscopy. *The Journal of Cell Biology* 91, 814–821.
- Kwon, M., Godinho, S.A., Chandhok, N.S., Ganem, N.J., Azioune, A., They, M., and Pellman, D. (2008). Mechanisms to suppress multipolar divisions in cancer cells with extra centrosomes. *Genes Dev.* 22, 2189–2203.
- Lacey, K.R., Jackson, P.K., and Stearns, T. (1999). Cyclin-dependent kinase control of centrosome duplication. *Proc. Natl. Acad. Sci. U.S.A.* 96, 2817–2822.
- Lane, H.A., and Nigg, E.A. (1996). Antibody microinjection reveals an essential role for human polo-like kinase 1 (Plk1) in the functional maturation of mitotic centrosomes. *The Journal of Cell Biology* 135, 1701–1713.
- Lange, B.M., and Gull, K. (1995). A molecular marker for centriole maturation in the mammalian cell cycle. *The Journal of Cell Biology* 130, 919–927.
- Lawo, S., Hasegan, M., Gupta, G.D., and Pelletier, L. (2012). Subdiffraction imaging of centrosomes reveals higher-order organizational features of pericentriolar material. *Nature Cell Biology* 14, 1148–1158.
- Lee, K., and Rhee, K. (2011). PLK1 phosphorylation of pericentrin initiates centrosome maturation at the onset of mitosis. *The Journal of Cell Biology* 195, 1093–1101.
- Lehtinen, M.K., and Walsh, C.A. (2011). Neurogenesis at the brain-cerebrospinal fluid interface. *Annu. Rev. Cell Dev. Biol.* 27, 653–679.
- Leidel, S., and Gönczy, P. (2003). SAS-4 is essential for centrosome duplication in *C. elegans* and is recruited to daughter centrioles once per cell cycle. *Dev. Cell* 4, 431–439.
- Leidel, S., and Gönczy, P. (2005). Centrosome duplication and nematodes: recent insights from an old relationship. *Dev. Cell* 9, 317–325.
- Leidel, S., Delattre, M., Cerutti, L., Baumer, K., and Gönczy, P. (2005). SAS-6 defines a protein family required for centrosome duplication in *C. elegans* and in human cells. *Nature Cell Biology* 7, 115–125.
- Lerit, D.A., and Rusan, N.M. (2013). PLP inhibits the activity of interphase centrosomes to ensure their proper segregation in stem cells. *The Journal of Cell Biology* 202, 1013–1022.
- Li, J., D'Angiolella, V., Seeley, E.S., Kim, S., Kobayashi, T., Fu, W., Campos, E.I., Pagano, M., and Dynlacht, B.D. (2013). USP33 regulates centrosome biogenesis via deubiquitination of the centriolar protein CP110. *Nature* 495, 255–259.
- Limbo, O., Chahwan, C., Yamada, Y., de Bruin, R.A.M., Wittenberg, C., and Russell, P. (2007). Ctp1 is a cell-cycle-regulated protein that functions with Mre11 complex to
-

- control double-strand break repair by homologous recombination. *Molecular Cell* *28*, 134–146.
- Lin, Y.-N., Wu, C.-T., Lin, Y.-C., Hsu, W.-B., Tang, C.-J.C., Chang, C.-W., and Tang, T.K. (2013a). CEP120 interacts with CPAP and positively regulates centriole elongation. *The Journal of Cell Biology* *202*, 211–219.
- Lin, Y.-C., Chang, C.-W., Hsu, W.-B., Tang, C.-J.C., Lin, Y.-N., Chou, E.-J., Wu, C.-T., and Tang, T.K. (2013b). Human microcephaly protein CEP135 binds to hSAS-6 and CPAP, and is required for centriole assembly. *Embo J* *32*, 1141–1154.
- Lingle, W.L., Barrett, S.L., Negron, V.C., D'Assoro, A.B., Boeneman, K., Liu, W., Whitehead, C.M., Reynolds, C., and Salisbury, J.L. (2002). Centrosome amplification drives chromosomal instability in breast tumor development. *Proc. Natl. Acad. Sci. U.S.A.* *99*, 1978–1983.
- Lingle, W.L., Lukasiewicz, K., and Salisbury, J.L. (2005). Deregulation of the centrosome cycle and the origin of chromosomal instability in cancer. *Adv. Exp. Med. Biol.* *570*, 393–421.
- Liu, X., and Erikson, R.L. (2002). Activation of Cdc2/cyclin B and inhibition of centrosome amplification in cells depleted of Plk1 by siRNA. *Proc. Natl. Acad. Sci. U.S.A.* *99*, 8672–8676.
- Loncarek, J., Hergert, P., and Khodjakov, A. (2010). Centriole reduplication during prolonged interphase requires procentriole maturation governed by Plk1. *Curr. Biol.* *20*, 1277–1282.
- Lucas, E.P., and Raff, J.W. (2007). Maintaining the proper connection between the centrioles and the pericentriolar matrix requires *Drosophila* centrosomin. *The Journal of Cell Biology* *178*, 725–732.
- Lukinavičius, G., Lavogina, D., Orpinell, M., Umezawa, K., Reymond, L., Garin, N., Gönczy, P., and Johnsson, K. (2013). Selective chemical crosslinking reveals a Cep57-Cep63-Cep152 centrosomal complex. *Curr. Biol.* *23*, 265–270.
- Lüders, J., and Stearns, T. (2007). Microtubule-organizing centres: a re-evaluation. *Nat Rev Mol Cell Biol* *8*, 161–167.
- Mahajan, M.A., Murray, A., and Samuels, H.H. (2002). NRC-interacting factor 1 is a novel cotransducer that interacts with and regulates the activity of the nuclear hormone receptor coactivator NRC. *Mol Cell Biol* *22*, 6883–6894.
- Mardin, B.R., and Schiebel, E. (2012). Breaking the ties that bind: New advances in centrosome biology. *The Journal of Cell Biology* *197*, 11–18.
- Mardin, B.R., Lange, C., Baxter, J.E., Hardy, T., Scholz, S.R., Fry, A.M., and Schiebel, E. (2010). Components of the Hippo pathway cooperate with Nek2 kinase to regulate centrosome disjunction. *Nature Cell Biology* *12*, 1166–1176.
- Marshall, W.F. (2008). The cell biological basis of ciliary disease. *The Journal of Cell Biology* *180*, 17–21.

-
- Marshall, W.F. (2009). Centriole evolution. *Curr Opin Cell Biol* 21, 14–19.
- Marshall, W.F., and Nonaka, S. (2006). Cilia: tuning in to the cell's antenna. *Curr. Biol.* 16, R604–R614.
- Marthiens, V., Rujano, M.A., Penner, C., Tessier, S., Paul-Gilloteaux, P., and Basto, R. (2013). Centrosome amplification causes microcephaly. *Nature Cell Biology* 15, 731–740.
- Matsumoto, Y., Hayashi, K., and Nishida, E. (1999). Cyclin-dependent kinase 2 (Cdk2) is required for centrosome duplication in mammalian cells. *Current Biology* 9, 429–432.
- Matsuo, K., Ohsumi, K., Iwabuchi, M., Kawamata, T., Ono, Y., and Takahashi, M. (2012). Kendrin Is a Novel Substrate for Separase Involved in the Licensing of Centriole Duplication. *Current Biology* 22, 915–921.
- Matsuura, K., Lefebvre, P.A., Kamiya, R., and Hirono, M. (2004). Bld10p, a novel protein essential for basal body assembly in *Chlamydomonas*: localization to the cartwheel, the first ninefold symmetrical structure appearing during assembly. *The Journal of Cell Biology* 165, 663–671.
- Mayor, T., Stierhof, Y.D., Tanaka, K., Fry, A.M., and Nigg, E.A. (2000). The centrosomal protein C-Nap1 is required for cell cycle-regulated centrosome cohesion. *The Journal of Cell Biology* 151, 837–846.
- Mennella, V., Keszthelyi, B., McDonald, K.L., Chhun, B., Kan, F., Rogers, G.C., Huang, B., and Agard, D.A. (2012). Subdiffraction-resolution fluorescence microscopy reveals a domain of the centrosome critical for pericentriolar material organization. *Nature Cell Biology* 14, 1159–1168.
- Meraldi, P., Lukas, J., Fry, A.M., Bartek, J., and Nigg, E.A. (1999). Centrosome duplication in mammalian somatic cells requires E2F and Cdk2-cyclin A. *Nature Cell Biology* 1, 88–93.
- Mogensen, M.M., Malik, A., Piel, M., Bouckson-Castaing, V., and Bornens, M. (2000). Microtubule minus-end anchorage at centrosomal and non-centrosomal sites: the role of ninein. *J. Cell. Sci.* 113 (Pt 17), 3013–3023.
- Morgan, D.O. (1997). Cyclin-dependent kinases: engines, clocks, and microprocessors. *Annu. Rev. Cell Dev. Biol.* 13, 261–291.
- Moritz, M., Braunfeld, M.B., Guénebaut, V., Heuser, J., and Agard, D.A. (2000). Structure of the gamma-tubulin ring complex: a template for microtubule nucleation. *Nature Cell Biology* 2, 365–370.
- Moritz, M., Braunfeld, M.B., Sedat, J.W., Alberts, B., and Agard, D.A. (1995). Microtubule nucleation by gamma-tubulin-containing rings in the centrosome. *Nature* 378, 638–640.
- Mottier-Pavie, V., and Megraw, T.L. (2009). *Drosophila* bld10 is a centriolar protein that regulates centriole, basal body, and motile cilium assembly. *Molecular Biology of the Cell* 20, 2605–2614.
-

- Nakagawa, Y., Yamane, Y., Okanou, T., Tsukita, S., and Tsukita, S. (2001). Outer Dense Fiber 2 Is a Widespread Centrosome Scaffold Component Preferentially Associated with Mother Centrioles: Its Identification from Isolated Centrosomes. *Molecular Biology of the Cell* *12*, 1687–1697.
- Nakamura, A., Arai, H., and Fujita, N. (2009). Centrosomal Aki1 and cohesin function in separate-regulated centriole disengagement. *The Journal of Cell Biology* *187*, 607–614.
- Nakazawa, Y., Hiraki, M., Kamiya, R., and Hirono, M. (2007). SAS-6 is a cartwheel protein that establishes the 9-fold symmetry of the centriole. *Curr. Biol.* *17*, 2169–2174.
- Nam, E.A., and Cortez, D. (2011). ATR signalling: more than meeting at the fork. *Biochem. J.* *436*, 527–536.
- Nigg, E.A. (2002). Centrosome aberrations: cause or consequence of cancer progression? *Nature Reviews Cancer* *2*, 815–825.
- Nigg, E.A. (2006). Origins and consequences of centrosome aberrations in human cancers. *Int. J. Cancer* *119*, 2717–2723.
- Nigg, E.A. (2007). Centrosome duplication: of rules and licenses. *Trends in Cell Biology* *17*, 215–221.
- Nigg, E.A., and Raff, J.W. (2009). Centrioles, centrosomes, and cilia in health and disease. *Cell* *139*, 663–678.
- Nigg, E.A., and Stearns, T. (2011). The centrosome cycle: Centriole biogenesis, duplication and inherent asymmetries. *Nature Cell Biology* *13*, 1154–1160.
- Noatynska, A., Gotta, M., and Meraldi, P. (2012). Mitotic spindle (DIS)orientation and DISease: Cause or consequence? *The Journal of Cell Biology* *199*, 1025–1035.
- O'Connell, C.B., and Khodjakov, A.L. (2007). Cooperative mechanisms of mitotic spindle formation. *J. Cell. Sci.* *120*, 1717–1722.
- O'Connell, K.F., Caron, C., Kopish, K.R., Hurd, D.D., Kempfues, K.J., Li, Y., and White, J.G. (2001). The *C. elegans* *zyg-1* gene encodes a regulator of centrosome duplication with distinct maternal and paternal roles in the embryo. *Cell* *105*, 547–558.
- O'Connell, K.F., Leys, C.M., and White, J.G. (1998). A genetic screen for temperature-sensitive cell-division mutants of *Caenorhabditis elegans*. *Genetics* *149*, 1303–1321.
- Oakley, B.R., Oakley, C.E., Yoon, Y., and Jung, M.K. (1990). Gamma-tubulin is a component of the spindle pole body that is essential for microtubule function in *Aspergillus nidulans*. *Cell* *61*, 1289–1301.
- Oakley, C.E., and Oakley, B.R. (1989). Identification of gamma-tubulin, a new member of the tubulin superfamily encoded by *mipA* gene of *Aspergillus nidulans*. *Nature* *338*, 662–664.
- Ohta, T., Essner, R., Ryu, J.-H., Palazzo, R.E., Uetake, Y., and Kuriyama, R. (2002). Characterization of Cep135, a novel coiled-coil centrosomal protein involved in

microtubule organization in mammalian cells. *The Journal of Cell Biology* 156, 87–99.

Okuda, M., Horn, H.F., Tarapore, P., Tokuyama, Y., Smulian, A.G., Chan, P.K., Knudsen, E.S., Hofmann, I.A., Snyder, J.D., Bove, K.E., et al. (2000). Nucleophosmin/B23 is a target of CDK2/cyclin E in centrosome duplication. *Cell* 103, 127–140.

Pagon, R.A., Adam, M.P., Bird, T.D., Dolan, C.R., Fong, C.-T., Stephens, K., Passenard, S., Kaindl, A.M., Titomanlio, L., Gerard, B., et al. (1993). Primary Autosomal Recessive Microcephaly (Seattle (WA): GeneReviews, University of Washington, Seattle).

Papari, E., Bastami, M., Farhadi, A., Abedini, S.S., Hosseini, M., Bahman, I., Mohseni, M., Garshasbi, M., Moheb, L.A., Behjati, F., et al. (2013). Investigation of primary microcephaly in Bushehr province of Iran: novel STIL and ASPM mutations. *Clin Genet* 83, 488–490.

Pearson, C.G., Osborn, D.P.S., Giddings, T.H., Beales, P.L., and Winey, M. (2009). Basal body stability and ciliogenesis requires the conserved component Poc1. *The Journal of Cell Biology* 187, 905–920.

Peel, N., Stevens, N.R., Basto, R., and al, E. (2007). Overexpressing centriole-replication proteins in vivo induces centriole overduplication and de novo formation. *Current Biology*.

Peel, N., Dougherty, M., Goeres, J., Liu, Y., and O'Connell, K.F. (2012). The *C. elegans* F-box proteins LIN-23 and SEL-10 antagonize centrosome duplication by regulating ZYG-1 levels. *J. Cell. Sci.* 125, 3535–3544.

Pelletier, L., Müller-Reichert, T., Srayko, M., Özlü, N., Schlaitz, A.-L., and Hyman, A.A. (2005). The *C. elegans* Centrosome during Early Embryonic Development. In *Centrosomes in Development and Disease*, E.A. Nigg, ed. (Weinheim, FRG: Wiley-VCH Verlag GmbH & Co. KGaA), pp. 225–250.

Pelletier, L., O'Toole, E., Schwager, A., Hyman, A.A., and Müller-Reichert, T. (2006). Centriole assembly in *Caenorhabditis elegans*. *Nature* 444, 619–623.

Pelletier, L., Özlü, N., Hannak, E., Cowan, C., Habermann, B., Ruer, M., Müller-Reichert, T., and Hyman, A.A. (2004). The *Caenorhabditis elegans* centrosomal protein SPD-2 is required for both pericentriolar material recruitment and centriole duplication. *Curr. Biol.* 14, 863–873.

Peters, J.-M. (2006). The anaphase promoting complex/cyclosome: a machine designed to destroy. *Nat Rev Mol Cell Biol* 7, 644–656.

Pfaff, K.L., Straub, C.T., Chiang, K., Bear, D.M., Zhou, Y., and Zon, L.I. (2007). The zebra fish *cassiopeia* mutant reveals that SIL is required for mitotic spindle organization. *Mol Cell Biol* 27, 5887–5897.

Piel, M., Meyer, P., Khodjakov, A., Rieder, C.L., and Bornens, M. (2000). The respective contributions of the mother and daughter centrioles to centrosome activity and behavior in vertebrate cells. *The Journal of Cell Biology* 149, 317–329.

Piel, M., Nordberg, J., Euteneuer, U., and Bornens, M. (2001). Centrosome-dependent exit

of cytokinesis in animal cells. *Science* 291, 1550–1553.

Portier, N., Audhya, A., Maddox, P.S., Green, R.A., Dammermann, A., Desai, A., and Oegema, K. (2007). A microtubule-independent role for centrosomes and aurora a in nuclear envelope breakdown. *Dev. Cell* 12, 515–529.

Puklowski, A., Homsy, Y., Keller, D., May, M., Chauhan, S., Kossatz, U., Grünwald, V., Kubicka, S., Pich, A., Manns, M.P., et al. (2011). The SCF-FBXW5 E3-ubiquitin ligase is regulated by PLK4 and targets HsSAS-6 to control centrosome duplication. *Nature Cell Biology* 13, 1004–1009.

Qiao, R., Cabral, G., Lettman, M.M., Dammermann, A., and Dong, G. (2012). SAS-6 coiled-coil structure and interaction with SAS-5 suggest a regulatory mechanism in *C. elegans* centriole assembly. *Embo J* 31, 4334–4347.

Quintyne, N.J. (2005). Spindle Multipolarity Is Prevented by Centrosomal Clustering. *Science* 307, 127–129.

Ramaswamy, S., Ross, K.N., Lander, E.S., and Golub, T.R. (2003). A molecular signature of metastasis in primary solid tumors. *Nat. Genet.* 33, 49–54.

Rieder, C.L., Faruki, S., and Khodjakov, A. (2001). The centrosome in vertebrates: more than a microtubule-organizing center. *Trends in Cell Biology* 11, 413–419.

Ring, D., Hubble, R., and Kirschner, M. (1982). Mitosis in a cell with multiple centrioles. *The Journal of Cell Biology* 94, 549–556.

Ritter, A.T., Angus, K.L., and Griffiths, G.M. (2013). The role of the cytoskeleton at the immunological synapse. *Immunol. Rev.* 256, 107–117.

Rodrigues-Martins, A., Riparbelli, M., Callaini, G., Glover, D.M., and Bettencourt-Dias, M. (2007a). Revisiting the role of the mother centriole in centriole biogenesis. *Science* 316, 1046–1050.

Rodrigues-Martins, A.A., Bettencourt-Dias, M.M., Riparbelli, M.M., Ferreira, C.C., Ferreira, I.I., Callaini, G.G., and Glover, D.M.D. (2007b). DSAS-6 Organizes a Tube-like Centriole Precursor, and Its Absence Suggests Modularity in Centriole Assembly. *Curr. Biol.* 17, 8–8.

Rogers, G.C., Rusan, N.M., Roberts, D.M., Peifer, M., and Rogers, S.L. (2009). The SCF Slimb ubiquitin ligase regulates Plk4/Sak levels to block centriole reduplication. *The Journal of Cell Biology* 184, 225–239.

Roque, H., Wainman, A., Richens, J., Kozyrska, K., Franz, A., and Raff, J.W. (2012). *Drosophila* Cep135/Bld10 maintains proper centriole structure but is dispensable for cartwheel formation. *J. Cell. Sci.* 125, 5881–5886.

Ruiz, F., Garreau de Loubresse, N., Klotz, C., Beisson, J., and Koll, F. (2005). Centrin deficiency in *Paramecium* affects the geometry of basal-body duplication. *Current Biology* 15, 2097–2106.

Salisbury, J.L., Suino, K.M., Busby, R., and Springett, M. (2002). Centrin-2 is required for

- centriole duplication in mammalian cells. *Current Biology* 12, 1287–1292.
- Schiebel, E., and Bornens, M. (1995). In search of a function for centrins. *Trends in Cell Biology* 5, 197–201.
- Schmidt, T.I., Kleylein-Sohn, J., Westendorf, J., Le Clech, M., Lavoie, S.B., Stierhof, Y.-D., and Nigg, E.A. (2009). Control of centriole length by CPAP and CP110. *Curr. Biol.* 19, 1005–1011.
- Schneider, C., Will, C.L., Makarova, O.V., Makarov, E.M., and Luhrmann, R. (2002). Human U4/U6.U5 and U4atac/U6atac.U5 Tri-snRNPs Exhibit Similar Protein Compositions. *Mol Cell Biol* 22, 3219–3229.
- Schöckel, L., Möckel, M., Mayer, B., Boos, D., and Stemmann, O. (2011). Cleavage of cohesin rings coordinates the separation of centrioles and chromatids. *Nature Cell Biology* 13, 966–972.
- Schwartz, R.S., Hildebrandt, F., Benzing, T., and Katsanis, N. (2011). Ciliopathies. *N Engl J Med* 364, 1533–1543.
- Sharma, N., Berbari, N.F., and Yoder, B.K. (2008). Ciliary dysfunction in developmental abnormalities and diseases. *Curr. Top. Dev. Biol.* 85, 371–427.
- Silkworth, W.T., Nardi, I.K., Scholl, L.M., and Cimini, D. (2009). Multipolar spindle pole coalescence is a major source of kinetochore mis-attachment and chromosome mis-segregation in cancer cells. *PLoS ONE* 4, e6564.
- Siller, K.H., and Doe, C.Q. (2009). Spindle orientation during asymmetric cell division. *Nature Cell Biology* 11, 365–374.
- Sir, J.-H., Barr, A.R., Nicholas, A.K., Carvalho, O.P., Khurshid, M., Sossick, A., Reichelt, S., D'Santos, C., Woods, C.G., and Gergely, F. (2011). A primary microcephaly protein complex forms a ring around parental centrioles. *Nat. Genet.* 43.
- Sir, J.-H., Pütz, M., Daly, O., Morrison, C.G., Dunning, M., Kilmartin, J.V., and Gergely, F. (2013). Loss of centrioles causes chromosomal instability in vertebrate somatic cells. *The Journal of Cell Biology* 203, 747–756.
- Sluder, G. (2005). Two-way traffic: centrosomes and the cell cycle. *Nat Rev Mol Cell Biol* 6, 743–748.
- Smith, E., Hégarat, N., Vesely, C., Roseboom, I., Larch, C., Streicher, H., Straatman, K., Flynn, H., Skehel, M., Hirota, T., et al. (2011). Differential control of Eg5-dependent centrosome separation by Plk1 and Cdk1. *Embo J* 30, 2233–2245.
- Song, M.H., Miliaras, N.B., Peel, N., and O'Connell, K.F. (2008). Centrioles: some self-assembly required. *Curr Opin Cell Biol* 20, 688–693.
- Sonnen, K.F., Gabryjonczyk, A.-M., Anselm, E., Stierhof, Y.-D., and Nigg, E.A. (2013). Human Cep192 and Cep152 cooperate in Plk4 recruitment and centriole duplication. *J. Cell. Sci.* 126, 3223–3233.

- Sonnen, K.F., Schermelleh, L., Leonhardt, H., and Nigg, E.A. (2012). 3D-structured illumination microscopy provides novel insight into architecture of human centrosomes. *Biol Open* *1*, 965–976.
- Sönnichsen, B., Koski, L.B., Walsh, A., Marschall, P., Neumann, B., Brehm, M., Alleaume, A.M., Artelt, J., Bettencourt, P., Cassin, E., et al. (2005). Full-genome RNAi profiling of early embryogenesis in *Caenorhabditis elegans*. *Nature* *434*, 462–469.
- Spektor, A., Tsang, W.Y., Khoo, D., and Dynlacht, B.D. (2006). Cep97 and CP110 Suppress a Cilia Assembly Program. *Cell* *130*, 678–690.
- Stearns, T., and Kirschner, M. (1994). In vitro reconstitution of centrosome assembly and function: the central role of gamma-tubulin. *Cell* *76*, 623–637.
- Stearns, T., Evans, L., and Kirschner, M. (1991). Gamma-tubulin is a highly conserved component of the centrosome. *Cell* *65*, 825–836.
- Stemm-Wolf, A.J., Morgan, G., Giddings, T.H., White, E.A., Marchione, R., McDonald, H.B., and Winey, M. (2005). Basal body duplication and maintenance require one member of the *Tetrahymena thermophila* centrin gene family. *Molecular Biology of the Cell* *16*, 3606–3619.
- Stevens, N.R., Dobbelaere, J., Brunk, K., Franz, A., and Raff, J.W. (2010a). *Drosophila* Ana2 is a conserved centriole duplication factor. *The Journal of Cell Biology* *188*, 313–323.
- Stevens, N.R., Raposo, A.A.S.F., Basto, R., St Johnston, D., and Raff, J.W. (2007). From stem cell to embryo without centrioles. *Current Biology* *17*, 1498–1503.
- Stevens, N.R., Roque, H., and Raff, J.W. (2010b). DSas-6 and Ana2 Coassemble into Tubules to Promote Centriole Duplication and Engagement. *Dev. Cell* *19*, 7–7.
- Stillman, B. (2005). Origin recognition and the chromosome cycle. *FEBS Lett* *579*, 877–884.
- Strnad, P., and Gönczy, P. (2008). Mechanisms of procentriole formation. *Trends in Cell Biology* *18*, 389–396.
- Strnad, P., Leidel, S., Vinogradova, T., Euteneuer, U., Khodjakov, A., and Gönczy, P. (2007). Regulated HsSAS-6 levels ensure formation of a single procentriole per centriole during the centrosome duplication cycle. *Dev. Cell* *13*, 203–213.
- Sunkel, C.E., and Glover, D.M. (1988). polo, a mitotic mutant of *Drosophila* displaying abnormal spindle poles. *J. Cell. Sci.* *89 (Pt 1)*, 25–38.
- Szollosi, D., Calarco, P., and Donahue, R.P. (1972). Absence of centrioles in the first and second meiotic spindles of mouse oocytes. *J. Cell. Sci.* *11*, 521–541.
- Tang, C.-J.C., Fu, R.-H., Wu, K.-S., Hsu, W.-B., and Tang, T.K. (2009). CPAP is a cell-cycle regulated protein that controls centriole length. *Nature Cell Biology* *11*, 825–831.
- Tang, C.-J.C., Lin, S.-Y., Hsu, W.-B., Lin, Y.-N., Wu, C.-T., Lin, Y.-C., Chang, C.-W., Wu, K.-S., and Tang, T.K. (2011). The human microcephaly protein STIL interacts with CPAP and is

- required for procentriole formation. *Embo J* 30, 4790–4804.
- Tanos, B.E., Yang, H.-J., Soni, R., Wang, W.-J., Macaluso, F.P., Asara, J.M., and Tsou, M.-F.B. (2013). Centriole distal appendages promote membrane docking, leading to cilia initiation. *Genes Dev.* 27, 163–168.
- Thein, K.H., Kleylein-Sohn, J., Nigg, E.A., and Gruneberg, U. (2007). Astrin is required for the maintenance of sister chromatid cohesion and centrosome integrity. *The Journal of Cell Biology* 178, 345–354.
- Thornton, G.K., and Woods, C.G. (2009). Primary microcephaly: do all roads lead to Rome? *Trends in Genetics* 25, 501–510.
- Tibelius, A., Marhold, J., Zentgraf, H., Heilig, C.E., Neitzel, H., Ducommun, B., Rauch, A., Ho, A.D., Bartek, J., and Krämer, A. (2009). Microcephalin and pericentrin regulate mitotic entry via centrosome-associated Chk1. *The Journal of Cell Biology* 185, 1149–1157.
- Tsang, W.Y., Bossard, C., Khanna, H., Peränen, J., Swaroop, A., Malhotra, V., and Dynlacht, B.D. (2008). CP110 suppresses primary cilia formation through its interaction with CEP290, a protein deficient in human ciliary disease. *Dev. Cell* 15, 187–197.
- Tsang, W.Y., Spektor, A., Vijayakumar, S., Bista, B.R., Li, J., Sánchez, I., Duensing, S., and Dynlacht, B.D. (2009). Cep76, a centrosomal protein that specifically restrains centriole reduplication. *Dev. Cell* 16, 649–660.
- Tsou, M.-F.B., and Stearns, T. (2006a). Mechanism limiting centrosome duplication to once per cell cycle. *Nature* 442, 947–951.
- Tsou, M.-F.B., and Stearns, T. (2006b). Controlling centrosome number: licenses and blocks. *Curr Opin Cell Biol* 18, 74–78.
- Tsou, M., Wang, W.J., George, K.A., Uryu, K., and Stearns, T. (2009). Polo kinase and separase regulate the mitotic licensing of centriole duplication in human cells. *Dev. Cell.*
- Uetake, Y., Loncarek, J., Nordberg, J.J., English, C.N., La Terra, S., Khodjakov, A., and Sluder, G. (2007). Cell cycle progression and de novo centriole assembly after centrosomal removal in untransformed human cells. *The Journal of Cell Biology* 176, 173–182.
- Uhlmann, F. (2003). Chromosome cohesion and separation: from men and molecules. *Current Biology* 13, R104–R114.
- van Beneden, E. (1876). Recherches sur les dicyemides, survivants actuels d'un embranchement des mésozoaires (Bull. Acad. royale de Belgique Ser. II).
- van Breugel, M., Hirono, M., Andreeva, A., Yanagisawa, H.-A., Yamaguchi, S., Nakazawa, Y., Morgner, N., Petrovich, M., Ebong, I.-O., Robinson, C.V., et al. (2011). Structures of SAS-6 suggest its organization in centrioles. *Science* 331, 1196–1199.
- van Breugel, M., Wilcken, R., McLaughlin, S.H., Rutherford, T.J., and Johnson, C.M. (2014). Structure of the SAS-6 cartwheel hub from *Leishmania major*. *Elife* 3, e01812.

- van der Voet, M., Berends, C.W.H., Perreault, A., Nguyen-Ngoc, T., Gönczy, P., Vidal, M., Boxem, M., and van den Heuvel, S. (2009). NuMA-related LIN-5, ASPM-1, calmodulin and dynein promote meiotic spindle rotation independently of cortical LIN-5/GPR/G α . *Nature Cell Biology* *11*, 269–277.
- Venoux, M., Tait, X., Hames, R.S., Straatman, K.R., Woodland, H.R., and Fry, A.M. (2013). Poc1A and Poc1B act together in human cells to ensure centriole integrity. *J. Cell. Sci.* *126*, 163–175.
- Verloes, A., Drunat, S., Gressens, P., and Passemard, S. (2013). Primary Autosomal Recessive Microcephalies and Seckel Syndrome Spectrum Disorders. GeneReviews.
- Vulprecht, J., David, A., Tibelius, A., Castiel, A., Konotop, G., Liu, F., Bestvater, F., Raab, M.S., Zentgraf, H., Izraeli, S., et al. (2012). STIL is required for centriole duplication in human cells. *J. Cell. Sci.* *125*, 1353–1362.
- Wadsworth, P., and Khodjakov, A. (2003). E pluribus unum: towards a universal mechanism for spindle assembly. *Trends in Cell Biology* *14*, 413–419.
- Wang, P.J., and Huffaker, T.C. (1997). Stu2p: A microtubule-binding protein that is an essential component of the yeast spindle pole body. *The Journal of Cell Biology* *139*, 1271–1280.
- Wang, W.-J., Soni, R.K., Uryu, K., and Tsou, M.-F.B. (2011). The conversion of centrioles to centrosomes: essential coupling of duplication with segregation. *The Journal of Cell Biology* *193*, 727–739.
- Warnke, S., Kemmler, S., Hames, R.S., Tsai, H.-L., Hoffmann-Rohrer, U., Fry, A.M., and Hoffmann, I. (2004). Polo-like kinase-2 is required for centriole duplication in mammalian cells. *Current Biology* *14*, 1200–1207.
- Wiese, C., and Zheng, Y. (2000). A new function for the gamma-tubulin ring complex as a microtubule minus-end cap. *Nature Cell Biology* *2*, 358–364.
- Wong, C., and Stearns, T. (2003). Centrosome number is controlled by a centrosome-intrinsic block to reduplication. *Nature Cell Biology* *5*, 539–544.
- Yamashita, Y.M., and Fuller, M.T. (2008). Asymmetric centrosome behavior and the mechanisms of stem cell division. *The Journal of Cell Biology* *180*, 261–266.
- Zhao, H., Zhu, L., Zhu, Y., Cao, J., Li, S., Huang, Q., Xu, T., Huang, X., Yan, X., and Zhu, X. (2013). The Cep63 paralogue Deup1 enables massive de novo centriole biogenesis for vertebrate multiciliogenesis. *Nature Cell Biology* *15*, 1434–1444.
- Zheng, X., Gooi, L.M., Wason, A., Gabriel, E., Mehrjardi, N.Z., Yang, Q., Zhang, X., Debec, A., Basiri, M.L., Avidor-Reiss, T., et al. (2014). Conserved TCP domain of Sas-4/CPAP is essential for pericentriolar material tethering during centrosome biogenesis. *Proceedings of the National Academy of Sciences* *111*, E354–E363.
- Zheng, Y., Jung, M.K., and Oakley, B.R. (1991). Gamma-tubulin is present in *Drosophila melanogaster* and *Homo sapiens* and is associated with the centrosome. *Cell* *65*, 817–823.

- Zheng, Y., Wong, M.L., Alberts, B., and Mitchison, T. (1995). Nucleation of microtubule assembly by a gamma-tubulin-containing ring complex. *Nature* *378*, 578–583.
- Zhu, F., Lawo, S., Bird, A., Pinchev, D., Ralph, A., Richter, C., Mueller-Reichert, T., Kittler, R., Hyman, A.A., and Pelletier, L. (2008). The mammalian SPD-2 ortholog Cep192 regulates centrosome biogenesis. *Curr. Biol.* *18*, 136–141.
- Zipperlen, P., Fraser, A.G., Kamath, R.S., Martinez-Campos, M., and Ahringer, J. (2001). Roles for 147 embryonic lethal genes on *C.elegans* chromosome I identified by RNA interference and video microscopy. *Embo J* *20*, 3984–3992.
- Zou, C., Li, J., Bai, Y., Gunning, W.T., Wazer, D.E., Band, V., and Gao, Q. (2005). Centrobin: a novel daughter centriole-associated protein that is required for centriole duplication. *The Journal of Cell Biology* *171*, 437–445.
- Zyss, D., and Gergely, F. (2009). Centrosome function in cancer: guilty or innocent? *Trends in Cell Biology* *19*, 334–346.

8. ACKNOWLEDGMENTS

First, I would like to thank Erich Nigg for giving me the opportunity to work as a PhD student in his lab. It was great to start with such an exciting project that quickly introduced me into the „world of centrosomes“. Thanks for helping me with critical decisions, but also for giving me the freedom to learn and organise things on my own (which usually is the harder, but more instructive way). Furthermore, I would like to thank Elena Nigg for excellent technical assistance and lab organisation, but also for being the „good soul“ of the lab in all these years. Also thank you Fabien Cubizolles for lab management and Zdenka Hage as well as Nadine Iberl for lots of support with administrative issues.

In the same manner, I would like to thank all my past and current labmates for support and friendship. Thanks first of all to Ina Maier, my former supervisor, for useful help especially in the beginning of my PhD. Thanks also to Luca Fava, Manuel Kaulich, Gernot Guderian, Gary Chan, Anna Santamaria Margalef, Manuel Bauer and Fabien Cubizolles for being good advisors and friends when I joined the group. Many thanks also go to all my „newer“ colleagues that joined later on, namely Conrad Eberhard von Schubert, Lukas Cajanek, Anna-Maria Gabryjonczyk, Patrick Redli, Eduard Anselm, Jasmine Bracher, Dominik Schnerch, Ana Amaro Meyer, Ana Stefanovic and Cristina Vigano. It was (is) always great to have you around for interesting discussions but also for sharing good moments. Special thanks also go to Anna-Maria Gabryjonczyk for joining some of my projects towards the end of my PhD.

Also, I would like to thank the imaging as well as the proteomics core facility of the Biozentrum, providing good and helpful services in live cell imaging/image analysis or mass spectrometry. Thank you Oliver Biehlmaier, Alexia Ferrand, Niko Ehrenfeuchter, Alexander Schmidt, Timo Glatter, Lars Molzahn, Jovan Simicevic and Erik Ahrné for your help.

Furthermore, I would like to thank Markus Affolter and Matthias Peter for participation in my advisory committee. Your input was very well appreciated. Also, I would like to thank York-Dieter Stierhof from the University of Tübingen for doing all this tedious

electron microscopy work that was needed to precisely analyze how STIL localizes to centrioles.

I am also very thankful to the Fellowships for Excellence Foundation (formerly called Werner Siemens Fellowship) for funding my salary and other expenses but also for providing a network of students and great study trips. Thanks also to Angie Klarer for her organisational activities all around the Fellowship program. I would also like to thank Henning Stahlberg for giving me the opportunity to do a rotation in his laboratory at the beginning of my PhD.

Last, but certainly not least, I would like to thank all my family and friends for supporting me throughout my life!